Doctoral thesis

Dot1-dependent Histone H3K79 methylation promotes the formation of meiotic double strand breaks in the absence of Histone H3K4 methylation in *Saccharomyces cerevisiae*

Mohammad Bani Ismail

September 2014

Laboratory of Genome and Chromosome functions
Department of Biological Science
Graduate school of science
Osaka University

Table of content

List of Abbreviations

AP	alkaline phosphatase
ATM	ataxia-telangiectasia-mutated
ATR	ATM- and Rad3-related
BSA	bovine serum albumin
° C	degree Celsius
Cdks	cyclin dependent kinase
CO	crossover
DAPI	6'-diamidino-2-phenylindole
D-Loop	displacement Loop
DNA	deoxyribonucleic acid
DSB	double strand break
DTT	dithiothreitol
EDTA	ethylenediaminetetraacetic acid
EtOH	ethanol
FACS	fluorescence-activated cell sorter
JMs	joint molecules
MI	meiosis I
MII	meiosis II
MES	2-(*N*-morpholino) ethane sulfonic acid
ml	milliliter
mJ	millijoules
µl	microliter
NCO	non-crossover
ORF	open reading frame
PAGE	polyacrylamide gel electrophoresis
PCR	polymerase chain reaction
PFA	paraformaldehyde
PBS	phosphate-buffered saline
RNase	ribonuclease
SAM	S-adenosylmethionine
SC	synaptonemal complex
SEI	single-strand invasion intermediate
SICs	synapsis initiation complex
SMC	structural maintenance chromosome
SUMO	small ubiquitin like modifier
TBS	Tris-buffered saline
TCA	trichloroacetic acid
UV	ultraviolet
V	volt
ZMM	zip, msh, mer

Abstract

In Eukaryotes, histone modifications play fundamental roles in regulating many cellular events during meiosis. Previous reports have shown a major role of the Set1-dependent histone H3K4 methylation during meiosis, in particular the initiation of meiotic recombination. Furthermore, other studies have shown roles of the Dot1-dependent histone H3K79 methylation in controlling the recombination checkpoint during meiosis. In this study, I analyzed the meiotic phenotype in mutants of the *DOT1* and *SET1* genes and also mutants of the histones H3K4 and H3K79. I confirmed the role of Set1-dependent H3K4 methylation in the formation of double strand breaks (DSBs), particularly for the initiation of meiotic recombination. Further, I identified a new role for Dot1-dependent H3k79 methylation in DSB formation in the absence of Set1-dependent H3K4 methylation. Moreover, I found that both Set1 and Dot1 control the formation of a meiosis-specific chromosome structure, the synaptonemal complex (SC). Importantly, Set1-dependent H3K4 methylation seems to modulate SC formation through the proper assembly of chromosome axes.

DSBs trigger DNA damage response mediated by Tel1/ATM and Mec1/ATR checkpoint kinases. The exact mechanisms by which these kinases are activated remain elusive. Here I present results on roles of Dot1-dependent H3K79 methylation in controlling signaling un-processed DSBs during defective recombination such as in the *rad50S* mutant, in which unprocessed DSBs accumulate and induce Tel1/ATM activation. Importantly, I showed that the histone H3K79 methylation mark might promote the activation of the Tel1/ATM leading to checkpoint activation, i.e., Hop1 phosphorylation. In conclusion, results described in this thesis confirm critical roles of histone modifications in regulating meiotic events such as chromosome functions.

Chapter 1. Introduction

Sexual reproduction is a common feature of eukaryotes, which provides the transmission of genetic information through generation. It also maintains accurate ploidy by achieving a highly organized form of cell division called “Meiosis”. During meiosis the genetic contents in a diploid cell is halved to produce haploid gametes, by undergoing two rounds of nuclear divisions after one round of DNA replication (Kerr et al., 2012). For many decades scientists have been studying meiosis in an attempt to understand the molecular events of meiotic cell cycle including DNA recombination, SC formation, protection of centromeric cohesin and many other aspects during meiosis.

Although the key events in meiosis have been identified, the exact molecular mechanisms as well as control of these events are far from full-understanding. In this thesis, I am studying the roles of histone modifications, and how they can regulate and influence many fundamental events during meiosis.

1-1. Meiosis

In order to understand how meiotic cell cycle machinery works, it is necessary to learn the logic of mitotic cell cycle. The mitotic cell cycle is divided into G1, S (synthesis), G2 and M (mitotic) phases. DNA replication takes place during the S phase, while chromosomes segregation and cytoplasm division occur during M phase. The meiotic cell cycle is also divided into G1, S, G2 and M phases, but there are quite some differences such as; first, the pre-meiotic S phase, when chromosomes duplicate, is longer than the mitotic one, second, during the meiotic G2 phase,

homologue pairs are connected to each other along the entire chromosomes to ensure their co-alignment at meiosis I, which is referred as chromosome synapsis, and third, during meiosis I (MI), the homologue chromosomes separate from each other, instead sister chromatids separate as happens in mitosis and meiosis II (MII) (Marston and Amon, 2004) (Fig. I).

The successful development at each stage of the cell cycle depends on successful completion of the stage before. This organized cell cycle is sustained and governed by the highly conserved family of proteins (Kerr et al., 2012). These controls ensure the formation of cells with a proper chromosome number not only during mitosis, but also during meiosis. In general, meiosis is a type of cell division, which gives rise to haploid gamete cells such as sperms and eggs with half DNA contents of parental diploid germ cells. Errors in the meiotic division lead to the generation of aneuploid gametes, which are the main cause of infertility, miscarriage and birth defect in humans.

1-1-1. Yeast as a model organism

Saccharomyces cerevisiae (*S. cerevisiae*) is a unicellular organism and one of the simplest eukaryotic organisms. Many important features and essential functions are conserved between yeast and humans. The yeast genome is packaged within the nucleus and contains chromosomes with over 12 million base pairs with about 6000 genes (Herskowitz, 1988). Yeast cells can divide and undergo many basic biological functions in a similar manner to human cells. About 20 percent of human diseases-associated genes have counterparts in the yeast (Herskowitz, 1988). This entitles yeast to be a suitable model to understanding the meiotic machinery. In the current study, I am using *S. cerevisiae* as a model in all the experiments described below.

1-1-2. Meiosis in *Saccharomyces cerevisiae*

S. cerevisiae exists in three specialized cell types. Among them, two cell types are haploid with an opposite sex, the mating type α and **a**. α and **a** cells mate efficiently, and the fusion between α and **a** cells leads to the formation of the diploid cell, which is unable to mate with either α or **a** type. Given sufficient nutrients, like the haploid cells, the diploid cells can proliferate vegetatively and undergo mitotic cell division by budding consequently, the original mother cell gives rise to a daughter cell. Upon nutritional starvation, diploids cells can undergo meiosis to generate haploid gametes, known as spores. These cells replicate their genome during S phase, followed by two rounds of cell divisions (MI and MII), which give rise to an ascus (tetrad). Ascus contains four haploid progeny each of which is protected with a spore coat (Herskowitz, 1988). Dissection of tetrads to spores followed by the characterization of genotypes of each spore cell has become a powerful tool in yeast genetics, and it has been used in combination with many established molecular biology procedures to investigate in more details the pathways that govern the cell cycle regulation and genome integrity.

1-1-3. Meiotic cell cycle

There are two phases of meiosis; meiosis I (MI) and meiosis II (MII). Before a dividing cell enters meiosis, it undergoes a period called interphase. Interphase is divided into three stages; G1, S and G2. During the G1 phase the cell determines whether it undergoes meiosis or not. The G1 phase is followed by the S phase or the so-called Pre-meiotic S phase. Upon nutrient starvation, budding yeast expresses two genes *IME1* and *IME2*. These genes regulate the initiation of meiosis by promoting

the entry into the pre-meiotic S phase and by expressing various genes necessary for meiosis (Marston and Amon, 2004). During the pre-meiotic S phase, DNA synthesis (replication) is triggered by the S-phase cyclin-dependent kinases, which consist of Cdc28 catalytic subunits along with S-phase specific cyclins, either Clb5 or Clb6 (Marston and Amon, 2004). As mentioned above, the pre-meiotic S-phase is longer than the pre-mitotic S-phase. This lengthening of S-phase remains poorly understood. The longer pre-meiotic S-phase might be important to ensure proper chromosome morphogenesis, in turns, this facilitates the interaction between homologous pairs and also ensures the faithful chromosomes segregation during G2 stage of MI.

1-1-4. Meiotic prophase

The first meiotic phase, MI, is preceded by an extended prophase (G2), which is considered as the most important phase during meiotic cell cycle. Many critical events take place throughout the prophase, for example, reciprocal recombination between homologues referred as crossover recombination, formation of the SC that keeps the homologous chromosomes connected, in addition to the recombination (pachytene) checkpoint. The prophase of MI is further divided into leptotene, zygotene, pachytene, diplotene, and diakinesis based on chromosome morphology (Zicker and Kleckner, 1998).

Leptotene :

Leptotene is the first stage of prophase of meiosis. In this stage, the replicated chromosomes are composed of two sister chromatids that start to condense into a chromosome axis with multiple chromatin loops inside the nucleus. The assembled chromosomes are called as “axial elements”. Later at this stage, DSBs occur to initiate recombination. After DSB formation, DSB ends are processed to create a single-

stranded DNA tail on which the meiotic recombination machinery with two RecA homologs, Rad51 and Dmc1, are assembled in the context of the axial element (Zickler and Kleckner, 1998; Borner et al., 2004; Page and Hawley, 2004). The axis-bound machinery is necessary for homology search with a duplex DNA on the homolog.

Zygotene :

During zygotene, the homologous chromosomes with axial elements become shorter and thicker, and line up with each other to engage in pairing. A short stretch of the SC, which is a ladder-like structure, is formed where the intimate juxtaposition occurs between two homologous regions of axial elements. At early zygotene, protein complexes involved in homologous recombination so termed the recombinasomes, are located as the early nodules (dense-stained structures). These recombinasomes correspond to DSBs, and are observed in the association with the chromosome axis (Zickler and Kleckner, 1998). The recombinase promotes the formation of a stable recombination intermediate called single-strand invasion intermediate (SEI), between single-stranded DNAs and its homologous partner duplex DNA. The zygotene stage is also known as the bouquet stage, where telomeres attached to nuclear envelops cluster at one area on the nucleus (Zickler and Kleckner, 1998).

Pachytene :

By the beginning of the pachytene stage, synapsed regions between homologous chromosome axes are extended along the entire lengths of chromosome, which is

described as the elongation of the SC, resulting in the formation of full length SCs. The two homologous chromosome axes are engaged together by the full length of SC, which is also referred to as “synapsis”. By mid- to late-pachytene the SC is fully matured, consisting of the paired axes called “lateral elements”, which are connected by the transverse filament (Page and Hawly, 2004). At this point the recombination develops from the SEI by capturing the other end of DSB to form a recombination intermediates containing double Holiday junctions (dHJs), (Kerr et al., 2012). The tight coordination between recombination progression and SC assembly from leptotene to pachyene is achieved by the ZMM (Zip, Msh, Mer) group of proteins, which marks the site of chromosome synapsis (Kerr et al., 2012). The resolution of dHJs to reciprocal crossover products occurs in the middle of pachytene accompanied with the disassembly of SC. This transition is under the control mechanism called recombination or pachytene checkpoint (below).

Diplotene :

The pachytene is followed by diplotene stage, during which meiotic chromosomes undergo decondensation. Moreover, the SC disassembles completely and chromosome losses most of the components. Furthermore, while sister arms of the chromosomes are highly connected, homologs become widely separated except at regions containing chiasmata. This region holds the chromosomes together throughout diakinesis prior to the onset of metaphase-I (Zickler and Kleckner, 1998; Page and Hawley, 2004).

Diakinesis to Meiosis I:

During the diakinesis phase, the chiasmata are most visible between homologs to ensure proper segregation. Later at this stage, which is followed by meiosis I metaphase, chromosomes moved around inside of the nuclei by the microtubules-directed motion at kinetochores. Once the tensions between all homologs are equal, the Securin prevents the activation of Separase, a protease with a cleavage activity to a kleisin subunit of cohesin complex. The activation of the Separase leads to the dissociation of the chromosome cohesion between sister chromatids from chromosome arms, while sister separation around kinetochores is protected by Shugoshin. As a result, two homologous chromosomes start to separate towards opposite poles at the MI. Sister chromatids are separated at MII by the second activation of the Separase together with the loss of Shugoshin (Marston and Amon, 2004).

1-1-5. Meiotic recombination

After the pre-meiotic DNA replication, the two sister chromatids are linked by cohesin. However, there is no connection between homologous chromosomes, this may cause unfaithful segregation of the chromosomes. To solve this issue, cells undergo a process called homologous recombination. Homologous recombination plays critical roles in the maintenance of the genome integrity, through the repair of DNA damage, such as DSBs. Homologous recombination refers to the exchange of DNA molecules with perfect DNA sequence homology between chromosomes, as reviewed in Handel and Schimenti (2010). It is required for both mitotic as well as meiotic cells. It is important for recovery of the collapsed DNA replication forks in S-phase by repairing DSBs or single strand gap. Furthermore, it is critical for the establishment of a tight connection between homologous chromosomes to ensure their

proper separation during the MI division. Moreover, meiotic recombination creates genetic diversity by reshuffling between allele of genes (Handel and Schimenti, 2010). The Rad52 group proteins (Rad50, Rad51, Rad52, Rad54, Rad55, Rad57, Rad59, Rdh54/Tid1, Mre11, and Xrs2) are a significant player in the homologous recombination process (Essers et al., 2002; Symington, 2002) in both mitotic and meiotic cell cycles.

While spontaneous DNA damage occurs along the genome at random, recombination events along the genome of meiotic cells are not random, rather show preferential locations called hotspots (Fukuda et al., 2008; Mets and Meyer, 2009). The location of the hotspots is influenced by chromatin structure and chromosome modifications. Recently, it has been shown that a recombination initiation site in yeast is marked by histone H3 lysine 4 tri-methylation (Borde et al., 2009), indicating an important role of epigenetic marks in meiotic cell cycle regulation and functions.

In meiosis, homologous recombination (Fig. II) is initiated by DSB formation at the recombination hotspots. Formation of the break is catalyzed by the topoisomerase-related protein Spo11, with the assistance of some other accessory proteins (Keeney et al., 1997; Page and Hawley, 2004; Handel and Schimenti, 2010). Spo11 protein dimer attacks the phospho-diester bonds in DNA strands using a hydroxyl group of tyrosine 135, resulting in covalent attachment of the protein to the 5'-end of the DNA at the DSB site.

The protein-DNA adduct is recognized by the MRX (Mre11, Rad50, Xrs2) complex. Together with Sae2 protein, the MRX complex then excludes Spo11 from the 5'-end, resulting in the formation of single stranded 3'-overhang tail, which extends hundreds to a few thousand nucleotides by the action of nucleases and helicases (Krogh and Symington, 2004; Nicolette et al., 2010). Single-stranded DNA

with 3'-end is covered with the bacterial RecA–related recombinase proteins, Rad51 and Dmc1, resulting in the formation of Dmc1/Rad51 nucleoprotein filaments (Bishop et al., 1992; Shinohara et al., 1992; Shinohara and Shinohara, 2004). The Dmc1/Rad51 nucleoprotein filaments, with Rad54 and Tid1 accessory proteins, start homology search for the homologous DNA sequence. Finding the match of the single-stranded DNA with the complementary strand of the homologous duplex DNA, results in the strand invasion of the single-stranded DNAs to the duplex to form a displacement loop (D-loop) (Krogh and Symington, 2004; Lao and Hunter, 2010). Subsequently, the transient D-loop is converted into stable SEI, which accompanied by the DNA synthesis from invaded DNA. Later, capturing of the extended SEI with the single-stranded DNA in the other DSB end, followed by the extensions of the 3'-overhang tail and the ligation of the gaps, leads to the formation of the dHJs. dHJs are resolved to create reciprocal crossovers (COs) (Matos et al., 2011). The formations of COs are highly regulated so that COs are distributed along chromosomes in a non-random way, in which every pair of homologs has at least one crossover. The presence of a CO at one position decreases the possibility of having another COs nearby, which is known as crossover interference (Borner et al., 2004).

1-1-6. Roles of Rad51 and Dmc1 proteins in meiotic recombination

S.cerevisiae Rad51 is 30% identical to the catalytic domain of the bacterial RecA protein, which is present in both mitotic and meiotic cells (Shinohara et al., 1992). On the other hand, Dmc1 is 45% identical to Rad51, with significant similarity to RecA and is expressed only during meiosis (Krogh and Symington, 2004). Rad51 and Dmc1 play essential roles in the conversion of DSBs to joint molecules (JMs), such as SEIs and dHJs during meiosis (Shinohara et al., 2000). Rad51 forms right-handed helical

filaments on single stranded DNA. It catalyses strand exchange between circular single-stranded DNA and homologous linear double-stranded DNA to form JMs (Shinohara and Ogawa, 1998). It is reported that *in vitro* Rad52 protein facilitates the formation of Rad51 filaments for strand exchange (Shinohara and Ogawa, 1998). Consistent with this, *in vivo* localization of Rad51 to the site of DSBs requires Rad52 as an essential factor for loading of Rad51 onto RPA-coated single stranded DNA (Krogh and Symington, 2004; Seeber et al., 2013). On the other hand, it is reported that Dmc1 protein plays an essential role in the repair between homologous non-sister chromatids during meiosis (Schwacha and Kleckner, 1997). The assembly of Dmc1 is promoted by Rad51 as well as a meiosis-specific protein complex, Mei5-Sae3 (Hayase et al., 2004). Rad51 and Dmc1 co-localize to form foci, which correspond to sites of DSBs during meiosis. This co-localization suggests that both proteins function together in the same recombination events such as inter-homolog recombination (Bishop, 1994; Shinohara et al., 2000). It is also reported that the *rad51* mutants exhibit partial defects in meiotic recombination and also create inviable meiotic products (Shinohara et al., 1992). On the other hand, the *dmc1* null mutant showed the accumulation of resected but unrepaired DSBs during meiosis as measured by some physical assays (Bishop et al., 1992). Collectively, the functions of Rad51 and Dmc1 are critical during meiotic recombination.

Rad50:

Efficient DSB formation and proper DNA ends resection require several proteins including the MRX complex (Mre11/ Rad50 /Xrs2). The recent model suggests that Spo11 is detached from DSB ends by a collaborative action of the MRX complex and Sae2 protein, then the resulting free 5'-ends are available for resection (Nicolette et al., 2010). Rad50 protein, a 153-kDa protein, contains N-terminal Walker A and C-terminal Walker B motifs that are linked with an α helical coiled-coil domain, where the other component of the MRX complex, Mre11, binds to form a heterotetramer. On the other hand, the third component, Xrs2, can interact directly with Mre11 (Aravind et al., 1999).

In yeast, *xrs2, rad50*, and *mre11* null mutants showed severe defects during meiosis; e.g. defects in meiotic DSB formation. Furthermore, like the *sae2* null mutant, the *rad50S* mutant, a non-null *rad50* mutant, showed accumulation of un-resected meiotic DSBs with the Spo11 covalently bound to the 5'-end (Krogh and Symington, 2004; Nicolette et al., 2010). These observations along with other studies confirm the critical role of DSB processing during meiotic cell cycle.

1-1-7. Synaptonemal complex

Proper homologous recombination and faithful chromosome segregation is intimately linked with the dynamics of chromosome pairing and synapsis during meiotic prophase. In yeast, it has been reported that DSB formation is required for synapsis, and, furthermore, the processing of the DSB ends is also vital for efficient synapsis (Roeder, 1997). In order to achieve the state of synapsis, chromosomes must pair in a ladder-like protein structure called synaptonemal complex (SC). SC is a tripartite ribbon between the homologous chromosomes, which is prominently seen in

pachytene (Fig. III). The SC is assembled, rearranged, and disassembled during the prophase of the MI. (See above, Page and Hawley, 2004).

SC formation starts at leptotene stage. Sister chromatids, which are connected through the cohesion begin to condense and become highly organized within the axial elements. As leptotene proceeds, bridges corresponding to a DSB site between homologs, known as axial associations, are formed. The formation of axial associations depends on Rad51and Dmc1. They function as a site for the assembly of synapsis initiation complexes (SICs), which are composed of a group of ZMM proteins including Zip1, Zip2, Zip3, Msh4, Msh5, Spo22, Spo16 and Mer3 (Nakagawa and Ogawa, 1999; Shinohara et al., 2008). Axial associations play an essential role in meiotic synapsis by helping the assembly of the SC and are important for the maturation of DSBs into meiotic COs (Chua and Roeder, 1998). The axial associations nucleate the formation of SC between the axial elements, and these axial elements are then incorporated in the SC structure as a part of lateral elements (Miyazaki and Orr-Weaver, 1994).

At zygotene stage, the two axial elements are joined together by the formation of a local short SC. During pachytene, chromosomes exhibit synapsis, holding the entire homologous chromosomes in such a way that, the lateral elements are paired together with each other through the connection by the central elements. As mentioned, the SC formation is promoted by the actions of the ZMM proteins. Among ZMMs, the binding of Zip3 to the axial associations, which recruits Zip2, and both Zip2 and Zip3 recruit the binding of Zip1, then the binding of Zip1 to the axial associations promotes the polymerization of the full length SC along the entire length of chromosomes by depositing Zip1 as a component of the transverse filament (Agarwal and Roeder, 2000). Following pachytene, SC disassembles and homologs

separate. Although the SC was discovered more than 50 years, the full picture of assembly and disassembly mechanisms of it remains far from complete.

1-1-7-1. Lateral elements

The conserved SC structure in most organisms is composed of two dense lateral elements holding sister chromatids which are connected to each other by less dense central elements (Hawley, 2011). Each lateral elements contains two sister chromatids with an axis with multiple chromatin loops. It is well known that chromosome cohesion holds the two sister chromatids during meiosis. The fact that cohesin is a basic component of chromosome axis structures indicates an important role of the cohesin in the maintenance of the SC structure between homologs. This connection between chromosome cohesion and SC raises the possibility that some proteins may have a dual function in both the sister chromatids cohesion and SC formation. The relationship between SC and chromosome cohesion can be explained as either the proper cohesion is required for proper recombination and mature SC, or SC might be required to maintain sister chromatids cohesion (Miyazaki and Orr-weaver, 1994).

In mitosis, cohesin is required to create cohesion between sister chromatids during chromosomes replication. Mitotic cohesin is composed of two structural maintenance chromosome (SMC) proteins, Smc1 and Smc3, and two non-SMC components, Scc1/Mcd1 and Scc3 (Hirand, 2002). On the other hand, cohesin is also required during meiosis where a cohesin member such as Scc1 is replaced by a similar protein called Rec8. During meiotic prophase, the cohesin complex binds along axial chromosomal cores (Eijpe et al., 2003). Rec8 and the other cohesin components are required for proper localization of lateral elements- associated

proteins. It has been reported that SC formation is abolished in *rec8* and *smc3* mutants (Klein et al., 1999).

Several studies showed the existence of other non-cohesin proteins involved in the formation of lateral elements. In yeast, *S.cerevisiae*, some meiosis-specific proteins such as Hop1 and Red1 play essential roles in the formation of lateral elements (Hollingsworth et al., 1990; Smith and Roeder, 1997). Other study showed that, in *red1* and *hop1* mutants, the SC failed to assemble normally (Loidl et al., 1994). The findings indicate important roles of not only cohesin, but also non-cohesin proteins in the normal assembly of the lateral elements and thus the SC formation.

Proteins in lateral/axial elements

Rec8:

Rec8 is a meiosis-specific α-kleisin subunit of cohesin and is a central component of the meiotic chromosome axis in budding yeast (Klein et al., 1999). Rec8 is expressed exclusively during meiosis and co-localizes with chromosomes cores in axial elements. Yeast Rec8 protein is required for the normal assembly of the lateral element protein Red1 on chromosomes, and also essential for the localization of the central element protein, Zip1 (Klein et al., 1999). Immunostaining analysis of chromosome spreads showed that Rec8 associates with chromosomes early during pre-meiotic DNA replication during leptotene and zygotene (Klein et al., 1999). Rec8 forms punctate distribution on chromosomes during early stages of prophase-I and, later at pachytene, forms continuous lines with a full length of SC (Klein et al., 1999). Furthermore, Rec8 is necessary for efficient meiotic recombination including the repair of DSBs and also for strand exchange between homologs (Klein et al., 1999).

During MI, cohesin must be removed along chromosomes arms, but should be maintained at centromeres (Klein et al., 1999). At the metaphase-I to anaphase-I transition, a protease known as Separase is activated, and the activated Separase cleaves Rec8, causing the removal of cohesin from chromosome arms, but not from kinetochores (Klein et al., 1999).

Red1:

Red1 is a meiosis-specific component of the lateral/axial elements and is also essential for coupling checkpoint signaling with SC formation (Thompson and Roeder, 1989; Hollingsworth and Ponte, 1997; De los Santos and Hollingsworth, 1999). Red1 forms homo-oligomers and physically interacts with Hop1 protein (Hollingsworth and Ponte, 1997). It has been reported that Red1 also physically interacts with Mek1 protein kinase (De los Santos and Hollingsworth, 1999). Wang et al. (2004) studied the interaction among Red1, Hop1 and Mek1, and proposed a model in which Hop1 first binds to chromosomes leading to the recruitment of the phosphorylated Red1 to chromosomes. Then, Mek1 binds to Red1 on chromosomes, and then Mek1 starts phosphorylation cascade that is involved in interhomolog recombination. Smith and Roeder (1997) studied the chromosomal localization of Red1 and found that Red1 expressed early during meiosis, localizes onto chromosome during leptotene, and that, later at pachytene, Red1 forms stretches of continuous staining disrupted by nonstaining regions, unlike continuous staining of Zip1 along the length of pachytene chromosomes. In addition, Smith and Roeder (1997) showed that Red1 and Hop1 show extensive co-localization, and that Hop1 localization depends on Red1, which confirmed the direct interaction between these two proteins.

Hop1:

Hop1 is a meiosis-specific protein, which plays an important role in the lateral elements assembly and the progression of homologous recombination (Hollingsworth et al., 1990). Hop1 N-terminus contains a region called HORMA domain involved in checkpoint function and chromosome synapsis, which is likely required to form a globular structure that might be involved in recognizing special chromatin associated with DSBs (Carballo et al., 2008; Hunter, 2008). Furthermore, Hop1 contains a Zinc finger domain required for DNA binding (Tung and Roeder, 1998; Page and Hawley, 2004). Hopl also contains a C-domain required for DSB-dependent Hop1 phosphorylation (Carballo et al., 2008; Hunter, 2008). Work by Carballo et al. (2008) identified a functional (S/T) Q cluster domain (SCD), which undergoes Tel1/Mec1-dependent phosphorylation in response to meiotic DSBs. The absence of Hop1 showed a defect in SC formation and, as expected, in the production of inviable yeast spores (Hollingsworth et al., 1990).

1-1-7-2. Central elements

In order to form a fully mature SC, the two lateral elements must be joined together by the assembly of central elements (transverse filaments) between them. Many studies have been carried out in order to understand the mechanism by which the central elements are formed and the functions of SCs by itself. Transverse filaments proteins are composed of an extended coiled coil-rich segment found in the center of the protein, sandwiched by largely globular domains of both ends of the coil (Sym et al., 1993; Page and Hawley, 2004). Other study by Dobson (1994) and Dong and Roeder (2000) showed that these transverse proteins form parallel dimmers through their coiled-coil regions. Transverse proteins are later arranged between the

chromosomes with C terminal along the lateral elements. The N-terminal from opposing dimmers interacts with each other in the center of the SC to form the central elements structure (Page and Hawley, 2004). Hunter (2003) claimed that these proteins act at the DSB sites, which will mature into a CO.

Zip1:

The Zip1 protein is a main component of the central region of the SCs. Zip1 is a coiled–coil protein that connect the space between the homologous chromosomes (Page and Hawley, 2004). Dong and Roeder (2000) suggested that the terminus globular domain of Zip1 makes up the central elements of the SC. The C-terminal amino acids 791-824 are essential for the binding of Zip1 to chromosomes (Tung and Roeder, 1998). Cytological analysis by Sym et al. (1993) showed that Zip1 starts to form a focus at late leptotene, followed by the formation of short stretches of Zip1 at zygotene. At pachytene stage, Zip1 forms continuous lines along the entire length of chromosomes, and starts to disappear shortly before the onset of nuclear division. Many studies showed that, in the *zip1* null mutant, SCs failed to assemble normally and showed many meiotic defects (Sym et al., 1993), which might reflect the role of the Zip1 protein in connecting the lateral elements of the SC. The absence of Zip1 showed many defects in recombination and homologous synapsis (Storlazzi et al., 1996). Further, analysis on the *zip1* recombination defects in *red1* background showed that Zip1 acts first on the recombination sites in a pathway independent of SC formation (Storlazzi et al., 1996). This is consistent with a role of Zip1 as the ZMM proteins (below).

1-1-8. ZMM proteins

Accurate segregation of homologous chromosomes during meiosis depends on a physical linkage between chromosomes called chiasma, which corresponds to crossover between parental DNA strands. Chiasma is formed during homologous recombination in the context of the SC (Chua and Roeder, 1998; Agarwal and Roeder, 2000; Lynn et al., 2007; Shinohara et al., 2008). ZMM proteins also called the synapsis initiation complex (SIC) play critical roles not only in the regulation of homologous recombination by promoting CO formation, but also in the SC assembly (Lynn et al., 2007; Shinohara et al., 2008). The ZMM consists of seven structurally diverse proteins, which are divided into three subgroups: subgroup I includes Zip1, Zip2, Zip3, subgroup II includes Msh4, Msh5 and possibly Mer3, subgroup III includes Spo22/Zip4 and Spo16 (Lynn et al., 2007; Shinohara et al., 2008).

As mentioned previously, Zip1 is a major central element component of the SC and also plays an additional role during recombination as the ZMM component (Storlazzi et al., 1996).

Zip2 is a meiosis–specific protein required for the initiation of chromosome synapsis. In the *zip2* mutant, Zip1 fails to localize to chromosomes, forming Zip1 aggregates called polycomplex, In their cytological analysis, Chua and Roeder (1998) also showed that Zip2 co-localizes with proteins involved in DSB formation and repair.

Zip3 is a meiosis-specific protein contains a RING finger required for SUMO (small ubiquitin-like modifier) E3 ligase activity (Agarwal and Roeder, 2000). It is suggested that Zip3 SUMO binding might be required for Zip3 association to chromosomes (Cheng et al., 2006; Lynn et al., 2007). Genome-wide mapping by Serrentino et al. (2013) showed a dynamic association of Zip3 with chromosomes;

first, it binds to centromeres independent of DSB formation, then localizes to meiotic chromosome axes to few sites only, and finally to DSB sites coupled with the formation of the JMs, a preferred intermediate for CO. Zip3 binding to chromosome arms reaches to maximum during pachytene stage. Furthermore, Borner et al. (2004) and Serrentino et al. (2013) both suggested that Zip3 marks the DSB site, which gives rise to CO products.

Zip4 also called Spo22 is a meiosis-specific protein induced early during meiosis and is required for chromosome synapsis. Zip4 is a component of the SIC. Zip4 interacts with Zip2 to form a unit, which might serve as a key factor to promote the Zip1 polymerization along chromosomes (Tsubouchi et al., 2006; Lynn et al., 2007).

Recent study by Shinohara et al. (2008) identified another member of ZMM called Spo16. Like other *zmm* mutants, the study showed that the *spo16* mutant has defects in both SC elongation and crossing-over, and, by their cytological analysis, that Spo16 often co-localizes with Zip1 and Zip3 with similar timing of focus formation. Furthermore, Shinohara et al. (2008) also showed that Spo16 localization depends on DSB formation since the *spo11-Y135F* mutant defective in DSB formation showed severely reduced levels of Spo16 on chromosomes.

ZMM subgroup II consists of highly conserved proteins including Mer3, Msh4 and Msh5. Mer3 protein is a meiosis-specific DNA helicase, with amino acid sequence of seven motifs characteristic of the DExH box type of DNA/RNA helicases (Nakagawa and Kolodner, 2002). Mer3 is involved in meiotic crossing-over, particularly for efficient conversion of DSBs to recombination intermediates (Nakagawa and Kolodner, 2002; Tsubouchi et al., 2006). Indeed, the *mer3* mutation

showed decreased frequencies of crossing-over, which leads to severe defects in meiotic progression (Nakagawa and Kolodner, 2002; Tsubouchi et al., 2006).

Msh4 and Msh5 are homologs of the bacterial protein MutS, which works in repair of mismatches in DNAs (Hollingsworth et al., 1995; Novak et al., 2001; Lynn et al., 2007). Msh4 and Msh5 are involved in meiotic recombination, chromosome synapsis and the regulation of CO distribution (Hollingsworth et al., 1995; Novak et al., 2001). The two proteins directly interact to form a heterodimer complex to localize on meiotic chromosomes as foci (Hollingsworth et al., 1995; Novak et al., 2001).

1-1-9. Recombination (pachytene) checkpoint

The highly regulated events during meiotic cell cycle must occur in an appropriate order to ensure accurate transmission of genetic information to progeny. Cell cycle checkpoints are control mechanisms that block or delay cell cycle progression and prevent the initiation of late events until earlier events have been successfully completed (Marston and Amon, 2004; Handel and Schimenti, 2010; Kerr et al., 2012). Recombination checkpoint also called pachytene checkpoint senses meiotic errors and eliminates unresolved defects, and delays or arrest meiotic cell cycle progression in response to the defects in meiotic prophase-I (Perez-Hidalgo et al., 2003; Handel and Schimenti, 2010; Kerr et al., 2012). Recombination checkpoint specifically monitors events during meiotic chromosome metabolism; DSB repair and/or probably chromosome synapsis (Perez-Hidalgo et al., 2003). Errors in meiotic DSB repair can activate this checkpoint causing an arrest at mid-pachytene of prophase-I in yeast, and induce apoptosis in mouse (Perez-Hidalgo et al., 2003). Signal transduction pathway during recombination checkpoint starts by the action of sensor proteins, which detect

DNA damage such as DSB ends or single-stranded DNAs. The sensor proteins generate a signal that is recognized and then transmitted by sensor protein kinases, leading to the activation of checkpoint effectors proteins that trigger various cellular responses to deal with the damage (Roeder and Bailis, 2000; Perez-Hidalgo et al., 2003; Marston and Amon, 2004). The recombination checkpoint requires the highly conserved protein kinases including Tel1/ATM (ataxia-telangiectasia-mutated) and Mec1/ATR (ATM- and Rad3-related) as a sensor kinase, and also the meiosis-specific chromosome axis proteins, Red1, Mek1 and Hop1. The signal transduction pathway mediated by the checkpoint clamp Rad17/Mec3/Ddc1 (the 9-1-1 complex in human) and its loader Rad24-RFC is also required for checkpoint activation. Pch2 (a meiosis-specific AAA+ ATPase) and a histone methyltransferase enzyme Dot1 are also responsible for the activation of the checkpoint (Roeder and Bailis, 2000; Perez-Hidalgo et al., 2003; Longhese et al., 2009; Kerr et al., 2012). Recombination checkpoint is activated upon or shortly after DSB formation. In response to un-resected DSB, Tel1 is recruited to the DNA damage through the interaction with a MRX component, Xrs2, leading to checkpoint activation (Usui et al., 2001; Clerici et al., 2001; Hochwagen and Amon, 2006; Longhese et al., 2009). Once the DSB termini are subjected to resection, the signaling activity of Tel1 is attenuated, although the mechanism on the Tel1 attenuation is not known yet. In the *dmc1* mutant where DSBs are hyperresected with accumulation of single-stranded DNAs due to the failure of the mutant to perform interhomolog repair, single-stranded DNAs lead Mec1-dependent checkpoint activation, which depends on its regulators, Rad24, Rad17, Mec3 and Ddc1 (Lydall et al., 1996; Hong and Roeder, 2002; Longhese et al., 2009). In response to these unresolved meiotic defects, the recombination checkpoint causes cell cycle arrest at mid-pachytene by preventing the activation of cyclin dependent

kinases (Cdks), which consist of a catalytic Cdc28 core protein and its regulator cyclins. Cdks are inhibited by the action of Swe1 kinase, which phosphorylates Cdc28 on Tyr19 by inhibiting its catalytic activity (Leu and Roeder, 1999; Hochwagen and Amon, 2006). The Swe1 activity is controlled by the checkpoint, once checkpoint is triggered, Swe1 becomes hyperphosphorylated. This phosphorylation plays a role in up-regulating Swe1 function (Leu and Roeder, 1999). Furthermore, upon the activation of the checkpoint, the level of Sum1, a transcriptional repressor which down-regulates pachytene exit factors, remains high. On the other hand, the transcription factor, Ndt80, which is required to exit from mid-pachytene, is also inhibited. As a result, the transcription of cyclin such as Clb1 and the other key cell cycle regulator for pachytene, Polo-like kinase Cdc5 is highly inhibited. Importantly, the activation of Cdc5 results in the resolution of dHJs and the disassembly of the SC (Page and Hawley, 2004; Sourirajan and Lichten, 2008; Kerr et al., 2012). Therefore, relative balance on amounts of both Sum1 and Ndt80 determines whether cells exit from mid-pachytene or not (Hunter, 2003; Page and Hawley, 2004; Kerr et al., 2012).

Pch2:

Pch2 (Pachytene checkpoint 2) is a conserved meiosis-specific AAA+ ATPase, originally found to be involved in a checkpoint during aberrant meiosis. Pch2 is expressed during meiosis and the expression level peaks at pachytene stage (San-Segundo and Roeder, 1999). Pch2 binds to chromosomes in the meiotic prophase-I and dissociates from chromosomes as meiotic division starts (San-Segundo and Roeder, 1999; Borner et al., 2008). Localization study of Pch2 protein on meiotic spreads by San-Segundo and Roeder (1999) showed that Pch2 predominantly localizes to the nucleolus, with small amounts of Pch2 detected in a punctate pattern

on synapsed chromosomes in wild type cells with co-localization with Zip1. The localization of Pch2 to the nucleolus requires Sir2 protein, an NAD-dependent histone deacetylase, which is also a component of the pachytene checkpoint. Furthermore, San-Segundo and Roeder (1999) also found that Pch2 tends to co-localize with Zip1, forming an aggregates called poly complex in mutant that fail to form SCs. Due to the fact that this protein plays multiple roles during meiotic cell cycle, it has been under intense investigation for many years. Borner et al. (2008) found that Pch2 controls localization/distribution of Zip1 proteins, such as the differential hyper-abundance of Zip1 and Hop1 along chromosomes, and showed that Pch2 is also required for the timely release of Hop1 from chromosomes during pachytene stage. Work by Farmer et al. (2012) suggested that Pch2 is involved in meiotic recombination, particularly in the DSB formation, by showing that the absence of Pch2 reduced levels of DSB mildly in *rad51 dmc1* background, but severely in the *sae2* mutant background. Recent studies by Ho and Burgess (2011) also showed a role for Pch2 in controlling interhomolog bias and regulating meiotic recombination checkpoint particularly in the response to unprocessed DSBs through the interaction with the Xrs2 protein. This in turn leads to the activation of an axial protein Hop1 as well as the downstream checkpoint kinase, Mek1. Defect in recombination activates Mec1/Tel1 kinases leading to the phosphorylation of Hop1 and subsequent activation of Mek1. Activated Mek1 then phosphorylates appropriate targets to activate the checkpoint. The activated checkpoint prevents phosphorylation of Ndt80 as a result inhibits the transcription of *Clb1* and other genes required for the exit from pachytene leading to cell cycle arrest.

1-2. The role of Chromatin structure during meiosis

Chromatin structures have been under intense investigation trying to find out how exactly the structures control and influence many fundamental processes during meiosis. Although many recent studies showed an important role of chromatin structure and dynamics in controlling many meiotic events such as DSB formation, homologous recombination, and SC formation (Kouzarides, 2007; Hernandez-Hernandez et al., 2009; Brachet et al., 2012), the exact molecular mechanisms behind the role of chromatin in organizing such these events remain largely unknown. Chromatin is a state in which DNA is highly organized and packaged in the cell in such a way to keep the DNAs fully functional. It consists of nucleosomes (histones) and non-histone proteins. The nucleosome is the basic structure unit of chromatin, consisting of an octamer of four core histone proteins (H2A, H2B, H3, H4), which is wrapped by 146 base pair of a duplex DNA. The linker histone H1 also plays a role in the chromatin structure by interacting with inter-nucleosomal DNA forming a higher level of chromatin organization state called the solenoid (Shilatifard, 2006; Kouzarides, 2007; Hernandez-Hernandez et al., 2009; Brachet et al., 2012). Each core histone consists of globular domain, which mediates histone-histone interaction, and N-terminal tail that is rich in basic amino acids, which extends from the surface of the nucleosome. The N-terminal tails of histones are subject to a large number of modifications which play a major role in establishing a higher chromatin structure and varieties of chromosome functions (Peterson and Laniel, 2004; Shilatifard, 2006), (Fig. IV).

1-2-1. Histone modifications

Histones are modified at many sites. These post-translational modifications include, acetylation, methylation (at lysine and arginine), phosphorylation, ubiquitylation, sumoylation, ADP ribosylation, deamination, and proline isomerization. The modifications are dynamics and rapidly changing, and their appearance depends on the signaling conditions within the cell (Peterson and Laniel, 2004; Kouzarides, 2007). The fact that some histone residues such as lysine can be mono-, di- or tri-methylated adds more complexity to the chromatin structure and may give enormous functional responses. Since histones are subject for many enzymatic activities and most DNA-mediated processes occurring in the context of chromatin, it is widely accepted an important role of histone modifications in controlling the chromatin structures to achieve distinct functional biological consequences (Bannister and Kouzarides, 2011). Histone modifications might function through two mechanisms. First, in order to unfold chromatin and change its structure by disrupting the contacts between nucleosomes or affecting the interaction between histones and DNA. The histone acetylation has the ability to neutralize the basic charge of lysine. The alteration in chromatin charge will bring structural consequences for the chromatin arrangement by weakening the interaction with negatively charged DNA molecules (Kouzarides, 2007; Hernandez-Hernandez et al., 2009; Bannister and Kouzarides, 2011). Second, histone modifications can affect the recruitment of non-histone protein to the chromatin itself, depending on the composition of the modification on one histone. Furthermore, Bannister and Kouzarides (2011) mentioned that different proteins have specific domains, which enable them to recognize specific histone modifications leading to the recruitment of such protein to the chromatin. For

example, the PHD fingers domain within the ING family proteins (ING1-5) can recognize the H3K4 tri-methylation. The ING proteins can recruit other chromatin modifiers such as histone acetyl transferases (HATs) (Bannister and Kouzarides, 2011).

1-2-2. Histone modification Cross-talk

The existence of such a huge number of histone modifications makes it very likely to create crosstalk between different modifications within the same histone or between different histones. This cross-communication between histone modifications might be achieved in different ways (Kouzarides, 2007; Bannister and Kouzarides, 2011). First, a competition occurs between different modification to modify a particular residue such as lysine residue, which can be acetylated, methylated or ubiquitylated (Shilatifard, 2006; Bannister and Kouzarides, 2011). In the other word, one modification at a residue inhibits the different modification on the same residue. Second, one modification depends on another as seen in *Saccharomyces cerevisiae*, where both histones H3K4 methylation by Set1 and H3K79 methylation by Dot1 are dependent upon histone H2BK123 ubiquitylation by Rad6-Bre1 (Shilatifard, 2006). Third, one modification can disrupt the binding of protein to another modified residue, such as phosphorylation of H3S10 disrupts the binding of HP1 to methylated H3K9 (Fischile et al., 2005; Shilatifard, 2006). Fourth, the participation between two different modifications to achieve more stable binding of some proteins to chromatin such as the binding of PHF8 to the H3K4 tri-methylated is strengthen by the acetylation of both H3K9 and H3K14 at the same histone tail (Vermeulen et al., 2010; Bannister and Kouzarides, 2011).

1-2-3. Roles of histone modifications during meiosis

Many lines of evidences suggest an important role of chromatin structure and dynamics in establishing the ideal chromatin environment to accomplish a successful meiotic cell cycle. As described earlier, histone modifications play a major role in creating such a unique chromatin design that may influences different cellular functions, such as DNA replication, gene transcription, DSB formation and repair, and SC formation (Kouzarides, 2007; Hernandez-Hernandez et al., 2009; Brachet et al., 2012). Studies on DNA repair during mitosis showed the involvement of histone modification in the repair mechanisms. Among these, the phosphorylation of the histone variant H2AX is catalyzed by the Mec1 and Tel1 checkpoint kinases (Mahadevaiah et al., 2001; Celeste et al., 2002; Brachet et al., 2012). This modification plays a role in DSB repair and response. Moreover, the histone H3K79 methylation by Dot1 protein helps the recruitment of the Rad9 at DSB sites for checkpoint activation (Huyen et al., 2004; Wysocki et al., 2005). And also the histone H4 acetylation by the histone acetyltransferase, NuA4, is likely to promote the opening of the chromatin to facilitate the access of repair proteins (Bird et al., 2002).

Histone modifications are also found to influence the recombination during meiosis. Recent studies showed that chromatin and recombination are closely linked during meiosis. The meiotic recombination events do not occur randomly on chromosomes, but do at specific sites called hotspots, suggesting that the recombination initiation sites are influenced by chromatin properties which are largely govern by histone modifications (Brachet et al., 2012). Based on the research on mouse spermatocytes, Mahadevaiah et al. (2001) showed that, the Spo11-induced DSB formation is accompanied with the appearance of γH2AX foci. The similar

phenomenon is observed during yeast meiosis (Brachet et al., 2012). Moreover, the histone H3K4 methylation was shown to be associated with DSB formation, and this modification is higher at DSB-rich regions compared with DSB-poor regions (Shilatifard, 2008; Borde et al., 2009). On their work, Rechet et al. (2006) and Govin et al. (2010) showed an important role of histone H3K56 acetylation and histone H3T11 phosphorylation for sporulation. Other studies suggest an important role of histone modifications in controlling the way by which meiotic DSBs are repaired to produce CO or just gene conversion (Shilatifard, 2008; Borde et al., 2009). All these examples confirm the critical role of histone modifications in controlling meiotic cell cycle events.

1-2-4. Histone methylation

Histone methylation is one of the most studied histone modifications that decorate histone tail within the nucleosome. Although histone methylation was discovered a long ago, the exact functional roles they play still remain to be determined. It has been shown that histones can be methylated on their lysine or arginine residues (Rechet et al., 2006; Govin et al., 2010). Two classes of histone methylation enzymes have been reported in various eukaryotes. The first class, the non-SET domain methyl-transferase, includes the Dot1 (disrupter of telomeric silencing 1) as the only member of this group, which methylates the histone H3 on lysine 79 (Sawada et al., 2004; Wysocki et al., 2005; Lazzaro et al., 2008). The second class includes the SET-domain-containing histone methyl-transferse, which methylates various N-terminal lysine and arginine residues of histones H3 and H4 leading to a wide range of cellular functions (Min et al., 2003; Shilatifard, 2006; Schulze et al., 2009). Histone methylation involves the enzymatic addition of the methyl group from the donor

substrate, S-adenosylmethionine (SAM), to lysine or arginine residues on histone H3 or H4. The addition of the methyl group has various effects on transcriptional regulation, faithful transmission of chromosomes during the cell division, protein targeting and signal transduction (Min et al., 2003; Shilatifard, 2006; Schulze et al., 2009). Lysine residues can be mono-, di-, or tri- methylated. On the other hand, arginine residues can only be mono- or di- methylated but can be found in either symmetric or asymmetric configurations (Berger, 2002; Shilatifard, 2006). Different studies have demonstrated roles of three methylation sites in transcription activation, including histone H3K4, H3K36 and H3K79, whose methylation are catalyzed by Set1, Set2, and Dot1 proteins, respectively. Also H3K4 methylation and H3K36 methylation have been implicated in transcriptional elongation as well (Min et al., 2003; Kouzarides, 2007; Li et al., 2007; Mosammaparast and Shi, 2010).

1-2-4-1. Histone H3K4 methylation

Histone H3K4 methylation in yeast is catalyzed by the Set1 protein complex, along the entire length of the open reading frame (ORF) of active genes where mono-methylation occur at the 3'-end, and the di-methylation is enriched at the middle, while tri-methylation is found to be localized to the 5'-end of the active gene (Shilatifard 2006; Kouzarides, 2007; Li et al., 2007). Set1 is found to be associated with RNA polymerase II (Pol II) at the beginning of ORF where it converts mono-methylation into di-methylation and eventually into tri-methylation (Dehe and Geli, 2006). In their study, Dehe and Geli (2006) suggested that Set1 could catalyze H3K4 mono-methylation independent of the conserved elongation complex, the PAF complex. The PAF complex participates in the recruitment of the histone H3K4 methyltransferase Set1 complex to elongating Pol II, and also the PAF complex

appears to regulate both histone H3K4 methylation and histone H2B ubiquitylation, reviewed in (Kouzarides, 2007; Li et al., 2007). The impact of this methylation mark on transcription activation is well studied, but little is known about its role in other chromosomal functions in meiosis. A recent studies by Sommermeyer et al. (2013) and Borde et al. (2009) showed that histone H3K4 tri-methylation is critical for DSB formation that initiates homologous recombination, and demonstrated that the absence of Set1 showed a dramatic reduction in the number of DSBs at the hottest hotspots examined. A work by Yamashita et al. (2004) also demonstrated a relationship between chromatin features and distribution of meiotic recombination events by analyzing the histone H2B ubiquitylation and found that the absence of this ubiquitylation leads to overall decrease in DSBs. Other studies by Borde et al. (2009) and Sommermeyer et al. (2013) suggested that one or more of the proteins required for DSB formation such as Mer2 can read the H3K4 tri-methylation, leading to the recruitment of DSB-forming machinery to generate the sites.

Set1:

Set1 protein contains a C-terminal motif with about 130 residues called the SET domain, which has been identified in many organisms, and also bears a conserved RNA recognition motif (Dehe and Geli, 2006). Set1 belongs to a component of the complex called COMPASS (complex proteins associated with Set1). COMPASS consists of Set1, Bre2, Swd1, Swd2, Swd3, Spp1, Sdc1 and Shg1. It is conserved from yeast to human (Krogan et al., 2003). Most of the complex subunits play important role in efficient H3K4 methylation (Dehe and Geli, 2006; Takahashi and Shilatifard, 2010). Work by Nislow et al. (1997) on the *set1* mutant phenotypes showed that the *SET1* gene is not required for viability, but that the deletion of *SET1* affects many cellular and growth related functions, including transcriptional

activation, telomere length regulation, rDNA silencing and meiotic differentiation. As COMPASS, Set1 is associated with the Pol II's repeat C-terminal domain (CTD) through the Paf1 complex, which consists of Paf1, Rtf1, Cdc73, Ctr9 and Leo1 (Krogan et al., 2003; Dehe and Geli, 2006). Unlike other SET-domain containing proteins, the presence of other COMPASS components is required for the full H3K4 methylation activity of Set1 (Shilatifard, 2006). Set1 is required for proper meiotic progression and the absence of Set1 leads to a delay of meiotic S-phase onset (Sollier et al., 2004). Furthermore, the deletion of the *SET1* showed a severe reduction of DSB formation. In the same study, it has been reported that Set1 is also required for the induction of middle meiotic gene expression (Sollier et al., 2004).

1-2-4-2. Histone H3K79 methylation

Histone H3K79 is methylated by Dot1 protein. Dot1 catalyzes mono-, di-, and tri-methylation of H3K79 (Sawada et al., 2004; Wysocki et al., 2005; Lazzaro et al., 2008). Similar to H3K4 methylation, mono-ubiquitylation of histone H2BK123 is also required for efficient histone H3K79 tri-methylation (Nislow et al., 1997; Krogan et al., 2003; Shilatifard, 2006). Histone H3K79 residue is located on the surface of the nucleosome, specifically on the top and bottom surfaces of the nucleosome disc, this unique position makes this residue accessible for the interaction with Dot1 in the context of chromatin but not when histone is free (Van Leeuwen et al., 2002). Work by Harrington and Andrews (1996) demonstrated that both Swi4 and Swi6 proteins are required for the histone H3K79 di-methylation but not for H3K79 tri-methylation. Both Swi4 and Swi6 are components of the SBF (SCB-binding Factor) complex that regulates the expression of several genes involved in cell cycle progression, linking the cell cycle progression to chromatin modification (Harrington and Andrews, 1996).

Histone H3K79 methylation is found to be important for the establishment of telomeric gene silencing. It is shown that the absence of either Dot1 or H3K79 methylation abolishes the silencing and reduces the association of Sir2 and Sir3 proteins to silent domains, suggesting an interaction between Dot1-mediated H3K79 methylation and Sir proteins (Van Leeuwen et al., 2002; Shilatifard, 2006).

H3K79 methylation is also found to have an important function during mitotic checkpoint activation by recruiting the Rad9 protein, which is facilitated by the interaction between the methylated H3K79 and the Rad9 Tudor domain. The interaction of Rad9 with the modification in turn leads to the activation of checkpoint kinase Rad53 after DNA damage in G1 cells (Lazzaro et al., 2008; Usui et al., 2009). Although this histone mark plays different roles during mitotic cell cycle, very little is known about the functions of the mark during meiotic cell cycle.

Dot1:

Dot1 protein, the histone H3K79 methyltransferse, was identified in a screen for high copy disruptors of telomeric silencing (Singer et al., 1998). Dot1 also showed a role in the silencing at *HML/HMR* and rDNA loci in the budding yeast. Dot1 protein contains a unique N-terminal helical domain with a high content of lysine residues and a conserved C-terminal domains consisting of seven-stranded β-sheet which harbors a binding site for the methyl-donor (SAM) and an active site pocket sided by conserved hydrophobic residues (Van Leeuwen et al., 2002; Sawada et al., 2004). In addition to the role of Dot1-dependent H3K79 methylation during mitotic cell cycle as described above, Dot1 was found to play different roles during meiosis. An early study by San-Segundo and Roeder (2000) found that Dot1 is required for meiotic prophase-I arrest or delay in *zip1* and *dmc1* mutants, and analyzed the localization of Dot1, which was

found to be enriched in the region of the nucleolus and also was observed on chromosomes.

Introduction figures:

Meiosis

Figure I:

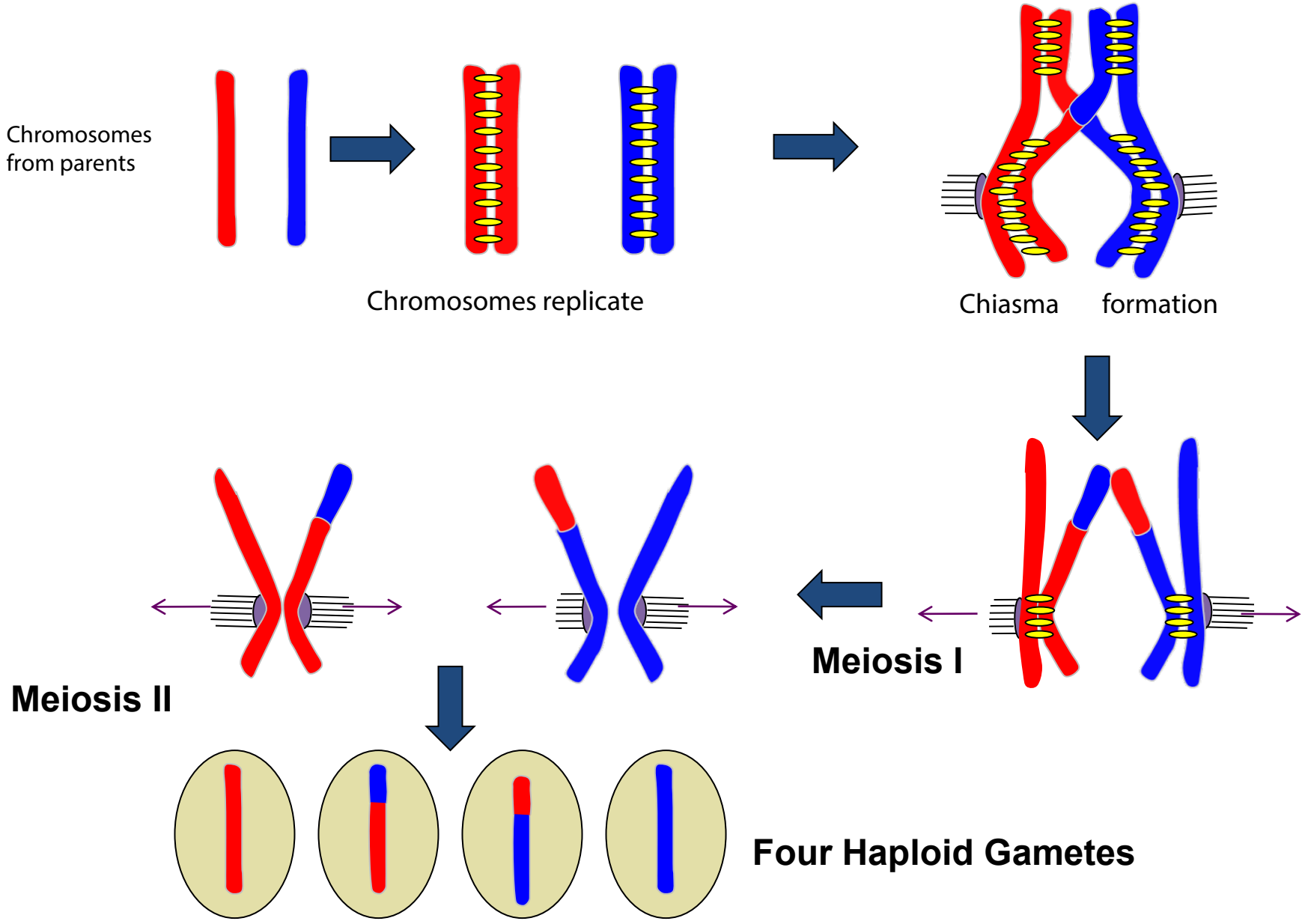

Meiotic recombination

Figure II:

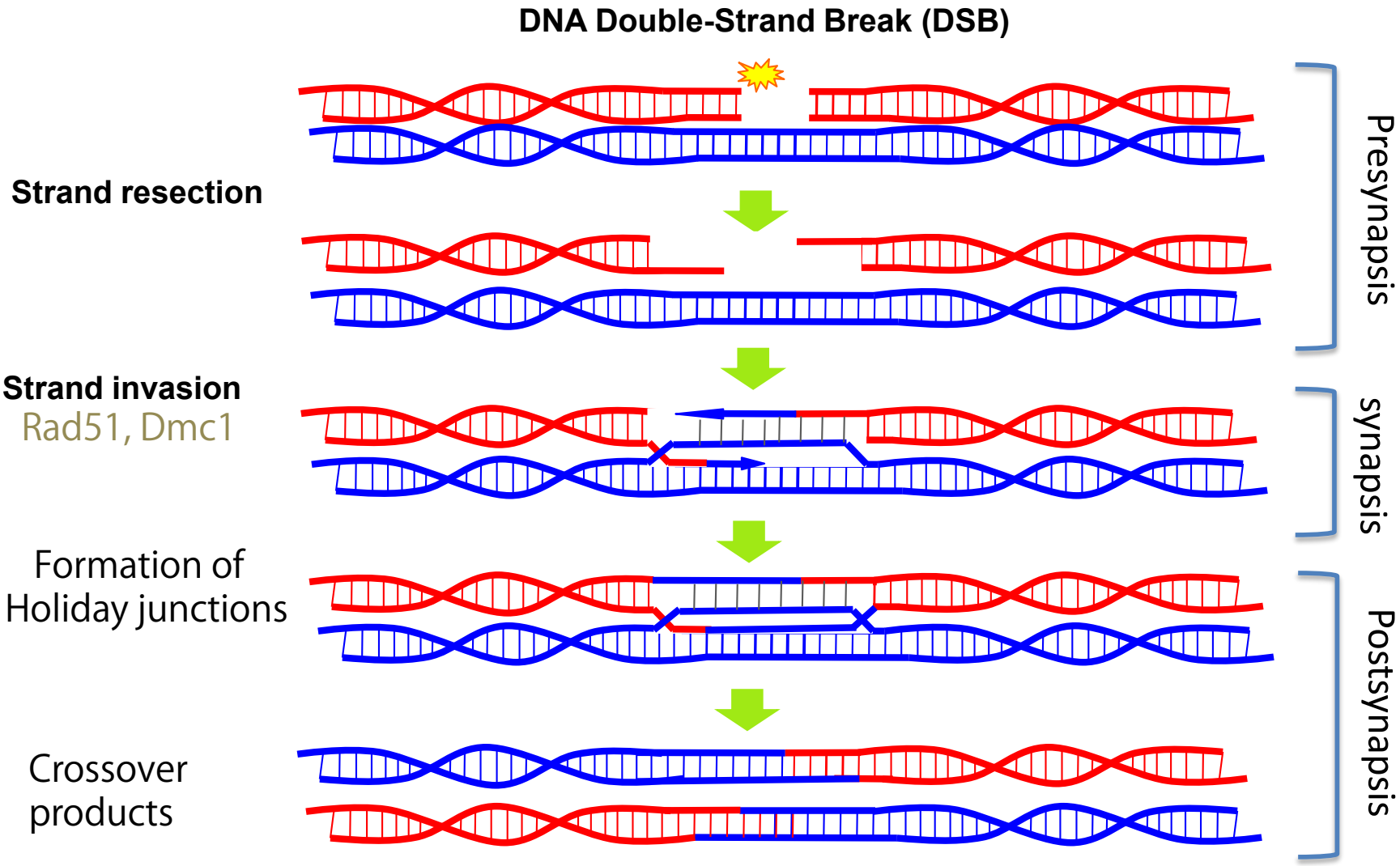

Synaptonemal complex

Figure III:

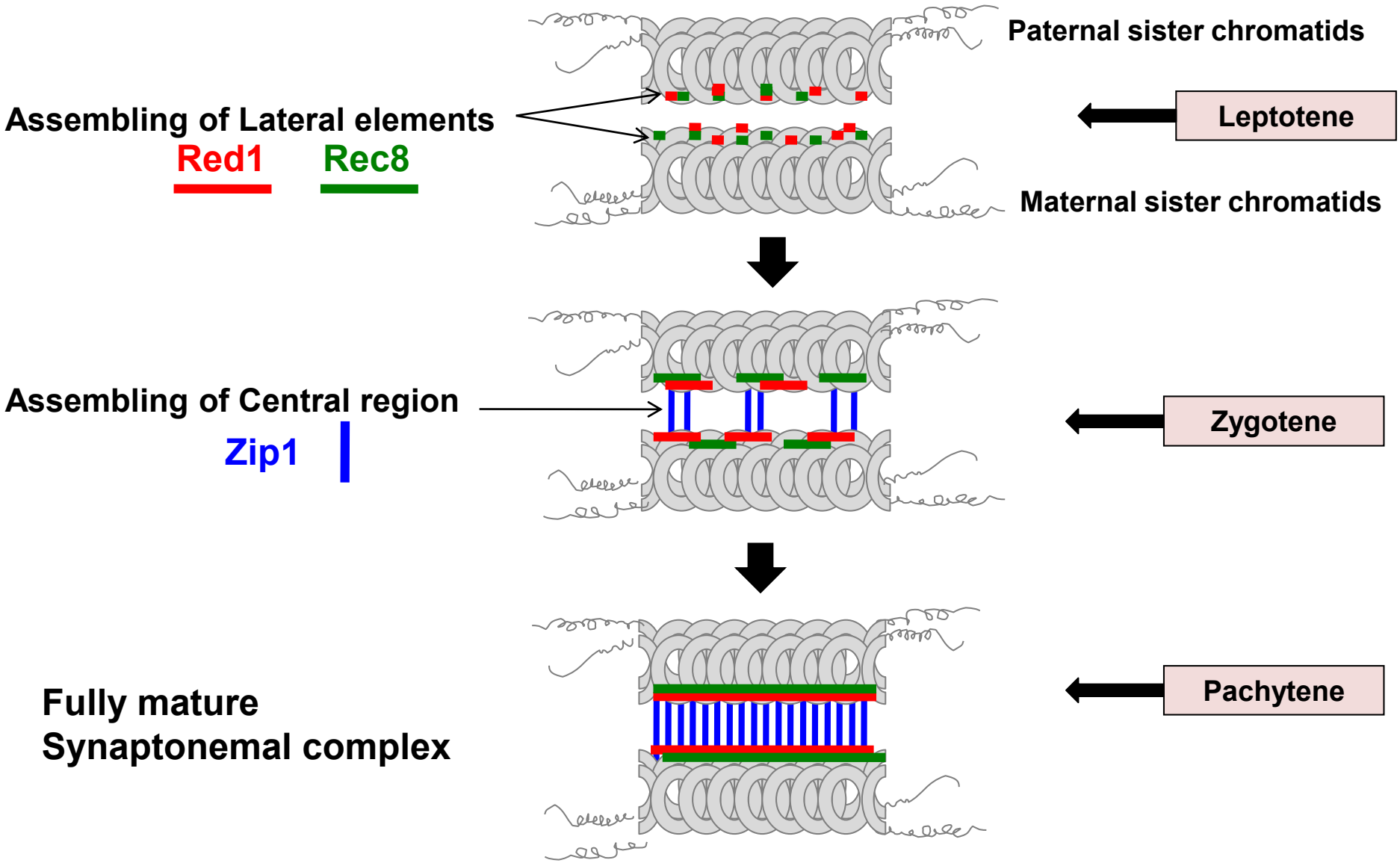

Figure IV:

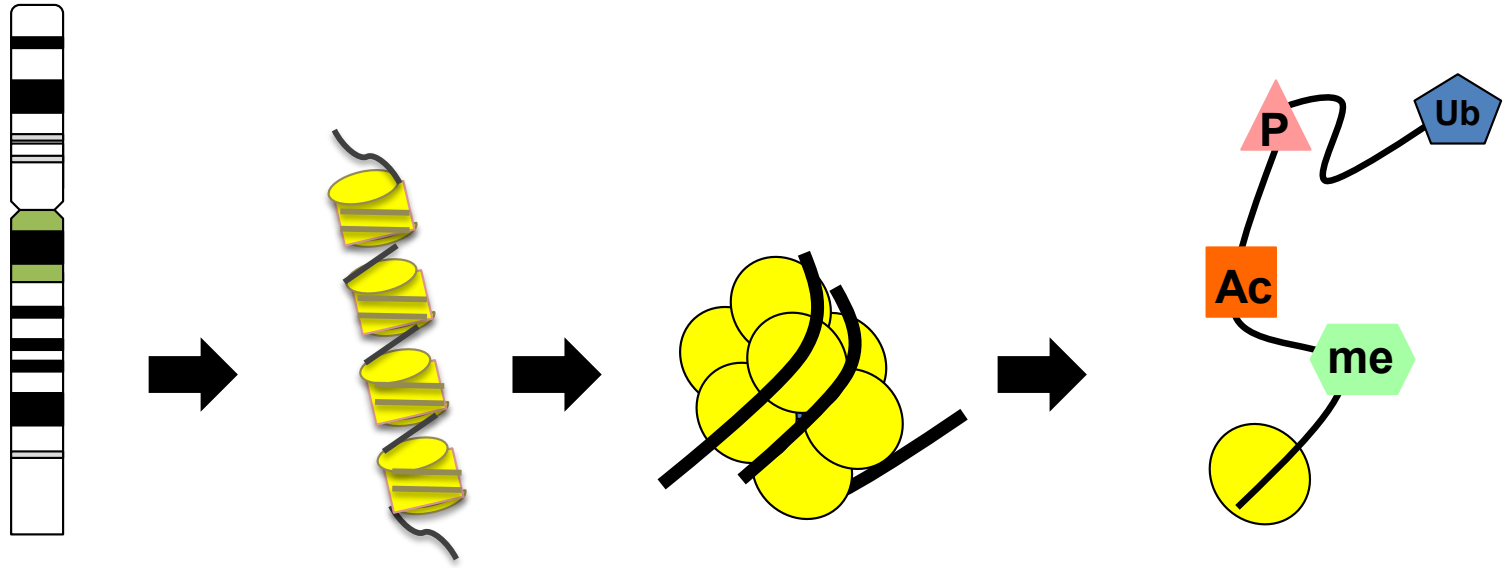
P
Ub
Ac
me
Chromosome
Chromatin
Nucleosome
Histone

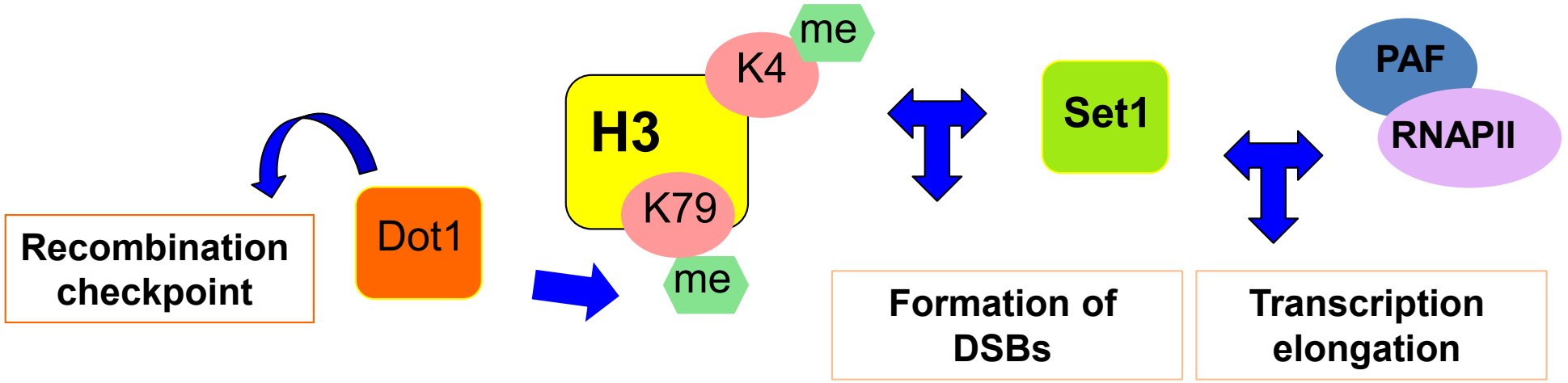
Recombination checkpoint
Dot1
me
K4
H3
K79
me
Set1
PAF
RNAPII
Formation of DSBs
Transcription elongation

Chapter 2: Materials and methods

2-1. Strains and plasmids

All strains used in this thesis were derived from the *S. cerevisiae* SK1 diploid strain NKY1551 (*MATa/MAT**a**, HO::LYS2/'', lys2/'', ura3/'', leu2::hisG/'', his4X-LEU2-URA3/his4B-LEU2, arg4-nsp/arg4-bgl*). The genotypes of strains used in this study are mentioned in Table 1. The *hht1-K79R hht2-K79R* strain was a generous gift from Dr. Takehiko Usui. The *hht1-K4R hht2-K4R* mutant was constructed by PCR-based mutagenesis. Briefly, wild type *HHT1* and *HHT2* genes were cloned into pBluescript II KS+ (Stratagene). PCR-based site-directed mutagenesis using mutant primers was carried out and the presence of the mutations was confirmed by DNA sequencing. The *hht1-K4R* and *hht2-K4R* mutant genes were cloned into YIP*lac*211 and pRS406, respectively. After digestion with *Kpn*I, the DNA was integrated by transformation for the selection of colonies with Ura+. The *URA3* gene was popped-out by counter-selection for the *ura*$^-$ phenotype on a 5-FOA (5-Fluroorotic Acid) plate. DNA sequencing using genomic DNA for candidates confirmed mutants. The primers used for strain construction are shown in Table 2.

2-2. Cytological analysis and antibodies

Immunostaining of chromosome spreads was performed as described below (Shinohara et al., 2000; Shinohara et al., 2003). Stained samples were observed using an epi-fluorescence microscope (BL51; Olympus) with a 100× objective (NA1.4). Images were captured by CCD camera (Cool Snap; Roper) and then processed using iVision software. For focus counting, about 100 nuclei were analyzed. Primary antibodies directed against Rad51 (guinea pig 1:500), Dmc1 (rabbit 1:500), Zip1

(rabbit 1:1000), Hop1 (guinea pig 1:500), Red1 (chicken 1:400), Rec8 (rabbit 1:1000) and Pch2 (rabbit 1:500) were used (Shinohara et al., 2008; Zhu et al., 2010). Fluorescent-labeled secondary antibodies (Alexa-fluor-594 and -488, Molecular Probes) directed against primary antibodies from the different species were used at a 1:2000 dilution. (Shinohara et al., 2008; Zhu et al., 2010). Antibodies against histone H3K4 tri-methylation and H3K79 tri-methylation were from Abcam (Cambridge, UK). Hop1 antibody was a gift from Dr. Miki Shinohara. Meiotic time course analysis for cytology was carried out 3 times and representative images are shown.

2-3. Western blotting

Western blotting analysis was performed according to standard procedure in Shinohara Lab., (Shinohara et. al., 2008). An aliquot of SPM culture was collected and cell precipitates were washed twice with 20% (w/v) trichloroacetic acid (TCA) and then cells were disrupted using a bead beater (Yasui Kikai Co. Ltd., Osaka, Japan). Precipitated proteins were recovered by centrifugation and then suspended in sodium dodecyl sulfate polyacrylamide gel electrophoresis (SDS-PAGE) sample buffer. After adjusting the pH to 8.8, samples were incubated at 95°C for 2 min. Following electrophoresis proteins were transferred from gel to Nylon membrane (Immobilon, MILLIPORE) with semi-dry transfer unit (ATTO TRANSWESTERN). Antibodies against Cdc5 (SantaCruz), Clb1 (SantaCruz), Hop1, Zip1, Rec8, and the **a-**subunit of rat tubulin (Serotec, UK) were used (Shinohara et al., 2008; Zhu et al., 2010). Antibodies against histone H3K4 tri-methylation and H3K79 tri-methylation were from Abcam (Cambridge, UK). Secondary antibodies conjugated Alkaline Phosphatase (Promega) were used at (1:7500) dilution. Proteins on the blots were detected by BCIP/NBT kit (Nacalai Tesque).

2-4. Preparation of *E. coli* plasmid DNA (Mini prep)

Preparation of *E. coli* plasmid was performed according to standard procedure in Shinohara Lab. *E. coli* single colony was inoculated into 1.5 – 2.0 ml LB liquid media containing ampicillin (50μg/ml) and incubated at 37°C over night. Next day, overnight culture was transferred into Eppendorf tubes, then centrifuged 10,000 rpm for 1min, and supernatants were removed completely using Pasteur pipette. Cells were suspended in 100 μl GTE buffer (50 mM Glucose, 25 mM Tris-HCL [pH 8.0], 10 mM EDTA) and vortexed until no pellet is observed. Followed by adding 200 μl Alkaline-SDS (0.2 N NaOH, 1% SDS) solution, and samples were inverted for five times, and then kept on ice for 5 min. 150 μl of 7.5 M Ammonium acetate was added and the samples were inverted again and kept on ice for at least 10 min, followed by centrifugation 15,000 rpm for 10 min at 4°C. Supernatants were transferred to new Eppendorf tubes containing 400 μl of 2-propanol, samples were inverted and centrifuged 15,000 rpm for 10 min at room temperature, washed with 70% (V/V) ethanol, and was followed by washing with 100 % (V/V) ethanol. The samples were dried for 10 min using centrifugal concentrator. 50-100 μl of 10:1 TE (10 mM Tris-HCL, 1mM EDTA) was added to dissolve DNA.

2-5. Yeast transformation (LiAc Method)

Yeast transformation was performed according to standard procedure in Shinohara Lab (Shinohara et. al., 2008). Yeast cells were inoculated into YPAD (1% Bacto Yeast Extract, 2% Bacto Peptone, 2% Glucose, 1% Adenine) liquid medium overnight. Overnight culture of yeast cells were diluted in 50-100 ml of YPAD (1/200 dilution) in 1L flask, and grown at 230 rpm at 30 °C using a shaker (Innova® 44) for 3

hours. Cells were centrifuged for 3 min at 3000 rpm using sterilized screw cap tubes, then washed twice in sterile distilled water, and centrifuged at 3000 rpm for 3 min. Cells were then suspended in 1ml of LiAc/TE (0.1M LiAc, 1X TE) and transferred to a new Eppendorf tube, and then centrifuged again at 5000 rpm for 1 min. Cells were suspended in 200 μl of LiAc/TE. 10 μl Carrier DNA (10mg/ml deoxyribonucleic Acid from salmon sperm, Wako Ltd) were added to the cells and mixed. 50 μl each of the cells were transferred to new Eppendorf tubes. Solution with Plasmid or DNA fragment (1-10μl) was added to each tube and mixed well. Followed by adding 350 μl of PEG/LiAc/TE (40% (w/v) PEG4000, 0.1M LiAc, 1x TE), cells were mixed well by inverting the tubes. The tubes were incubated with rotation at 30°C for 30 min. The cells were incubated at 42°C for 15 min using heat block or water bath. Cells were centrifuged at 5000 rpm for 1 min. Supernatants were removed by aspirator. Cells were suspended in 1 ml YPAD, incubated for 3-6 hours or overnight, and centrifuged at 1500 rpm for 2 min. The pellets were suspended in 100 μl of PBS (Phosphaste Buffered Saline) or TE and spread on selective medium plates.

2-6. Yeast Genomic DNA preparation

Genomic DNA was isolated according to standard procedure in Shinohara Lab. Briefly, yeast cells were inoculated into 2-3 ml YPAD liquid medium overnight. Cells were harvested in Eppendorf tubes. Pellets were suspended in 500 μl of Zymolase buffer (10mM NaPO4, 10mM EDTA, 0.1M β-Mercaptoethanol, 100μg/ml Zymolase 100T), vortexed for mixing, and then incubated at 37° for 30 min. Cells were lysed by adding 5 μl of ProtenaseK (10mg/ml) and 100 μl of Lysing buffer (0.25M EDTA, 0.5M Tris base, 2.5% (w/v) SDS), mixed well, and incubated at 65°C for 1 hour. During this incubation, tubes were mixed at least twice. 100 μl of 5 M Potassium

Acetate solution was added to the cell suspension, mixed well by shaking, and followed by incubating on ice for at least 15 min. Cells were centrifuged at 15000 rpm for 10 min. Supernatants were transferred to new Eppendorf tubes containing 500μl of cold 100% (V/V) EtOH (ethanol). Samples were inverted gently 5 times and centrifuged at 12000 rpm for 30 sec. Supernatants were removed and pellets were washed with 1ml of 70% (V/V) EtOH. Samples were dried for 10 min by centrifugal concentrator. DNAs were suspended with 500 μl of 1X TE, which was followed by RNaseA treatment with 10mg/ml RNaseA at room temp for 30 min. 500 μl of 2-propanol was added to samples and inverted gently for 5 times, and then centrifuged at 15000 rpm. Supernatants were removed, and pellets were washed with 70% (V/V) EtOH and were followed by washing with 100% (V/V) EtOH. Samples were dried up for 10 min, and DNAs were suspended with 100-200 μl of 1X TE buffer.

2-7. Meiosis Time course

Meiosis time course was performed according to standard procedure in Shinohara lab (Shinohara et al., 2008). Yeast cells was spread on the YPG (1% Bacto Yeast Extract, 2% Bacto Peptone, 2% Glycerol) plate from freezing stock (-80°C), incubated at 30°C for 12 hours, and then streaked on YPAD plates and incubated for further 2 days at 30°C for producing single colonies. A single diploid colony was inoculated in 3 ml of liquid YPAD medium and incubated overnight in rotator at 30°C. 1ml of the culture was added to 100 ml of SPS (0.5% Bacto Yeast Extract, 1% Bacto Peptone, 0.17% Yeast Nitrogen base, 1% Potassium acetate, 1% Potassium hydrogen phalate, 0.5% Ammonium sulfate) and incubated for 16-17 hours at 30°C with 230 rpm, shaker (Innova® 44). Next day, the SPS culture was centrifuged using a 50 ml screw cap tube and then pellets were washed twice with sterilized distilled water. Yeast cells were

suspended in SPM (0.3% Potassium acetate, 0.02% Raffinose) and incubated at 30°C at 230 rpm, and samples were collected at each time point.

2-8. Meiotic Nuclear Spreads: Lipsol Method

5 ml of SPM culture containing yeast cells was collected in a 15 ml conical screw cap tube, centrifuged, and pellets were resuspended in 1 ml of ZK buffer (25mM Tris-HCL [pH 7.5], 0.8M KCl). 20μl of 1M DTT (Dithiothreitol) was added and samples were incubated for 2 min at room temperature with gentle mixing. The samples were spun again and pellets were resuspended in fresh 1 ml of ZK buffer. 5μl of Zymolaze buffer (5mg/ml zymolase 100T, 2% glucose, 50mM Tris [pH7.5]) was added, and samples were incubated for 30 min in 30°C incubator with rotating. To check spheroplasting, water was added to an aliquot of sample on slide glass, and watched under light microscope in which cells shows bursting. After checking that more than 80% of cells became a spheroplast, samples were centrifuged and washed with 1ml MES/Sorbitol (0.1M MES [pH6.5], 1M sorbitol) using Pasteur pipette. The samples were centrifuged again, and pellets were resuspended in 1ml of MES/Sorbitol and kept at 4°C for usage of spreading later. For chromosome spreads, using micropipette, 20μl of above cell suspension was spotted on a clean glass slide (S2441 micro slide glass, Matsunami glass IND., LTD). To cell suspension, 40μl of PFA/sucrose (4% PFA (Paraformaldehyde [SIGMA-ALDRICH], 3.4% sucrose) was added and swirled briefly. Then, 80μl of 1% Lipsol was added and swirled again, cells were incubated for 20 sec and watched under light microscope until about 80-90% of cells were lysed. After confirming full lysis, 80μl of the PFA/sucrose was added to fix the cells. A glass pasture pipette was passed lengthwise along the top of the drop to spread

liquid all over entire surface of the slide. The slides were dried to a very thick honey from 4 hours to overnight and were stored in a plastic black microscope box at -20°C.

2-9. Immunostaining of Chromosomes Spreads

Immunostaining was performed according to standard procedure in Shinohara lab (Shinohara et al., 2008). Slides with chromosome spread prepared as described above were dipped in 0.2% photoflo (Photo-Flo 200 solution Kodak) for 2min using Coplin jar. The slides were air-dried for 5-10 min, and were blocked for 15 min using 0.5ml TBS/BSA (1x TBS [20mM Tris pH7.5, 0.15M NaCl], 1% BSA [albumin from bovine serum, SIGMA]). Then, the blocking buffer was drained onto a paper towel, and 90µl of TBS/BSA solution with primary antibody was added to slides, and covered with a cover slip and incubated overnight at 4°C or 2 hours at room temperature in a moist chamber. The cover slip was removed by submersion at 45° angle in the washing buffer (1x TBS). The slides were washed for 10 min 3 times in 1xTBS using Coplin jar.

90µl of TBS/BSA solution with secondary antibody solution (1/2000) dilution of fluorochrome-conjugated IgG in TBS/BSA was added to slides and incubated for 2 hours at room temperature in a dark moist chamber. The cover slip was removed and slides were washed as above, and then washed with water for 2 min. Once slides were completely dry, 15µl (three drops) of mounting medium (Vecta Shield with 0.2mg/ml DAPI) was added to slides and covered with coverslip, which was followed by sealing with nail polish and storing in a dark box. Stained samples were observed using an epi-fluorescence microscope as mentioned above.

2-10. Southern Blotting

Southern blotting was performed as described previously (Shinohara et al., 2003). Isolated DNA samples from SPM were digested with proper restriction enzyme, for the detection of DSBs or for CO/NCO. DNA was digested in 100μl of solution with *PstI* (20,000 U/ml) for DSBs, and was digested with *XhoI/MluI* (*XhoI* 4U/μl / *MluI* 20,000U/ml) for CO/NCO overnight at 37 °C. Next day, samples were subject to precipitation for DNA using Sodium acetate with 100% (V/V) EtOH, and pellets were suspended with 30μl of 1X TE buffer and kept for 4-5 hours to dissolve the DNAs. After DNA was completely dissolved, electrophoresis was performed using a 0.7% or 0.6 % of southern agarose gel (size 35cmx15cm) in 1X TAE buffer (Tris base, acetic acid, EDTA) with Voltage of 75 V overnight for the detection of DSBs, and Voltage of 50-65 V for 36~48 hours for the detection of CO/NCO. Once electrophoresis has finished, agarose gel was cut according to lab manual, treated by 0.25 M HCl with shaking for 20 min, followed by Alkali solution (0.6M NaCl, 0.2M NaOH) treatment for 15 min twice, and then gel was neutralized with 25mM Na-phosphate buffer [pH 6.5] with shaking for 40 min. The DNAs in the gel was transferred onto membrane (Hybond-N; GE Healthcare), by capillary transfer as described in lab manual for at least 12 hours. For crosslinking the DNA, membranes were irradiated using the UV crosslinker (Stratalinker® UV Crosslinker) and UV irradiated with 120 mJ/cm^2 (Autocrosslink Mode: 1200 microjoules (x 100)). Later, membranes were hybridized according to Shinohara lab protocol. Briefly, membrane was inserted in a hybridization bottle containing 25ml of hybridization buffer (7% SDS, 1M Na-Phosphate buffer, 0.5M EDTA), and incubated more than 30 min at 65°C. Meanwhile, 50ng of probe DNA was dissolved in 10.5μl of 1X TE buffer, 2.5μl of

primer DNA (Amersham Megaprime DNA labeling kit; GE healthcare) was added and sample was boiled at 95°C for 5 min, followed by adding 2.5µl of reaction mix, 2µl of dCTP, 2µl of dTTP, 2µl of dGTP and 2.5µl of α-^{32}P-dATP (37MBq), then 1µl of Klenow fragment was added to the mix and incubated for15 min at 37°C. The probe DNA solutions were then transferred to a G-50 spun column, and centrifuged in a new Eppendorf tube for 1 min at 4°C. After boiling at 95°C for 5 min and chilled on ice, probes DNAs were added to the bottle containing 25 ml of fresh hybridization buffer. The membrane was incubated at 65°C for more than 12 hours. Next day, the membranes were washed 3 times using washing buffer (0.1 % SDS, 1M Na-Phosphate buffer, 0.5M EDTA) at 65°C. Membranes were dried up and contacted with IP plate (BAS IP MAGAZINE 20x40, Fuix) for 5-8 hours. Followed by scanning the membrane using IP reader (BAS2000 II Fujix). Probes used for Southern blotting were "Probe 155" for CO/NCO, and "Probe 291" for DSBs detection (Storlazzi et al., 1995). Image Gauge software (Fujifilm Co. Ltd., Tokyo, Japan) was used to quantify the CO/NCO and DSBs bands.

2-11. FACS Analysis

1.5 ml of cell culture from SPM was harvested and centrifuged for 3 min at 3000 rpm, and then, pellets were resuspended with 1.0 ml of 70% (V/V) EtOH and kept in -20°C. Cells were centrifuged and washed with 1ml of buffer-A (0.2M Tris-HCl, 0.05M EDTA) and washing was repeated twice. Cells were resuspended with 0.5ml buffer-A and sonicated at 10% amplitude using a sonicator (Branson Digital sonifier). Followed by the addition of 0.2 mg/ml RNase-A, and incubation at 37°C for 4 hour, with mixing for several times. Cells were centrifuged and resuspended with 0.5ml of buffer-A containing 16 µg/ml of PI (Propidium Iodide) solution, samples were

incubated at room temperature for 30 min, then FACS (Fluorescence activated cell sorter) analysis was performed using (BD FACSCalibur™).

2-12. CHEF-Southern: Chromosome-wide meiotic DSB detection

Chromosome-wide meiotic DSB detection was performed as described previously **(**Murakami et al., 2011). Briefly, DNA Plugs were prepared using 1.8 % LMP (Low melting point) agarose mix, 125 mM EDTA [pH7.5]. Agarose gel was melted and incubated at 45~50°C until used. 15ml of meiotic culture was harvested and washed twice with 5ml of 50 mM EDTA [pH7.5]. Samples were centrifuged and pellets were resuspended with100 µl of 50 mM EDTA [pH7.5] and transferred to an Eppendorf tube. 100µl of cell suspension tube was incubated at 40°C for ~ 30 sec. 200 µl of pre-warmed 40°C LMP/Solution 1 (For 5 samples, 0.83 ml of 1.8 % LMP agarose mix and 0.17 ml Plug DNA solution 1 (Plug DNA solution 1, 0.17 ml/5 samples: 5 % β-mercaptethanol, 1.5 mg/ml Zymolyase 100T in SCE (1M sorbitol, 0.1M sodium citrate, 0.06M EDTA, [pH 7.0]). Tube was rotated until Zymolyase is dissolved and tube was placed on ice until use), mixed just before use and placed at 40°C. The LMP/Solution 1 was added to the cell suspension and vortexed well immediately. 90 µl of each of LMP/Solution 1/cells was transferred into plug mold and kept on bench until solidified. Samples blocks were pushed out of the plug mold and transferred to 15ml tube containing 3ml of Plug DNA solution 2 (7.5% β-mercaptoethanol, 450mM EDTA [pH 7.5], 10mM Tris-HCl [pH 7.5], 0.01mg/ml RNase-A). Samples were inverted gently and incubated at 37°C for one hour. Plug DNA solution 2 was removed carefully and replaced with 3 ml of Plug DNA solution 3 (1% SDS, 250mM EDTA [pH 7.5], 10mM Tris HCl [pH 7.5], 1mg/ml Proteinase K). Samples were inverted gently for several times and incubated at 50 °C for overnight. In the

following day, Plug DNA solution 3 was removed and replaced with 3 ml of 50 mM EDTA [pH7.5] plugs were incubated on rotator for 15 min (twice). 50 mM EDTA was removed carefully and replaced with 4 ml of Plug DNA storage solution (50% Glycerol, 50mM EDTA [pH 7.5]) and incubated on rotator for 20 min. DNA plugs were transferred to an Eppendorf tubes containing DNA storage solution and stored at (-20°C). 150ml of 1.3% LMP agarose gel was prepared in a gel mold (gel size 20 cm x 14 cm), and kept at 55°C for a few hours to equilibrate. DNA plugs were cut out one third and immersed in 1.5ml of the filter-sterilized 0.5X TBE in a 2 ml Eppendorf tube and rotated for 15 minutes. DNA plugs were taken out of the tubes and placed on the well in agarose and sealed with one drop of the 1.3 % agarose gel and kept for 5 min. Comb was inserted in the gel casting stand and gel was poured slowly and left to set for 30 min at room temperature. CHEF apparatus (CHEF- DR III system, BIO RAD) was assembled and the gel was equilibrated to the buffer for 15 minutes. Pulse field electrophoresis was started, 15.1s initial switch time; 25.1s final switch time; 120^{o} switch angle; 6V/cm; 46 h run time (14 cm W x 21 cm H), 30.5 h (21 cm W x 14 cm H); Pump speed 85. Once electrophoresis was finished the transfer to membrane (Hybond N+) was performed: briefly, the gel was stained for 30 min in 0.5µg/ml ethidium bromide, was rinsed in water for 5 min and then photographed. Gels were placed in the UV crosslinker (Stratalinker® UV Crosslinker) and UV irradiated with 180 mJ/cm^2 (Energy mode: 1800 microjoules x 100). The gel was equilibrated in 500 ml of PFGE transfer buffer (0.6 M NaCl, 0.4 N NaOH) for 20 min. Gels were transferred as described earlier, then membrane was hybridized according to Shinohara lab protocol using different probes as follows. For Chromosome III, *CHA1* probe was prepared using F-CHA1-IIIL probe: GTGGTTCCTACAGCGACAAAG and R-CHA1-IIIL probe:

CCAACGCTTCTTCCAAGTCC. For Chromosome V, *RMD6* probe was prepared using F-RMD6-VL probe: ATGTCAGCTTGCCCTTGCAACATCG and R- RMD6-VL probe: CTACAATCTATGATTTCCCAACTC.

2-13. Tetrad Dissections

In order to check the spore viability, haploids parental strains were patched together on YPAD for 4 hours at least and then spread on sporulation plates (0.3% Potassium acetate, 0.02% Raffinose) then incubated at 30˚C overnight, after which tetrads were dissected and viable spores were counted. For each strain, 100 tetrads were dissected on the dissection plate. Dissection was carried out using Zeiss Axioskop 40 microscope.

Chapter 3

Dot1-dependent histone H3k79 methylation is critical for DSB formation and also SC assembly in the absence of histone H3K4 methylation.

3-1. Results:

3-1-1. Set1 and Dot1 play differential roles during meiosis

Previous reports described the role of Set1-mediated histone H3K4 methylation in DSB formation and the role of Dot1-dependent histone H3K79 methylation in signaling for defective SC formation (San-Segundo and Roeder, 2000; Sollier et al., 2004). In order to understand in more details the role of these methyltransferases during meiosis, here I analyzed the meiotic phenotypes of the *set1* and *dot1* single mutants. I also constructed the *set1 dot1* double mutant in the SK1 background and characterized meiotic phenotypes of the double mutant together with single mutants. Since spore viability reflects the fidelity in meiotic cell cycle such as chromosome segregation, so I first analyzed the spore viability in these mutants compared to wild type, as shown in Fig. 1. Haploid parental (a and a) strains of wild type, *dot1*, *set1* and *set1 dot1* were patched together on YPAD plates for at least four hours, then on sporulation plates and then incubated at 30°C overnight, after which tetrads were dissected and viable spores which gave colonies on the plate were counted. As reported previously (San-Segundo and Roeder, 2000; Sollier et al., 2004), the *dot1* single mutant exhibits wild-type spore viability with 96.8% compared to 97.5% seen in wild type, suggesting an appropriate meiotic cell cycle division in the *dot1*. The *set1* single mutant showed a slight reduction to 86.8% relative to wild type.

Importantly, the double mutant, *set1 dot1*, showed synergistic reduction in spore viability to 46.5% compared to either single mutants (Fig. 1 A), indicating that Set1 and Dot1 work independently in meiosis and that both of them has a unique contribution to meiotic events. Then, I compared the distribution of viable spores per a tetrad and found that the double mutant is more biased towards 4-, 2-, and 0- viable spores rather than 3- and 1- viable spores (Fig. 1 B), suggesting non-disjunction of homologous chromosomes at MI in the double mutant, which is caused by a defect in meiotic prophase-I.

In order to characterize the role of Dot1 and Set1 during meiosis, and to investigate the effect of the absence of both histone methylation H3K4 and H3K79 on meiotic cell cycle progression, I carried out 4', 6-Diamidino-2-phenylindole (DAPI) staining. For meiotic time course analysis, cells were incubated in pre-sporulation medium (SPS) for 16-17 hours, transferred to sporulation medium (SPM), and samples were collected at the indicated times. Then, cells were fixed in 50% ethanol and stained with DAPI. Positive nuclei were counted for 1, 2, and 3/4 DAPI-staining bodies in a cell under epi-fluorescent microscope. DAPI staining showed that the *dot1* mutant exhibits a wild-type like entry into meiosis (Fig. 1 C). As reported previously (Sollier et al., 2004), the *set1* single mutant delays the entry of MI by 2 hours relative to wild type, which is probably caused by delay in the meiotic S-phase. The *set1 dot1* double mutant cells exhibit a 2.5 hours delay in entry into MI, which is slightly later than *set1* single mutant, suggesting differential roles of Set1 and Dot1 in the progression of meiosis I.

Later, I analyzed the pre-meiotic S-phase DNA replication in these strains by FACS analysis as described in Material and methods (Fig. 1D). As shown in Fig.1D, the *dot1* single mutant showed little delay in the progression of pre-meiotic S-phase

compared to wild type. On the other hand, both *set1* single mutant and *set1 dot1* double mutant cells showed 1-1.5 hour delay in the onset of pre-meiotic S-phase and also both mutants finish DNA replication with 1-1.5 hour delay compared to wild type cells.

Furthermore, I also analyzed the expression level of different proteins by western blotting, including some SC components, Rec8, Zip1 and Hop1 as well as the expression level of the Clb1 cyclin and the polo-like kinase Cdc5 (Fig. 1 E, F). The expression of both Clb1 and Cdc5 are required for exit from mid-pachytene and for the metaphase-anaphase transition. In wild type, expression of both Clb1 and Cdc5 was observed around 5 hours, consistent with the DAPI analysis described above. The expression of Zip1, Hop1, Rec8 and Red1 in the wild type started around 2 hours, and then modified forms of these proteins were observed at late times, as indicated by the existence of slowly-migrating multiple bands on western blots.

The *dot1* single mutant showed similar expression of Cdc5 and Clb1 around 5 hours compared to wild type. Also, Rec8, Hop1, Red1 and Zip1 expression pattern in the *dot1* mutant was almost similar to those in wild type. On the other hand, the *set1* single mutant and the *set1 dot1* double mutant showed a 3-hour delay in the appearance of Cdc5 and Clb1. Also these mutants showed 1-hour delay in the appearance of phosphorylated Hop1 around 4 hours compared to wild type where Hop1 phosphorylation was observed around 3 hours. Furthermore, the *set1* single mutant and the *set1 dot1* double mutant also showed a 3-hour delay in the disappearance of both Rec8 and Red1 compared to the wild type.

In order to know the role of Set1 and Dot1 during meiotic recombination, and to further study their histone H3-dependent methylation effects on DSB formation and

repair, I analyzed meiotic DSB formation and recombinant formation at a recombination hotspot, the *HIS4-LEU2* locus (Cao et al., 1990), (Fig. 2). Genomic DNAs from cells harvested at different times were analyzed for DSB or reciprocal recombinants as described in Material and Methods (Shinohara et al., 2003). Genomic DNAs was digested using *MluI* and *XhoI* for crossover/non-crossover (CO/NCO), or *PstI* for DSB detection as indicated in Fig. 2. A, and F. On DSB blots, full-length fragments, that do not contain meiotic DSBs, is indicated by "P" fragments. Meiotic DSB formation produces two shorter DNA fragments at the two major DSB sites in the *HIS4-LEU2* locus, as shown as DSB I and DSB II. In the wild-type cells, DSB started at 2 hours, peaked at 4 hours and then gradually disappeared. The *dot1* single mutant exhibits kinetics of DSB formation during meiosis that is almost the same as in the wild type. The DSB bands appeared smeared due to resection of the 5'-ends. As reported (Sollier et al., 2004), the *set1* single mutant showed a delay in DSB appearance by 2 hours compared to wild type, and peaks at 5 hours with reduced steady-state levels of DSBs at site I to 18% of the levels seen in the wild type, confirming a role of Set1 in efficient DSB formation. The *set1 dot1* double mutant showed similar kinetics seen in *set1* single mutant and a similar level of steady-state DSBs as seen in the *set1* single mutant, suggesting that Dot1 does not play a role in DSB formation at the *HIS4-LEU2* locus in the absence of Set1 (Fig. 2 B, D). Next, I examined the formation of CO and NCO, which can be distinguished using restriction site polymorphisms around DSB site I from parental DNA (Fig. 2 C, E). In the wild-type cells, formation of both CO and NCO started around 3 hours and gradually levels of CO/NCO were increased. In the *dot1* mutant the formation of both CO and NCO was delayed by 1 hour compared to wild type, but final CO and NCO levels in the *dot1* mutant are almost similar to those in the wild type. The *set1* single mutant

showed a delay in the formation of recombinants by 2 hours and also showed decreased level of COs to 35% and NCOs to 25% of levels in the wild type, supporting a role for Set1 in efficient meiotic recombinant formation. Furthermore, the levels of CO and NCO in the *set1 dot1* double mutant were comparable to those in *set1* single mutant. These results support a role of Set1 in efficient meiotic recombinant formation.

3-1-2. Dot1 plays a role in DSB formation in the absence of Set1

Homologous recombination is very important to ensure proper chromosome segregation during meiosis. In order to know whether the histone methylation by Set1 and Dot1 has any impact on DSB formation and meiotic recombination along the genome or not, I performed immunostaining analysis for the localization of Rad51 and Dmc1 to meiotic chromosomes. The cooperation of Dmc1 and Rad51 is essential for interhomolog recombination (Schwacha and Kleckner, 1997; Shinohara et al., 1997). As described above, Rad51, a RecA homolog, is involved in both meiotic and mitotic recombination (Shinohara et al., 2000). As shown previously (Bishop, 1994), Rad51 shows punctate staining on meiotic chromosomes that corresponds with sites of ongoing recombination (Miyazaki et al., 2004). As shown in Fig. 3 A, B, in wild-type cells, Rad51 appeared after 2 hours, peaked at 4 hours and gradually disassembled from chromosomes as DSB is repaired. The *dot1* single mutant showed little defects in Rad51 assembly, which started at the same time as wild type. Interestingly, the mutant showed faster dissociation of Rad51 from chromosomes compared to wild type. On the other hand, in *set1* single mutant, the appearance of Rad51 foci delayed by 2 hours compared to wild type, consistent with the delay of the onset of the pre-meiotic S phase. Compared to that in wild type, percentages of Rad51

focus-positive nuclei in the mutant were dramatically reduced at 3 hours. The *set1* mutant showed delay in the dissociation of Rad51 foci from chromosomes. Importantly, in the *set1 dot1* double mutant, Rad51 focus formation is delayed for 1 hour compared to *set1* single mutant, peaked at 5 hours, and Rad51 gradually dissociated from chromosomes slower than the *set1* single mutant, suggesting a role for Dot1 in meiotic DSB repair in the absence of Set1.

During the analysis on Rad51 staining, I noticed that the *set1 dot1* double mutant showed less number of Rad51 foci on chromosome spreads. So, in order to confirm this observation, I counted Rad51 focus number on chromosomes on each spread. As shown in Fig. 3 C, blue numbers indicates an average of Rad51 foci per a nucleus. The average numbers of Rad51 foci per focus-positive cell represent the steady-state numbers of DSBs in a cell. In wild type and *dot1* single mutant, an average of Rad51 foci at 4 hours is 36±10 (n = 78) and 32±12 (n = 89), respectively. The *set1* showed reduction in Rad51 foci number compared to *dot1* single mutant and wild type with an average number of 21±8.8 (n = 79) at 6 hours. Importantly, *set1 dot1* cells showed more reduction in Rad51 focus number compared to *set1* single with an average number of 17±6.6 (n = 116) at 6 hours. Moreover, mutations in the *SET1* and/or *DOT1* genes show similar effects on the kinetics analysis of Dmc1 as those seen for Rad51 foci (Fig. 3 A, B). These results suggest that Dot1 plays a role in DSB formation in the absence of Set1.

To further confirm the reduction of DSB formation seen in *set1* single mutant and *set1 dot1* double mutant, I constructed the *set1 dmc1* and the *set1 dot1 dmc1* for further analysis. The *dmc1* mutant, which is defective in the repair of DSBs with accumulates the Rad51 foci (Bishop et al., 1992), which enables me to measure levels of DSBs in the mutants precisely. Strains were confirmed for selective markers and

by PCR. As described above, I counted a number of Rad51 foci in the *dmc1* background, as described in Fig. 4. First, I checked meiotic progression in these stains compared to wild type (Fig. 4, A). As reported by San-Segundo and Roeder (2000), the *dot1* mutation partially suppresses *dmc1*-induced cell cycle arrest. Importantly, in the *dmc1 set1 dot1* triple mutant, *dmc1* arrest was alleviated to a greater extent than does the *dmc1 dot1* double mutant alone. As expected, all strains with the *dmc1* mutation accumulate Rad51-focus-positive cells (Fig. 4, B, C). Next, I counted Rad51 focus number in all strains, as shown in Fig. 4, D. The average number of foci in the *dmc1* and *dmc1 dot1* mutants at 3 hours are 41±13 (n = 41) and 42±17 (n = 30), respectively. The *dmc1 set1* mutant showed a reduced number of foci with 34±12 (n = 42) at 5 hours relative to wild type. This suggests a role of Set1 in DSB formation. Importantly, the *dmc1 set1 dot1* triple mutant showed a decreased number of foci to 19±6.9 (n = 52) at 4 hours, which is lower than that in the *dmc1 set1* double mutant. This result confirms a role of Dot1 in DSB formation in the absence of Set1.

To further confirm the role of Dot1 in DSB formation in the absence of Set1, I analyzed the efficiency of DSB formation along the whole chromosome, as described in Fig. 5. Chromosomal-length DNAs were prepared after immobilizing cells in agarose plugs as described in Material and methods. Chromosomes were fractionated using a CHEF-DRIII pulsed field gel electrophoresis system (BioRad). After the transfer to nylon membrane under denaturing conditions, genomic DNAs were hybridized with the DNA probe specifically recognizing a specific location on ends of chromosomes III or IV. As shown in Fig. 5 A, the *dmc1 set1 dot1* triple mutant showed more reduction in overall DSB formation compared to *dmc1 set1* double mutant. I also quantified the DSB levels in these mutants (Fig. 5 B) in which values plotted with standard deviation bars are the mean of three independent experiments.

The *dmc1 set1 dot1* triple mutant showed a big reduction in DSB formation in region I, region II and region IV compared to *dmc1 set1* double mutant. The *dmc1 set1* double mutant not only reduced DSB formation at some regions, but also increased DSB formation at several regions. On the other hand, other regions showed a slight reduction in DSB formation, which may indicate a reduction in DSB formation in a locus-dependent manner. I also checked the DSB formation on chromosome IV, which is the longest chromosome in yeast, as shown in Fig. 5 E, F. I could observe a reduction in DSB formation in the *dmc1 set1 dot1* triple mutant compared to *dmc1 set1* double mutant as indicated in quantification results in Fig. 5 E, where most regions on chromosome IV showed a significant reduction in DSB formation in the *dmc1 set1 dot1* triple mutant compared to *dmc1 set1* double mutant.

The levels of DSB in the *set1 dot1* double mutant at the *HIS4-LEU2* locus were comparable to these in *set1* single mutant. In order to confirm the locus-dependent manner effect of Dot1, I analyzed DSB formation on the *YCR048W* locus on chromosome III as described in Fig. 5 C, D. As shown in the quantification on results of two independent experiments, the *dmc1 set1 dot1* triple mutant showed clear reduction in DSB formation compared to *dmc1 set1* double mutant at this locus. All these results described here confirm an important role of Dot1 in DSB formation in the absence of Set1.

3-1-3. Set1 and Dot1 play a role in chromosome morphogenesis

Previously, the role of two histone H3 methyltransferases Dot1 and Set1 in chromosome morphogenesis had not been described carefully. Based on the fact that the absence of Set1 showed reduction in DSB formation, and since cell cycle events are connected to each other and earlier events may affect later events, I thought that

this reduction in DSB formation, which may be caused directly by absence of Set1-dependent histone H3 methylation, might affect chromosome morphogenesis and dynamics during meiosis. So I analyzed the SC formation by immunostaining for Zip1, which is a component of the central region of the SC (Sym et al., 1993), (Fig. 6). Meiotic nuclear spreads were stained with anti-Zip1 antibody as described in the Materials and methods. Zip1 staining was classified into three classes: dots, partial lines and full lines, which may correspond to the leptotene, zygotene and pachytene stages, respectively (Fig. 6 A, B). Immunostaining results revealed exclusive contributions of Set1 and Dot1 to SC formation. In wild-type cells, dotty Zip1 localization was observed around 2 hours, followed by the formation of short lines of Zip1 and then the assembly of Zip1 along the entire length of SCs around 4 hours. At later time points, Zip1 started to disassemble gradually from chromosomes and almost disappeared form chromosomes by 8 hours. The *dot1* single mutant showed almost wild-type kinetics for Zip1 assembly and disassembly, except that dotty staining of Zip1 appeared earlier in the *dot1* cells relative to wild type (Fig. 6 B). The *set1* single mutant showed clear defects in SC assembly (Fig. 6 A, B). The appearance of Zip1 dotty staining is delayed by 1 hour, probably due to a delay in the S-phase. Moreover, the elongation of Zip1 is partially impaired in *set1* single mutant, as indicated by the reduced frequencies of full lengths of SCs. Furthermore, the SC disassembly occurred 1 hour later than wild type. Consistent with the defect in SC assembly in the *set1* single mutant, the mutant accumulates an aggregate of Zip1 referred as to polycomplex which is rarely seen in wild-type cells (Fig. 6 A, B). The *set1 dot1* double mutant showed more defects in Zip1 elongation and greater delay in the Zip1 disassembly than did the *set1* single mutant. In the *set1 dot1* double mutant, only dotty staining of Zip1 is predominantly seen with a high fraction of Zip1

polycomplex, indicating a severe defect in SC elongation in the mutant. These results suggest an important role of Dot1 in SC formation in the absence of Set1.

In order to analyze the SC defects seen in the *set1* mutant in more details, I also analyzed the association of Hop1 to chromosomes. As mentioned earlier, Hop1 is a component of the chromosome axis and is required for SC formation as well as meiotic recombination (Holligsworth et al., 1990). As shown in Fig. 6 A, C, in wild-type cells, Hop1 showed punctate staining in early MI, and disassembled from chromosomes by late prophase. Hop1 staining in the *dot1* single mutant was similar to that seen in wild type, although, as seen for Zip1, Hop1 loading occurs slightly earlier in the *dot1* compared to wild type. Importantly, the *set1* single mutant showed 1-hour delay in the assembly of Hop1 foci compared to the wild type, and 3 hours delay in the disassembly from chromosomes. Furthermore, *set1* cells showed elongated lines of Hop1, which are rarely seen in the wild type (Fig. 6 A, D). In some *set1* cells, two lines of Hop1 are aligned side-by-side, suggesting that homologous chromosomes pairing takes place at a significant level, but full synapsis is impaired in the *set1* single mutant. The *set1 dot1* double mutant showed very similar patterns of Hop1 staining compared to the *set1* single, but with greater fractions of cells with long Hop1 lines and delayed disappearance of Hop1 from chromosomes relative to the *set1* single mutant. This is consistent with the role of Dot1 in the SC formation in the absence of Set1 (Fig. 6 A, C, D). Double staining of Zip1 and Hop1 in the wild-type cells clearly showed that Zip1 signal is lost from Hop1 enriched regions (Borner et al., 2008) (Fig. 6 A). The accumulation of long lines of Hop1 along the chromosomes in the *set1* mutant is possibly consistent with the fact that Set1 is required for Zip1 elongation.

To further confirm the role of Set1 in SC formation, I also analyzed the localization of another chromosome axis protein, Red1 (Rockmill and Roeder, 1988) as well as the localization of the meiosis-specific Kleisin, Rec8 (Klein et al., 1999). Red1 works together with Mek1/Mre4 as well as Hop1 in both meiotic recombination and chromosome morphogenesis (Hollingsworth and Ponte, 1997). As shown in Fig. 7 A, B, both Rec8 and Red1 initially appeared as dotty staining like Hop1, but later, unlike Hop1, both Rec8 and Red1 form discontinuous lines as the SC elongates (Smith and Roeder, 1997). As shown in Fig. 7, wild type and *dot1* single mutant showed beads-in-line staining for both Rec8 and Red1, indicating a normal assembly of lateral elements. Furthermore, the *set1* and *set1 dot1* double mutant showed some defects in the SC formation, as indicated by the delay in the assembly and disassembly of both Red1 and Rec8. There is also little thick staining of chromosomes in these mutants compared to thick chromosome staining in wild type and *dot1* single mutant. The *set1* single mutant and *set1 dot1* double mutant tend to form thin lines of Red1/Rec8 staining compared to the thick lines seen in the wild type and *dot1* single mutant, consistent with the lack of closely juxtaposed chromosome axes in the mutants. Interestingly, *set1* single mutant and *set1 dot1* double mutant do accumulate aggregates of Red1 and Rec8, which are rarely seen in the wild type, and also not formed in other SC-deficient mutants such as the *dmc1* mutant (Fig. 7 C). At 6 hours, about 35% of *set1* single mutant cells contain Red1 and Rec8 aggregates while 55% at 5 hour in the *set1 dot1* double mutant did contain the aggregates. In the Red1-Rec8 aggregates (polycomplex-like structure), Red1 shows bipolar staining on large Rec8-block (Fig. 7 A, C). These results indicate that Set1 plays critical role in SC elongation and that Dot1 is important for SC formation only

in the absence of Set1. Set1 might play a specialized role in the organization of the chromosome axis containing Red1 and Rec8 for synapsis.

3-1-4. Dot1 is required for proper Pch2 localization in the absence of Set1

As shown in Fig. 6, both *set1* single mutant and *set1 dot1* double mutant showed accumulation of Hop1 along chromosomes. A previous report by Borner et al. (2008) demonstrated that the absence of Pch2 exhibits delayed unloading of Hop1 from chromosomes, shown by continuous and uniform lines of Hop1 staining. Moreover, they showed a differential Hop1/Zip1 hyper-abundance seen along wild-type pachytene chromosomes, which is regulated by Pch2. These suggest that Pch2 is required for timely release of Hop1 from chromosomes. So, I analyzed the localization of Pch2 in different strains as shown in Fig. 8. Pch2 localization in wild type started around 2 hours after the induction of meiosis, peaked at 3 hours, and gradually disassembled from chromosomes (Fig. 8 A). The *dot1* single mutant showed similar kinetics of Pch2-loading compared to wild-type cells. In wild type and *dot1* single mutant, Pch2 was observed as aggregates at the nucleolus, indicated by the white arrow, and also as short stretches on chromosomes (Fig. 8 B), consistent with the previous study (Borner et al., 2008). On the other hand, both *set1* single mutant and *set1 dot1* double mutant showed similar kinetics where Pch2 localization started at 3 hours, peaked at 6 hours, and disappeared by 12 hours, to wild type (Fig. 8 A). Moreover, in *set1* single mutant and *set1 dot1* double mutant, I could clearly notice the formation of Pch2 polycomplex as indicated by a yellow arrow in Fig. 8 B, which is completely different from the nucleolus localization of Pch2 seen in wild type and *dot1* single mutant. In the *set1 dot1* double mutant, Pch2 localization was

observed as dotty staining at chromosomes compared to *set1* single mutant where Pch2 chromosomal localization showed a kind of short stretches similar to wild type, suggesting a defect in Pch2 localization in the *set1 dot1* double mutant. Double immunostaining of Zip1 and Pch2 in *set1* single mutant and *set1 dot1* double mutant showed that Pch2 polycomplex co-localizes with Zip1 polycomplex, as shown in Fig. 8 D, with a higher fraction of Pch2/Zip1 polycomplex seen in the *set1 dot1* double mutant than the *set1,* (Fig. 8 C). These results may suggest that Dot1 plays an important role in proper Pch2 localization in the absence of Set1.

3-1-5. The histone H3K4 mutant is defective is SC formation

So far I showed by cytological analysis that the absence of histone methylation by Set1 and Dot1 induced a clear defect in the SC formation, suggesting a redundant role of both Set1 and Dot1 in SC assembly with Set1 playing a major role in SC elongation. I also found the role of Set1 in the normal assembly of axial and lateral elements. To confirm the role of Set1 in meiotic chromosome metabolism through the epigenetic mark catalyzed by Set1, I constructed the histone H3K4 point mutant, *hht1-K4R hht-2K4R* (hereafter, *hht1-2-K4R*). The budding yeast has two histone H3 identical copies, *HHT1* on chromosome II and *HHT2* on chromosome XIV. Here, I mutated the two copies by sequential PCRs as described in Material and methods. First, I confirmed the absence of H3K4 tri-methylation by western blotting, where *hht1-2-K4R* double mutant showed complete loss of H3K4 tri-methylation during meiosis compared to wild type (Fig. 9 A). Then, I checked spore viability of the mutant (Fig. 9 B) and found that the *hht-1-2-K4R* double mutant showed wild-type spore viability with no clear defect in sporulation. To check the meiotic progression, I also performed DAPI staining as described above. The *hht1-2-K4R* double mutant

showed a greater delay (2 hours) in the entry into meiosis I than does the *set1* single mutant (Fig. 9 C). Except for this delay, the *hht1-2-K4R* double mutant nearly recapitulates the meiotic phenotype of the *set1* single mutant. The *hht1-2-K4R* double mutant showed reduced DSB levels as indicated by immunostaining of Rad51 and Dmc1 in Fig. 9 D, E. Rad51 staining showed a big delay in the Rad51 localization on chromosomes as described in Fig. 9 E, and also that a steady-state number of Rad51foci in the *hht1-2-K4R* double mutant is, on average, 26±6.8 (n = 143) at 6 hours (Fig. 9 F), confirming the role of histone H3K4 methylation in DSB formation (Borde et al., 2009). The *hht1-2-K4R* double mutant also showed a defect in the SC assembly, as indicated by Zip1 and Hop1 double immunostaining (Fig. 9 G, H). The *hht1-2-K4R* double mutant showed delay in the assembly of Zip1 protein to chromosomes. Moreover, as seen in *set1* single mutant, in the *hht-1-2-K4R* double mutant, the elongation of Zip1 is partially impaired, as indicated by the reduced frequencies of full lengths of Zip1 staining and a high fraction of Zip1 polycomplex. In the *hht1-2-K4R* double mutant, Hop1 staining pattern was similar to that in the *set1* single mutant. I could clearly observe the accumulation of Hop1 on chromosomes, forming long lines as seen in the *set1* single mutant.

Later, I constructed the *dot1 hht1-2-K4R* triple mutant to confirm my previous results, regarding the role of Dot1 in the DSB formation and SC assembly in the absence of Set1-dependent H3K4 methylation. I first checked spore viability as shown in Fig. 9 B, and importantly the *dot1 hht1-2-K4R* triple mutant showed a big reduction in spore viability with 63.5% compared to the wild type. I also checked meiotic progression in this mutant, which showed a delay in the entry into MI, as seen in the *set1 dot1* double mutant (Fig. 9 C). Then, I analyzed the DSB formation by immunostaining for Rad51 and Dmc1 as shown in Fig. 9 D, E. The *dot1 hht1-2-K4R*

triple mutant showed a big reduction in Rad51-focus number with an average of 17±5.6 (n = 140) at 6 hours compared to the *hht1-2-K4R* double mutant (Fig. 9 F). Also the *dot1 hht1-2-K4R* triple mutant showed more defects in the SC formation compared to the *hht1-2-K4R* double mutant as described in Fig. 9 G, H. Immunostaining of Zip1 and Hop1 showed that the *dot1 hht1-2-K4R* triple mutant failed to form mature SCs, only with dotty staining of Zip1 and a high fraction of polycomplex as seen in this mutant. Furthermore, the accumulation of Hop1 between the homologous chromosomes is observed in this mutant. These results described here clearly suggest a role for Set1 in the DSB formation as well as SC formation through the methylation of histone H3K4. Furthermore, these results support the idea described above that the Dot1 plays a role in DSB formation as well as SC assembly in the absence of Set1-dependent H3K4 methylation.

3-1-6. Histone H3K79 methylation is critical for DSB formation as well as the synaptonemal complex assembly

In order to know the involvement of histone H3K79 methylation in DSB formation, I also used a strain with histone H3K79 mutations (*hht1-K79R, hht2-K79R*, hereafter *hht1-2-K79R*). The absence of histone H3K79 tri-methylation was confirmed by western blotting using an anti-histone H3K79 tri-methylation antibody (Fig. 10 A). Then, I checked the meiotic progression and found that the meiotic progression of the mutant was similar to wild type with no clear defect (Fig. 10 B). I also found the spore viability in the *hht1-2-K79R* double mutant with wild type spore viability of 96.5 %, indicating that this methylation mark is not required for spore formation (Fig. 10 C). Later, I constructed the *set1 hht1-2-K79R* triple mutant and, importantly, this mutant showed a defect in meiotic progression (Fig. 10 B). Spore viability in the *set1*

hht1-2-K79R triple mutant was reduced to 47.8 % compared to wild type, similar to the reduction in spore viability as seen in *set1 dot1* double mutant in Fig. 1. I also found that the *set1 hht-2-K79R* triple mutant is defective in DSB formation, as shown by immunostaining for Rad51 and Dmc1 (Fig. 10 D). This mutant showed a decreased number of Rad51 foci with an average of 12±3.5 (n = 62). Furthermore, the *set1 hht1-2-K79R* triple mutant showed defect in the SC formation as observed from Zip1 staining (Fig. 10 E). I found that the *set1 hht1-2-K79R* triple mutant recapitulates the meiotic phenotypes of the *set1 dot1* double mutant. This result supports the idea that Dot1-dependent histone H3K79 methylation promotes meiotic DSB formation and also required for normal SC formation in the absence of Set1.

3-1-7. Rad9 might have a meiotic function in the absence of Set1

Results described above in this thesis suggest an important role of Dot1-dependent histone H3K79 methylation in DSB formation in the absence of Set1. Previous reports demonstrated that, the histone H3K79 methylation is recognized by the Tudor domain of Rad9 protein in yeast (Grenon et al., 2007; Lydal et al., 1996). According to Lydal et al. (1996), Rad9 is not critical for meiotic checkpoint activation, which makes it arguable that Rad9 plays a role during meiotic cell cycle or even contributes to DSB formation. Since Dot1 plays a role in DSB formation only in the absence of Set1, this encouraged me to explore the possibility that Rad9 might play a role in DSB formation in the absence of Set1. So here, I characterized the meiotic phenotypes of the *set1* and *rad9* single mutants, and I also constructed and characterized the *set1 rad9* double mutant in the SK1 background. As usual, I first analyzed the spore viability in the *set1 rad9* double mutant as shown in Fig. 11 A. As reported previously by Weber and Byers (1992), the *rad9* single mutant exhibits wild-type spore viability

with 98%. Importantly, the *set1 rad9* double mutant showed slight reduction in spore viability with 80.5% compared to *set1* single mutant with 86.8%, indicating that Rad9 might contribute to meiotic events only in the absence of Set1. In order to characterize the role of Rad9 during meiosis, I performed DAPI staining as described above. DAPI staining revealed that, the *rad9* single mutant showed no clear delay in the entry into MI compared to wild type (Fig. 11 B). As shown in Fig. 1, the *set1* single mutant delayed the entry of MI by 2 hours relative to wild type. The *set1 rad9* double mutant cells exhibit a 4 hours delay in entry into MI, which is later than *set1* single mutant, suggesting differential roles of Set1 and Rad9 in the progression of meiosis.

In order to address whether Rad9 has any impact on DSB formation and meiotic recombination in the absence of Set1 or not, I carried out immunostaining analysis for the association of Rad51 to chromosomes. Rad51 staining showed a big delay in the Rad51 localization on chromosomes in the *set1 rad9* double mutant compared to *set1* single mutant, consistent with the delay in the meiotic cell cycle seen in the mutant (Fig. 12 A). The Rad51 focus numbers were comparable in both *set1* single mutant and *set1 rad9* double mutant. Rad51foci number in the *set1 rad9* double mutant is, on average, 24±6.8 (n = 58) at 8 hours compared to an average of 24±10.3 (n = 49) at 8 hours in *set1* single mutant, indicating that Rad9 does not contribute to DSB formation in the absence of Set1. Based on the fact that the *set1 rad9* double mutant showed a big delay in meiotic progression compared to *set1* single mutant, and since cell cycle events are connected to each other and earlier events may affect later events, I thought that this meiotic delay might affect chromosome morphogenesis and dynamics during meiosis. So I analyzed the SC formation by immunostaining for Zip1, (Fig. 13 A, B). The *set1* single mutant showed clear defects in SC assembly as mentioned above. The *set1 rad9* double mutant

showed similar immunostaining of Zip1 as seen in *set1* single mutant. In the *set1 rad9,* the appearance of Zip1 dotty staining is delayed by 1 hour compared to *set1* single mutant. Moreover, the elongation of Zip1 is partially impaired in both *set1* single mutant and *set1 rad9* double mutant. As indicated by the reduced frequencies of full-length SCs. Consistent with the defect in SC assembly in the *set1* single mutant and *set1 rad9* double mutant, both *set1* single mutant and *set1 rad9* double mutant accumulate Zip1 polycomplex. Since the absence of Rad9 did not show any additive defect in the assembly of the SC in the absence of Set1, these results suggest that Rad9 does not contribute to the SC formation in the absence of set1.

Figure 1

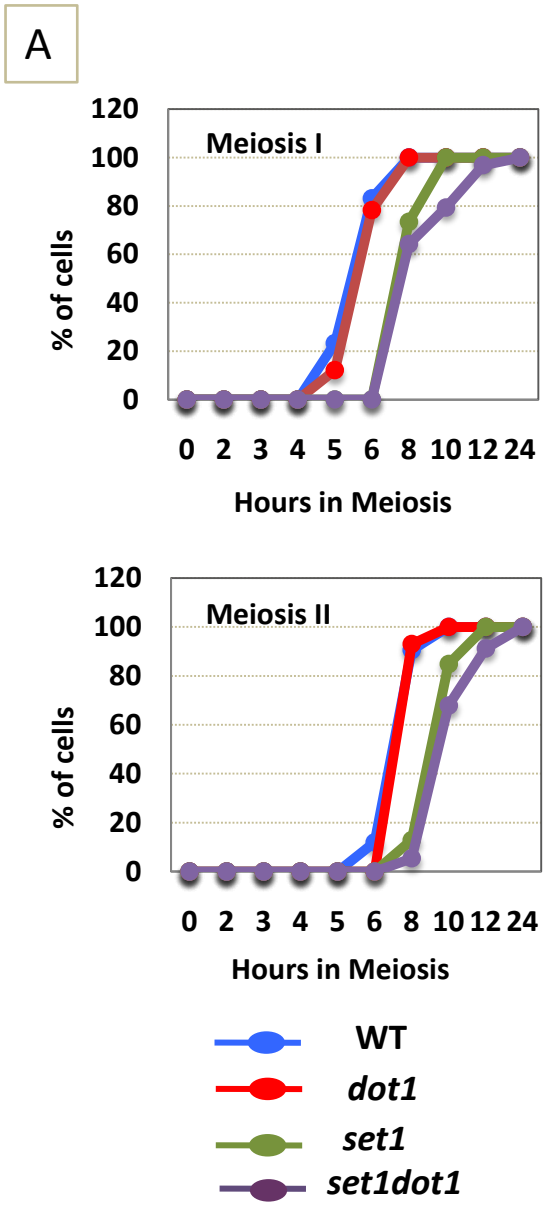
A
Meiosis I
% of cells
120
100
80
60
40
20
0
0 2 3 4 5 6 8 10 12 24
Hours in Meiosis
Meiosis II
% of cells
120
100
80
60
40
20
0
0 2 3 4 5 6 8 10 12 24
Hours in Meiosis
WT
dot1
set1
set1dot1

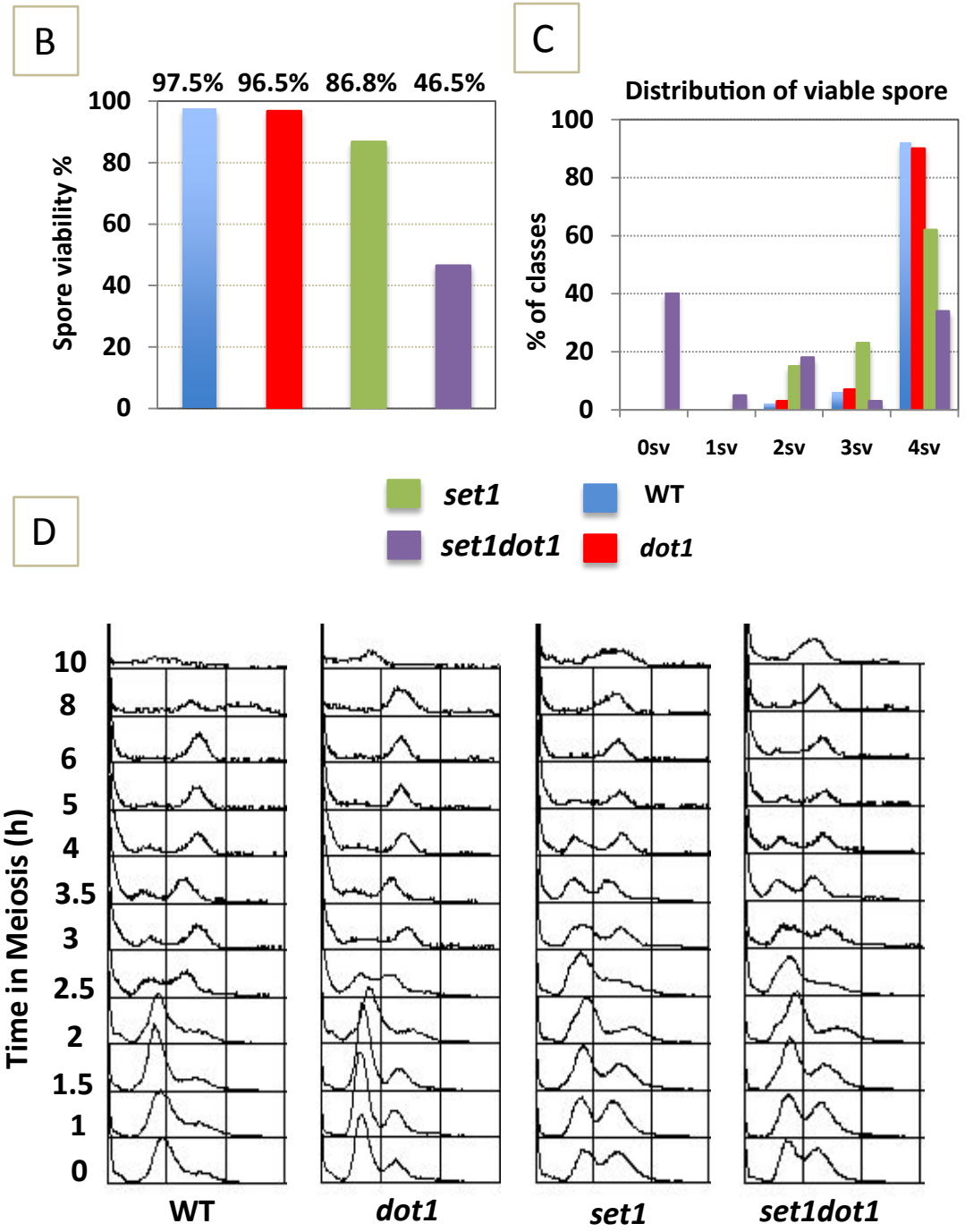
B
97.5% 96.5% 86.8% 46.5%
Spore viability %
100
80
60
40
20
0
C
Distribution of viable spore
% of classes
100
80
60
40
20
0
0sv 1sv 2sv 3sv 4sv
set1
WT
set1dot1
dot1
D
Time in Meiosis (h)
10
8
6
5
4
3.5
3
2.5
2
1.5
1
0
WT
dot1
set1
set1dot1

Figure 1

E

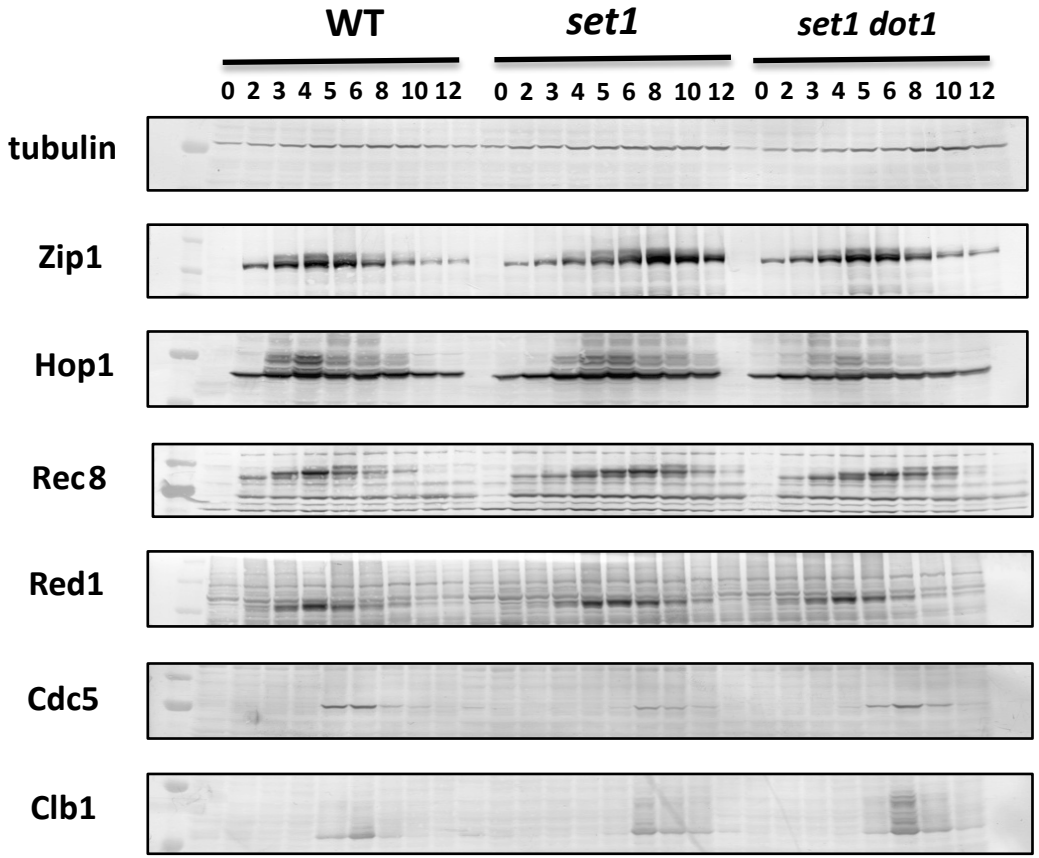
WT
set1
set1 dot1
0 2 3 4 5 6 8 10 12
0 2 3 4 5 6 8 10 12
0 2 3 4 5 6 8 10 12
tubulin
Zip1
Hop1
Rec8
Red1
Cdc5
Clb1

F

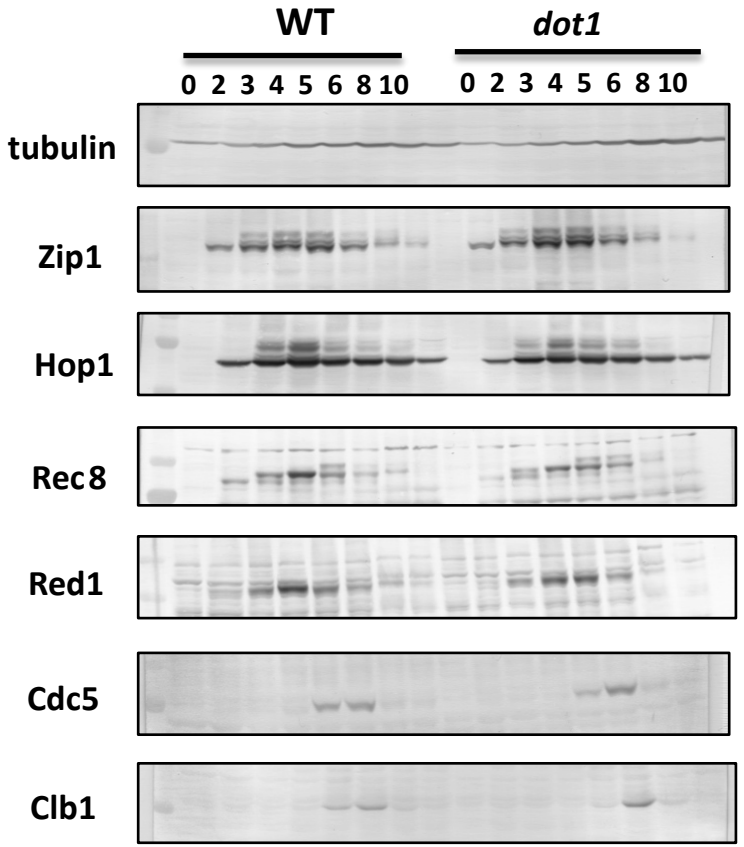
WT
dot1
0 2 3 4 5 6 8 10
0 2 3 4 5 6 8 10
tubulin
Zip1
Hop1
Rec8
Red1
Cdc5
Clb1

Figure 2

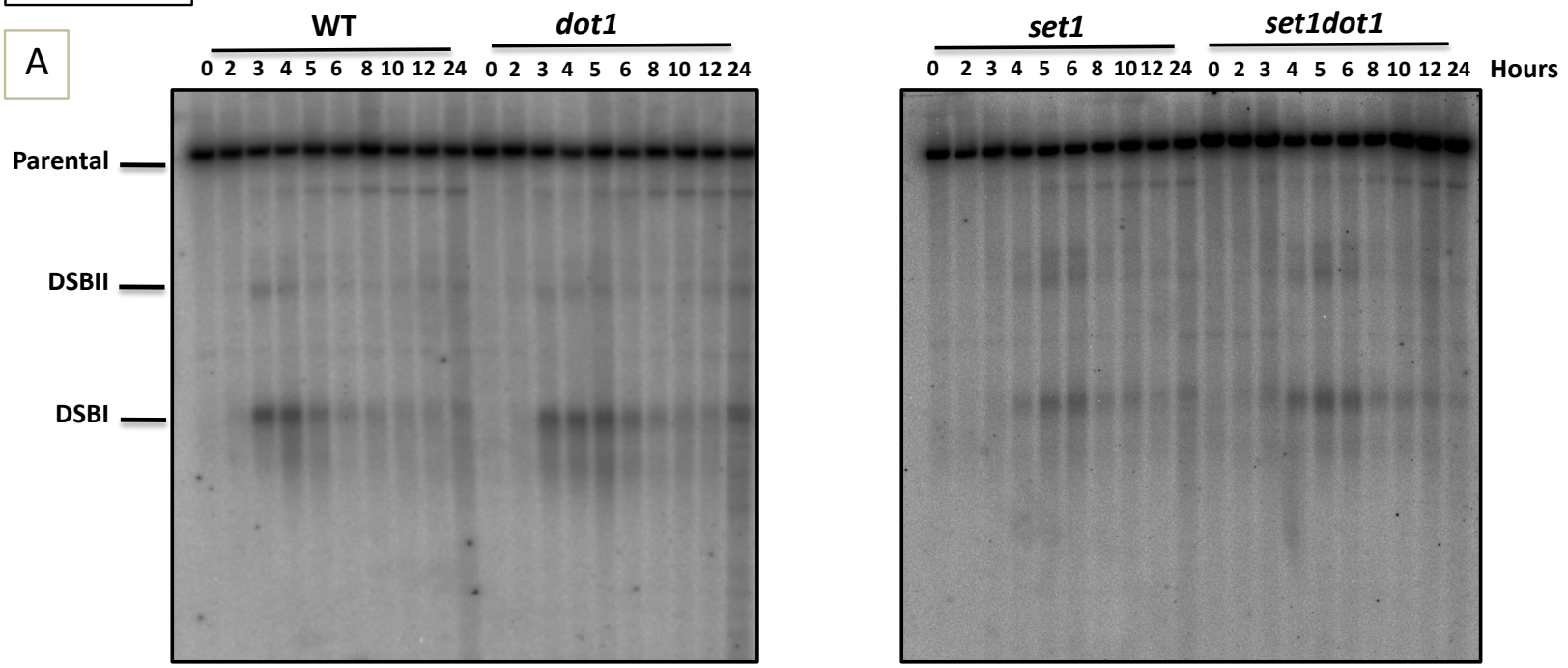
A
WT
dot1
set1
set1dot1
0 2 3 4 5 6 8 10 12 24
Hours
Parental
DSBII
DSBI

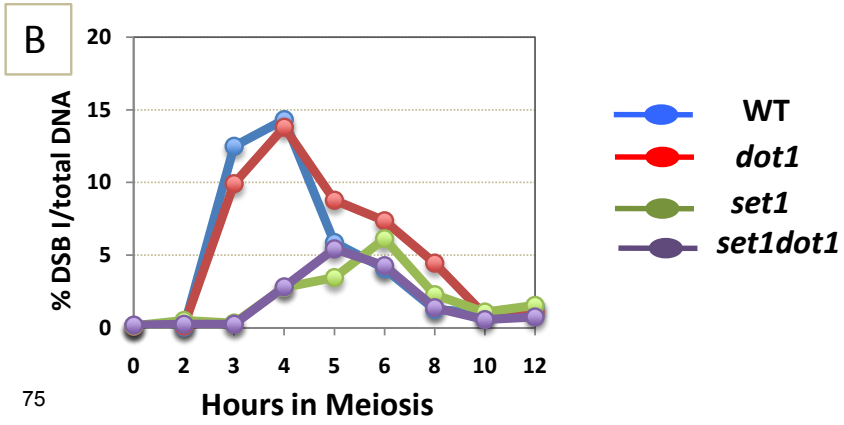
B
% DSB I/total DNA
Hours in Meiosis
WT
dot1
set1
set1dot1

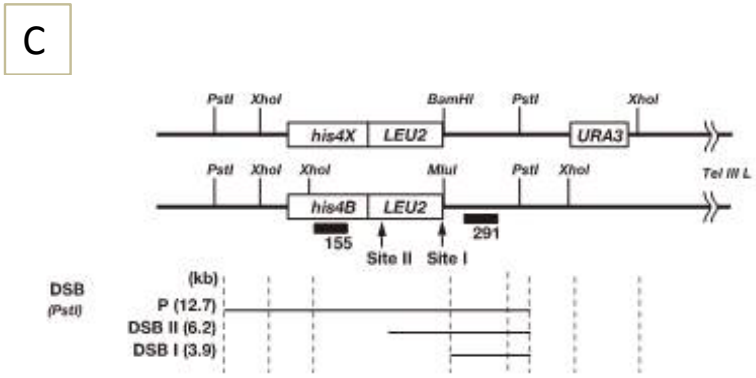
C
PstI
XhoI
BamHI
MluI
his4X
LEU2
URA3
his4B
Tel III L
155
291
Site II
Site I
DSB
(PstI)
(kb)
P (12.7)
DSB II (6.2)
DSB I (3.9)

Figure 2

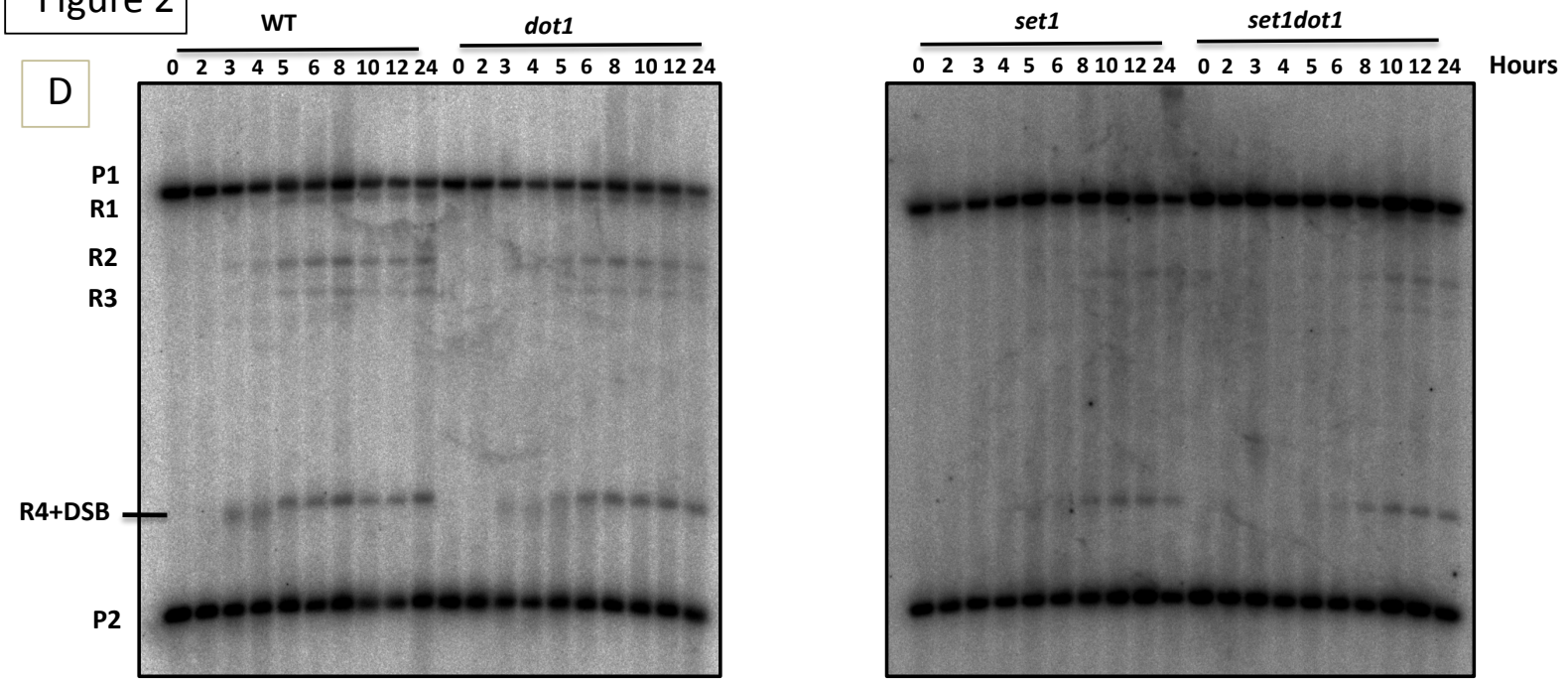
D
WT
dot1
set1
set1dot1
0 2 3 4 5 6 8 10 12 24
Hours
P1
R1
R2
R3
R4+DSB
P2

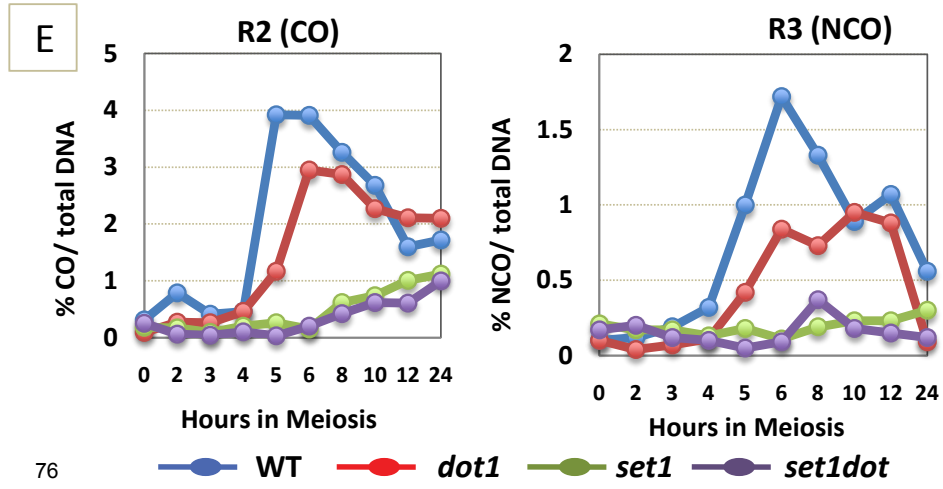
E
R2 (CO)
% CO/ total DNA
Hours in Meiosis
R3 (NCO)
% NCO/ total DNA
Hours in Meiosis
WT
dot1
set1
set1dot

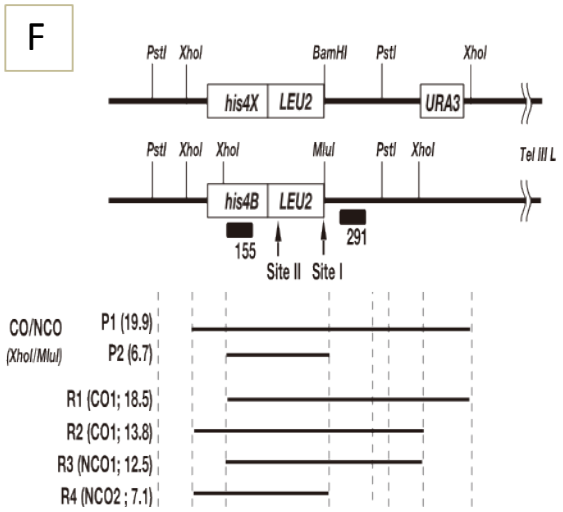
F
PstI XhoI BamHI PstI XhoI
his4X LEU2 URA3
PstI XhoI XhoI MluI PstI XhoI
Tel III L
his4B LEU2
155
291
Site II
Site I
CO/NCO
(XhoI/MluI)
P1 (19.9)
P2 (6.7)
R1 (CO1; 18.5)
R2 (CO1; 13.8)
R3 (NCO1; 12.5)
R4 (NCO2 ; 7.1)

Figure 3

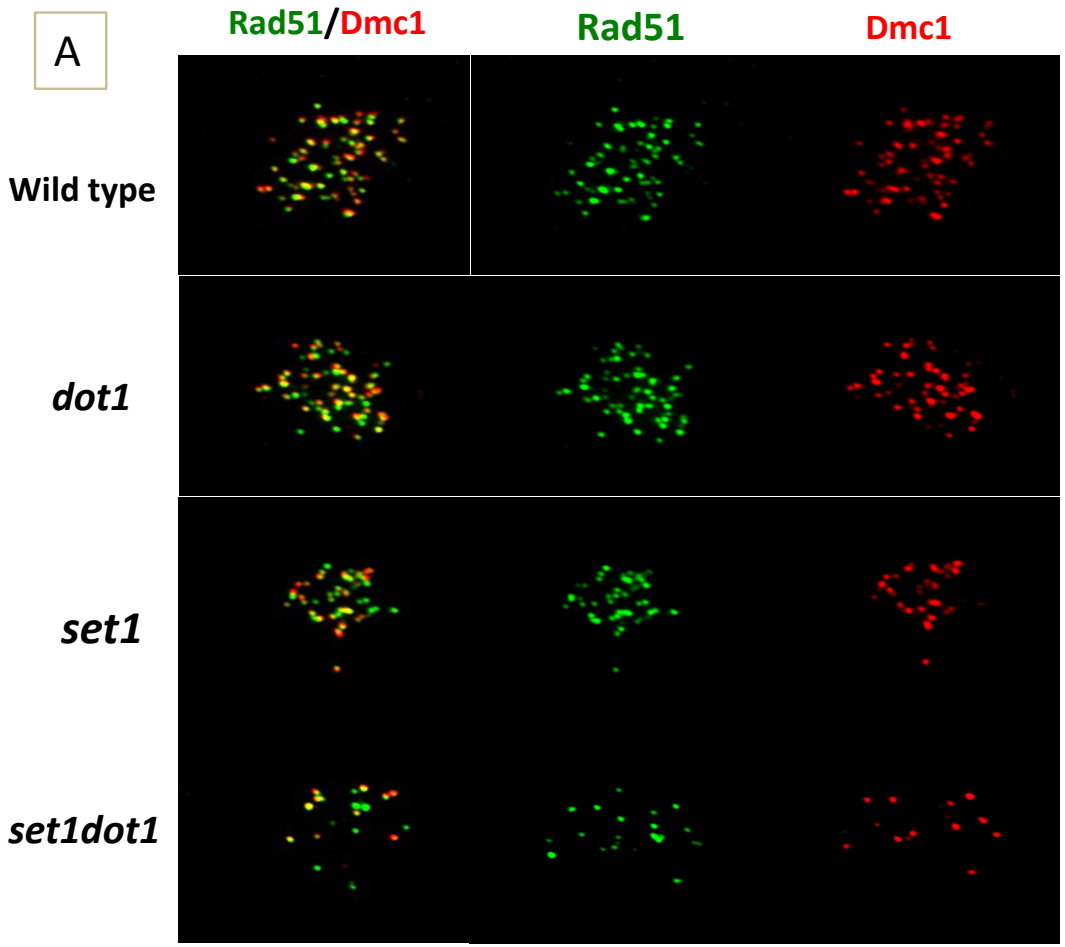
A
Rad51/Dmc1
Rad51
Dmc1
Wild type
dot1
set1
set1dot1

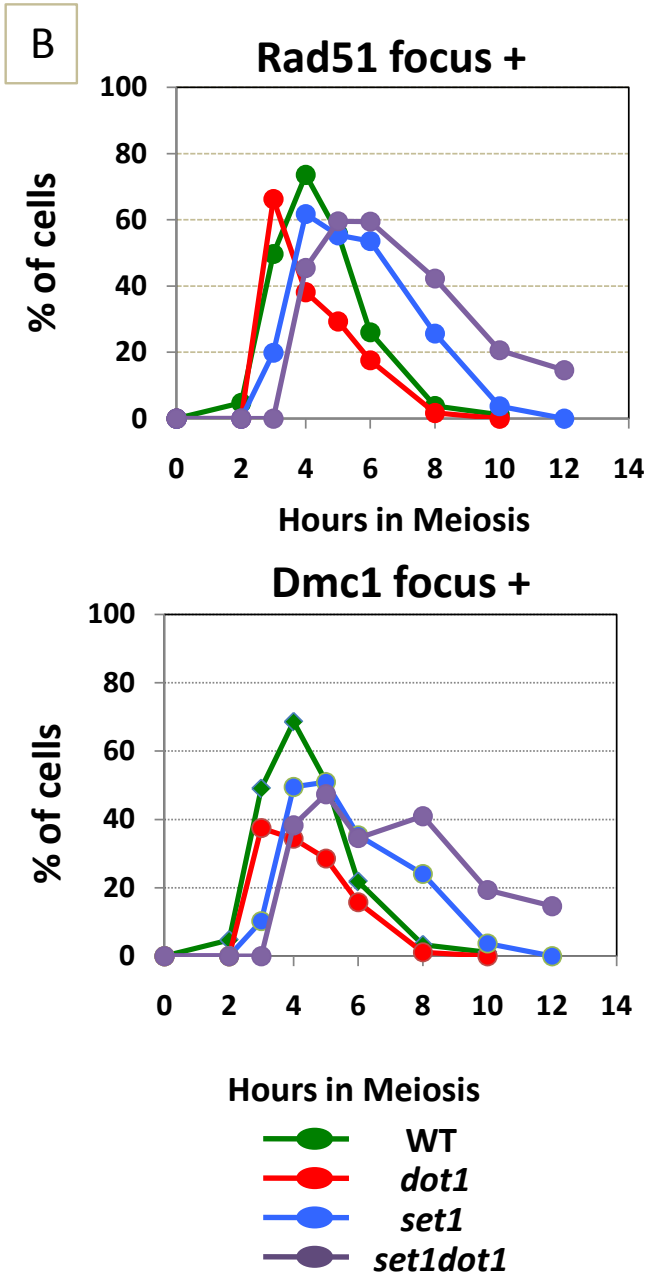
B
Rad51 focus +
% of cells
100
80
60
40
20
0
0 2 4 6 8 10 12 14
Hours in Meiosis
Dmc1 focus +
% of cells
100
80
60
40
20
0
0 2 4 6 8 10 12 14
Hours in Meiosis
WT
dot1
set1
set1dot1

Figure 3

C

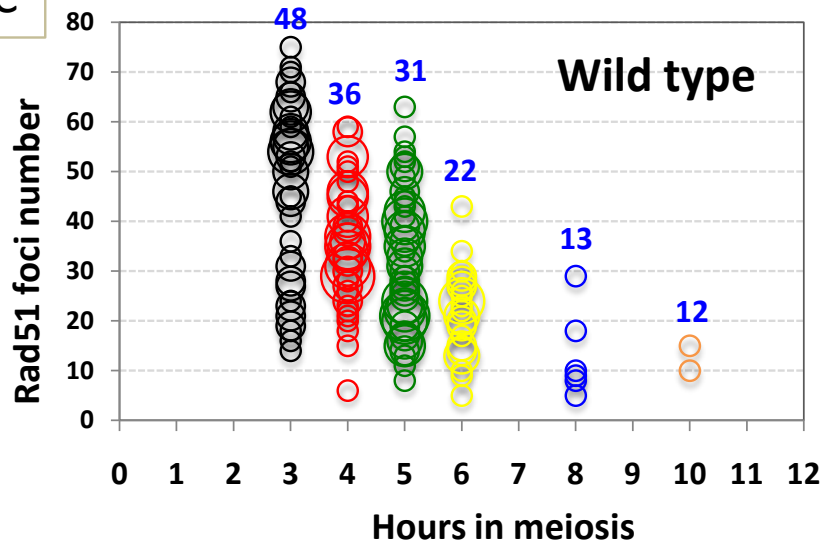
Wild type
Rad51 foci number
Hours in meiosis
48
36
31
22
13
12

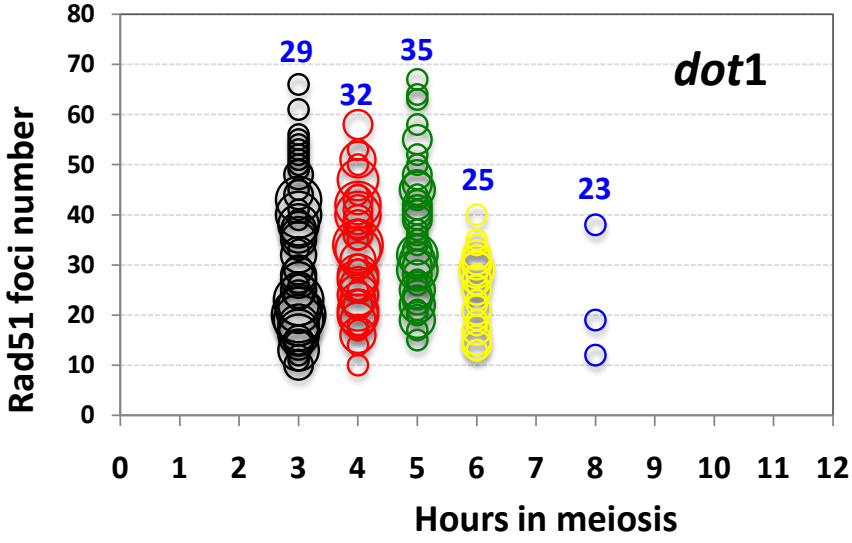
dot1
Rad51 foci number
Hours in meiosis
29
32
35
25
23

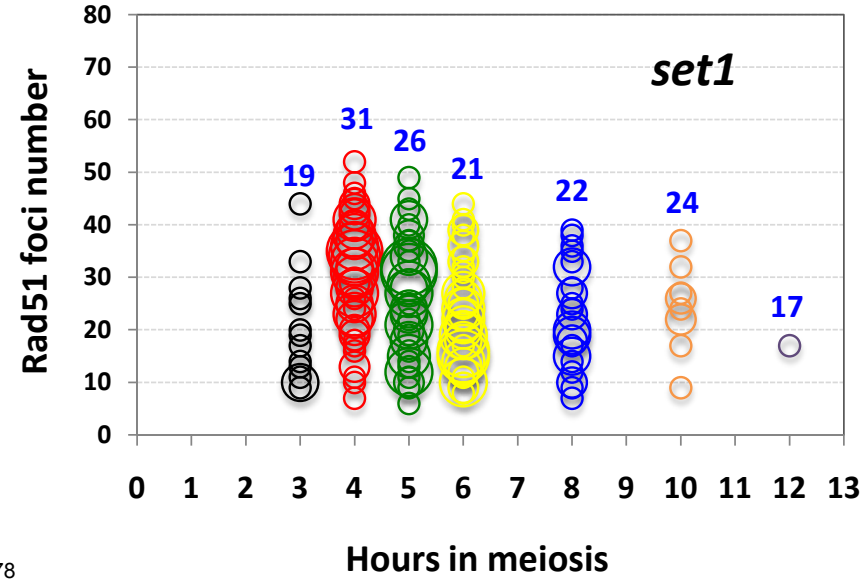
set1
Rad51 foci number
Hours in meiosis
19
31
26
21
22
24
17

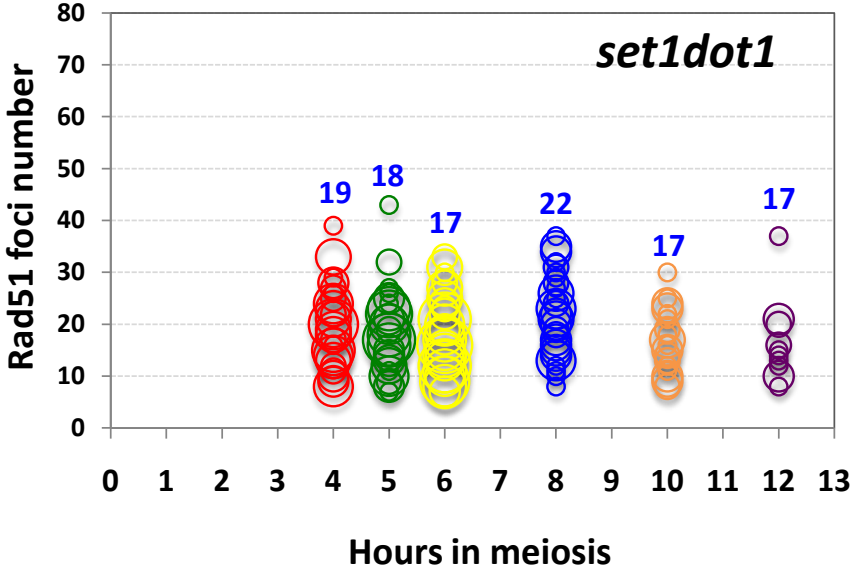
set1dot1
Rad51 foci number
Hours in meiosis
19
18
17
22
17
17

Figure 4

A

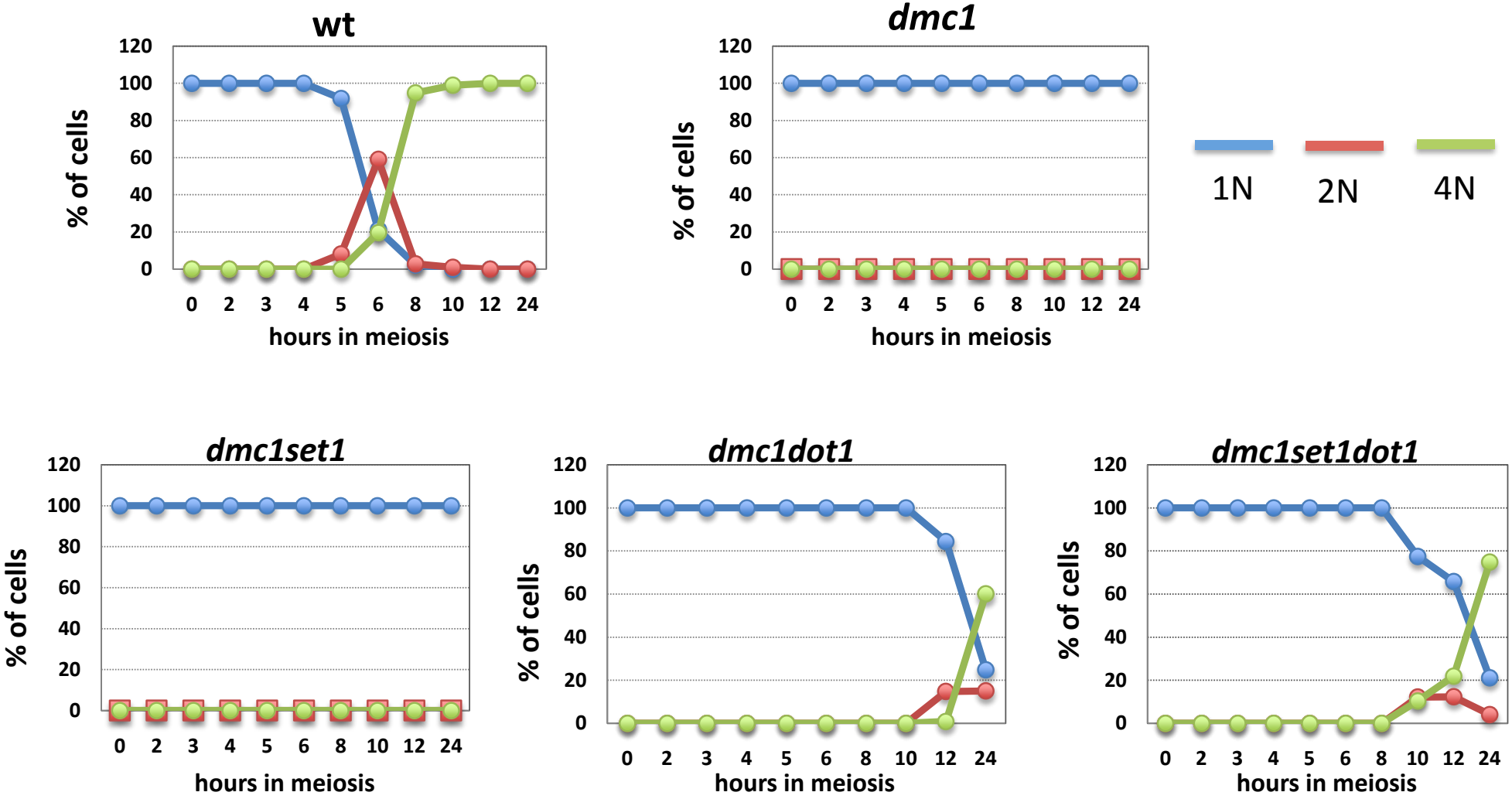
wt
dmc1
dmc1set1
dmc1dot1
dmc1set1dot1
% of cells
hours in meiosis
0 2 3 4 5 6 8 10 12 24
0 20 40 60 80 100 120
1N
2N
4N

Figure 4

B

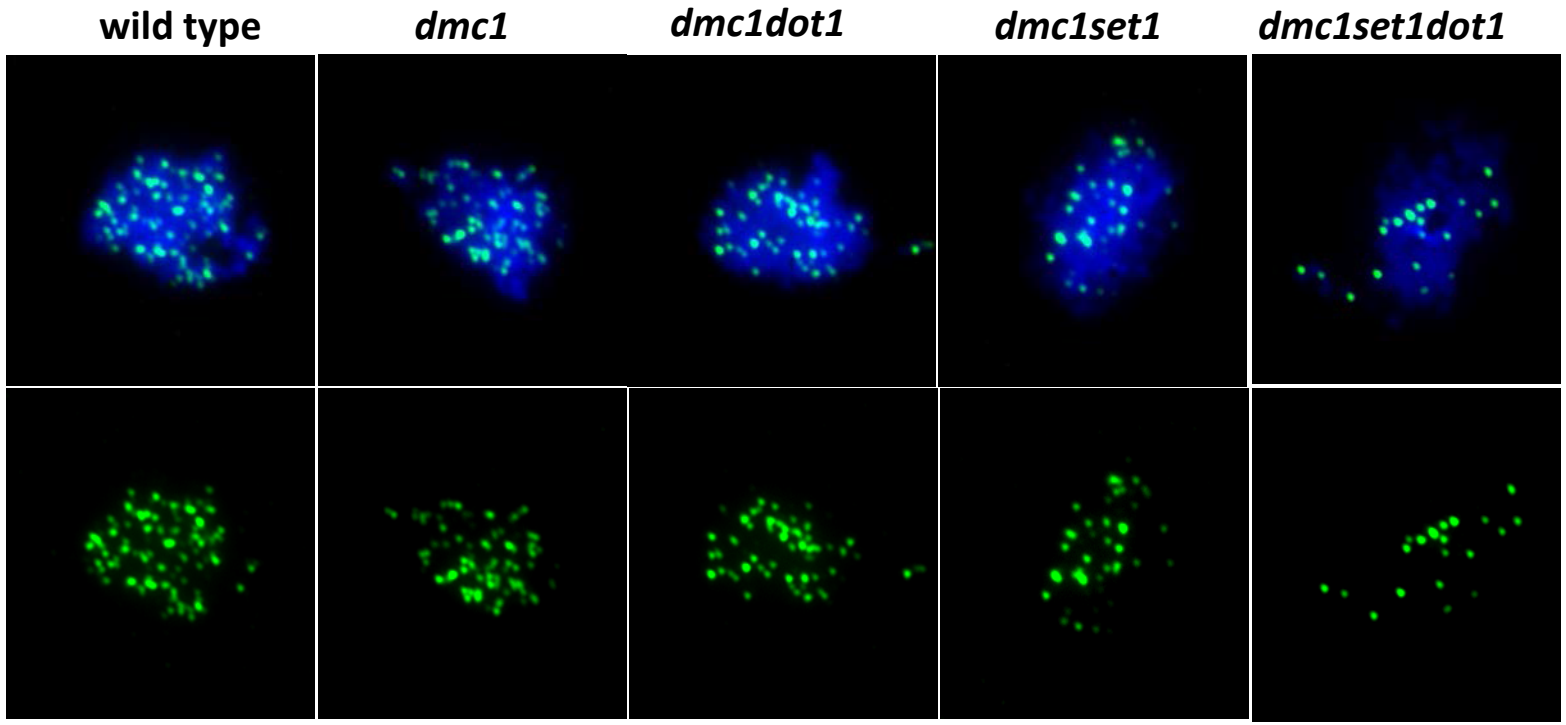
wild type
dmc1
dmc1dot1
dmc1set1
dmc1set1dot1
+DAPI
Rad51

C

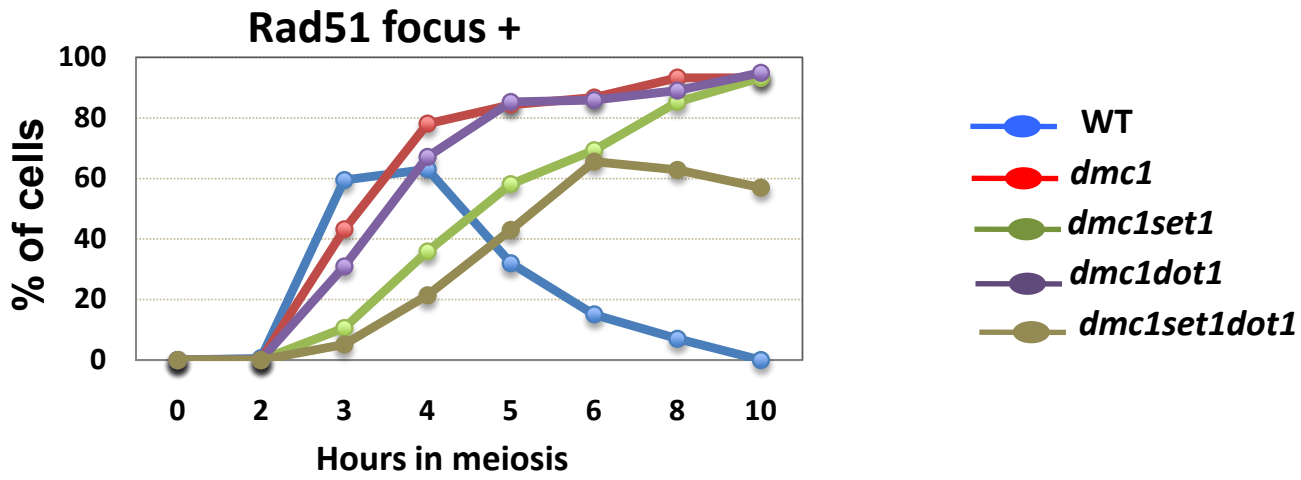
Rad51 focus +
% of cells
100
80
60
40
20
0
0
2
3
4
5
6
8
10
Hours in meiosis
WT
dmc1
dmc1set1
dmc1dot1
dmc1set1dot1

Figure 4

D

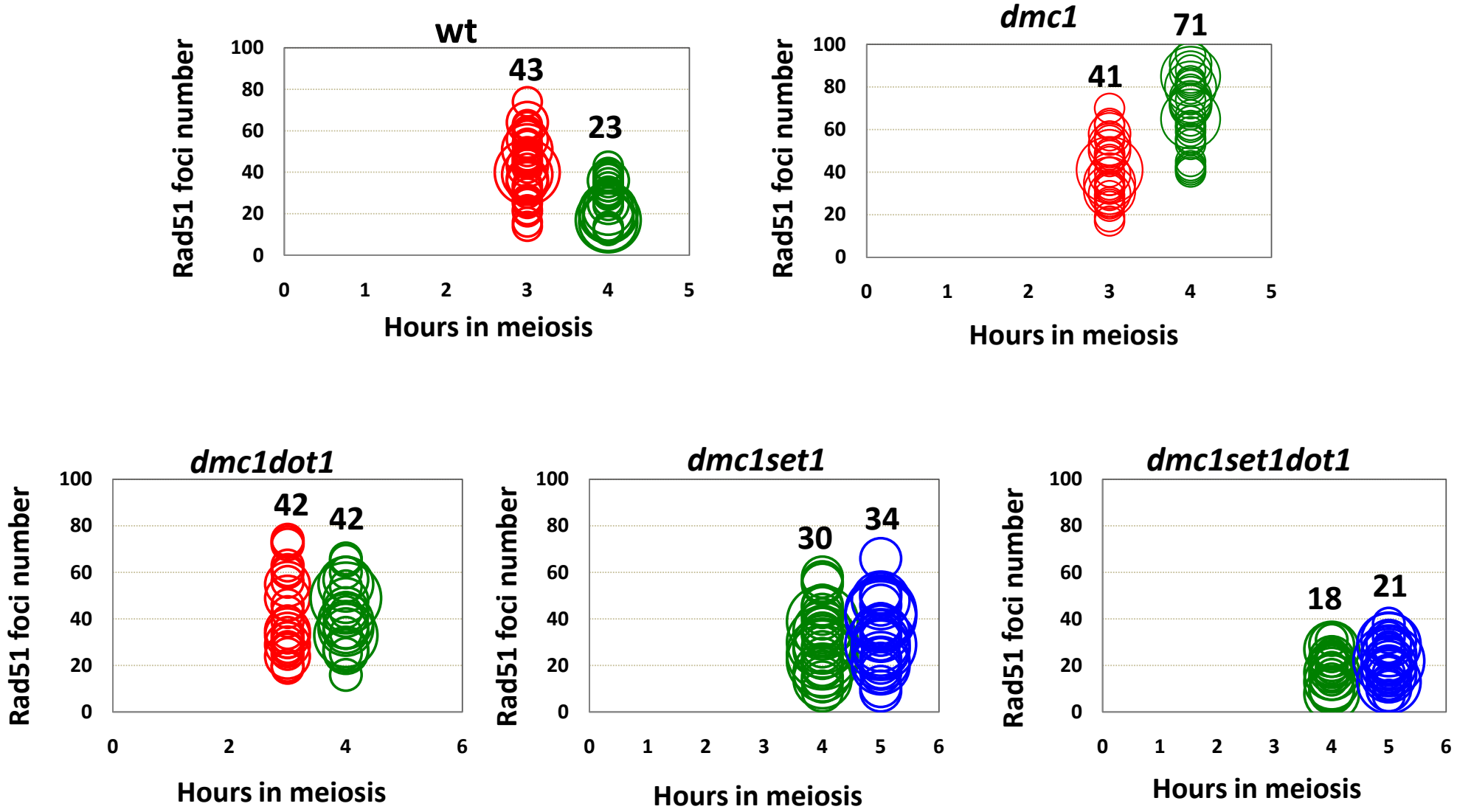
wt
43
23
Rad51 foci number
Hours in meiosis
dmc1
41
71
Rad51 foci number
Hours in meiosis
dmc1dot1
42
42
Rad51 foci number
Hours in meiosis
dmc1set1
30
34
Rad51 foci number
Hours in meiosis
dmc1set1dot1
18
21
Rad51 foci number
Hours in meiosis

Figure 5

A

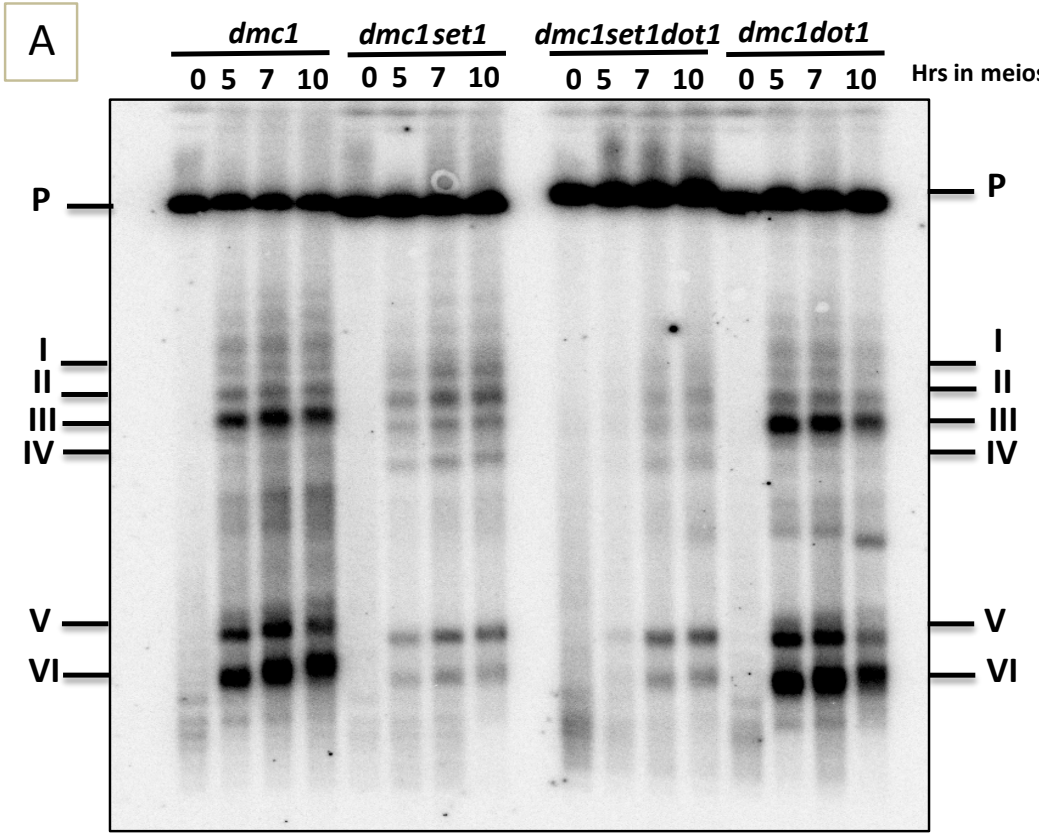
dmc1
dmc1set1
dmc1set1dot1
dmc1dot1
0 5 7 10
Hrs in meiosis
P
I
II
III
IV
V
VI

B

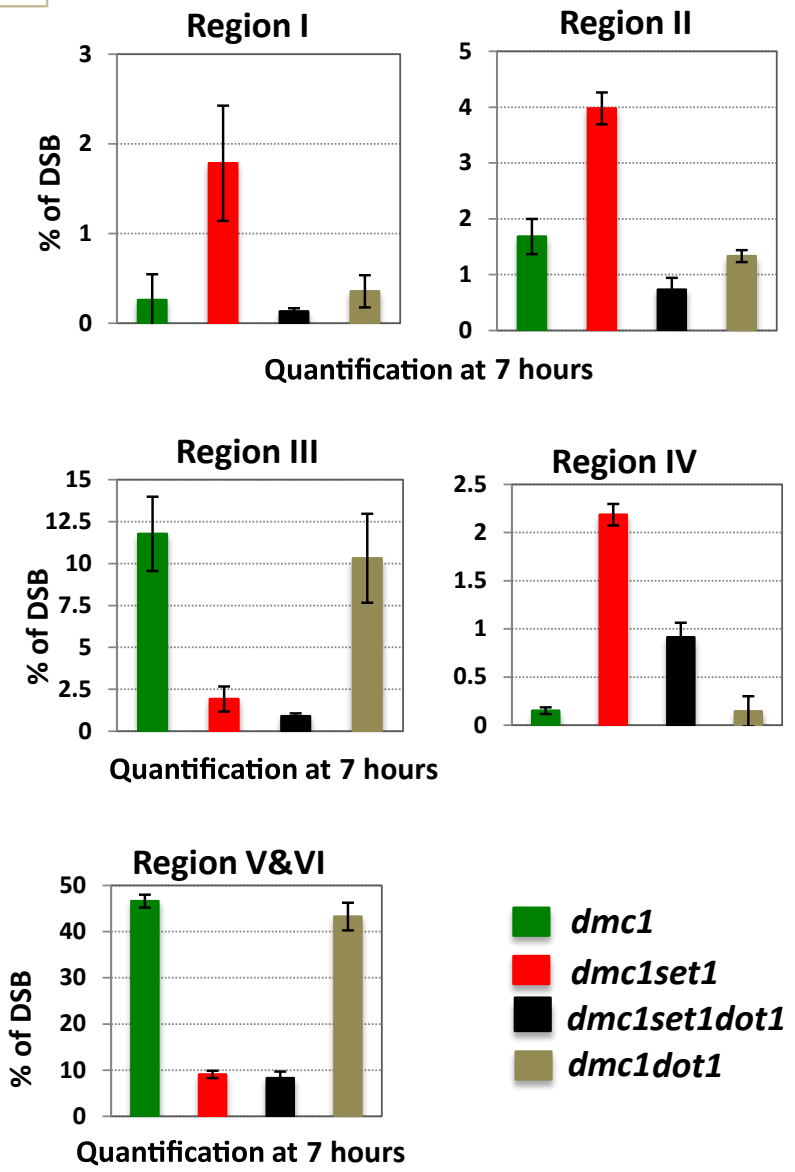
Region I
% of DSB
Quantification at 7 hours
Region II
Region III
Region IV
Region V&VI
dmc1
dmc1set1
dmc1set1dot1
dmc1dot1

Figure 5

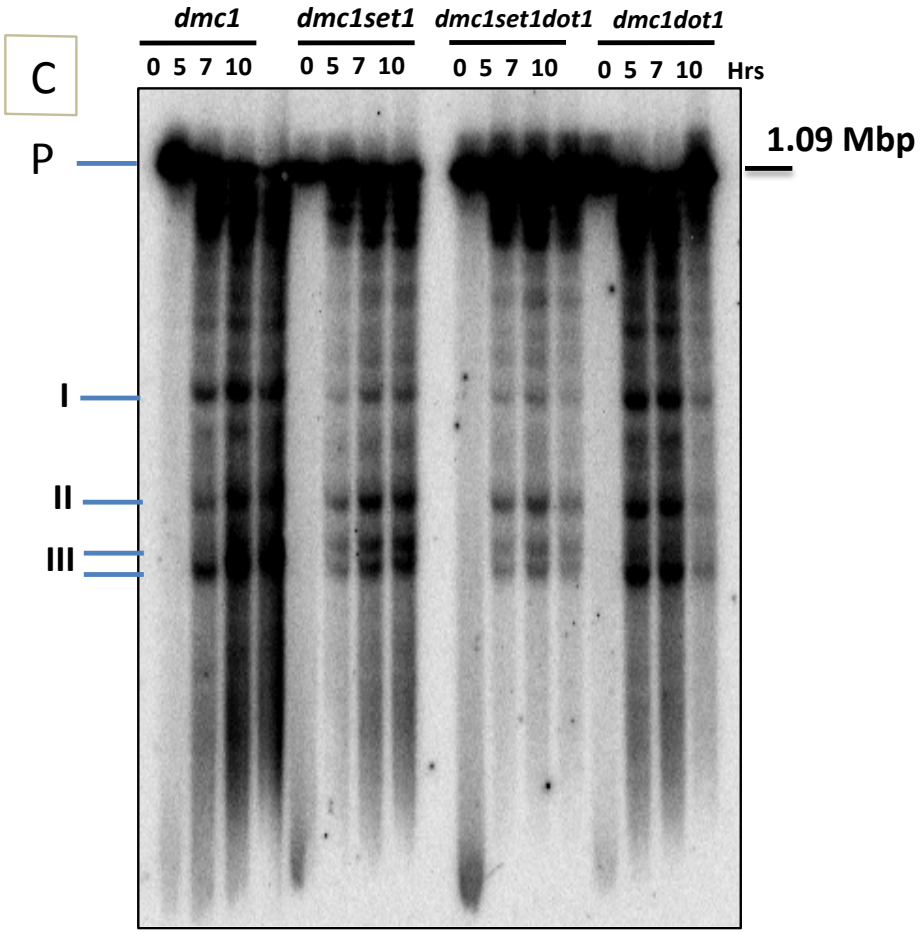
C
dmc1
dmc1set1
dmc1set1dot1
dmc1dot1
0 5 7 10
0 5 7 10
0 5 7 10
0 5 7 10
Hrs
1.09 Mbp
P
I
II
III

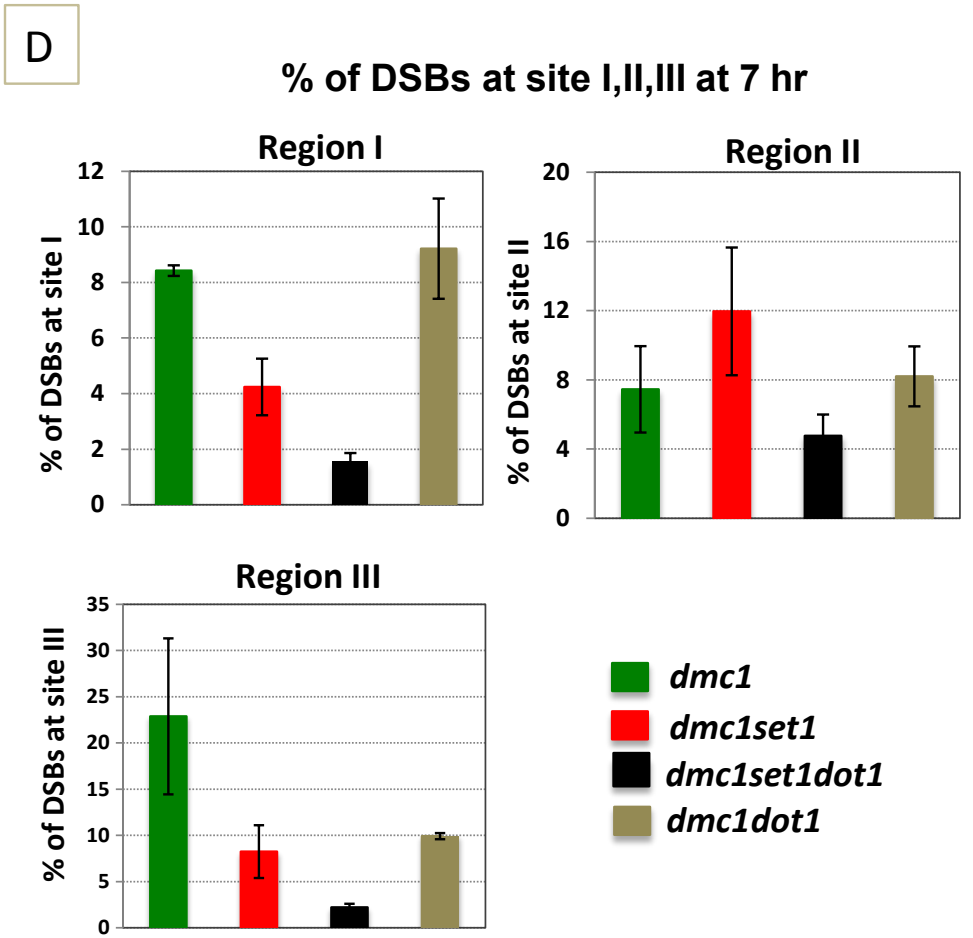
D
% of DSBs at site I,II,III at 7 hr
Region I
% of DSBs at site I
Region II
% of DSBs at site II
Region III
% of DSBs at site III
dmc1
dmc1set1
dmc1set1dot1
dmc1dot1

Figure 5

E

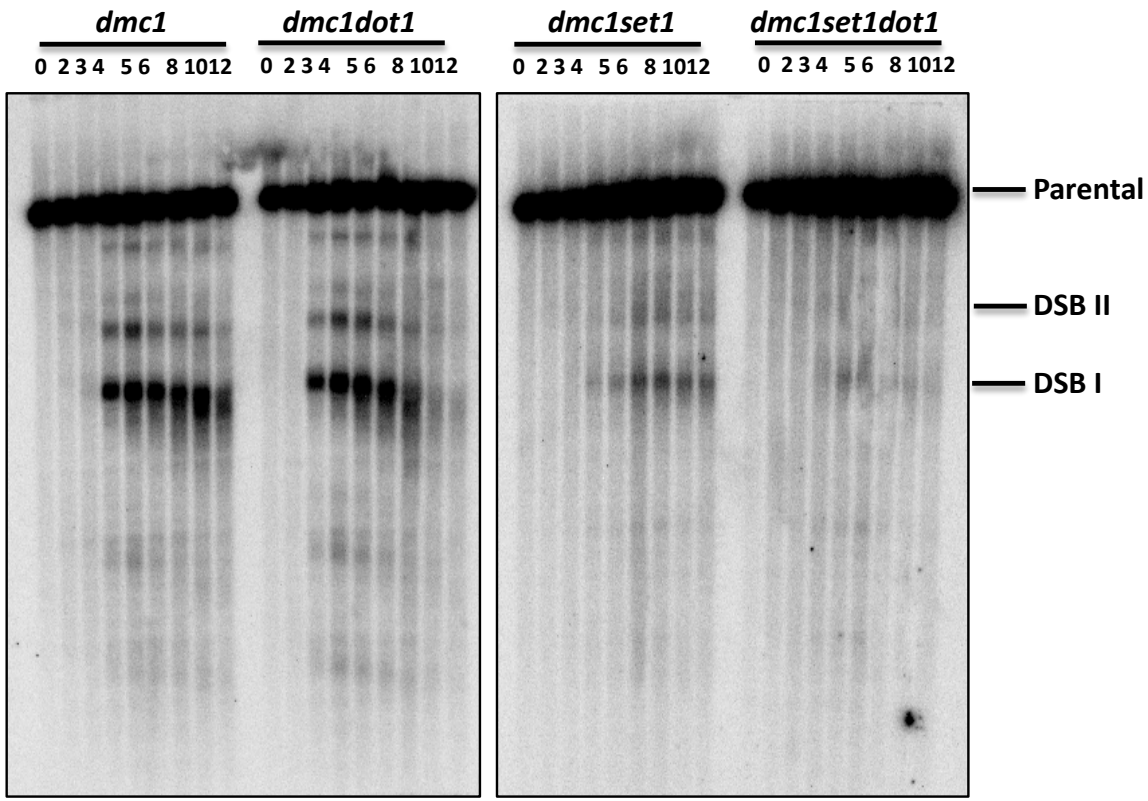
dmc1
dmc1dot1
dmc1set1
dmc1set1dot1
0 2 3 4 5 6 8 10 12
0 2 3 4 5 6 8 10 12
0 2 3 4 5 6 8 10 12
0 2 3 4 5 6 8 10 12
Parental
DSB II
DSB I

F

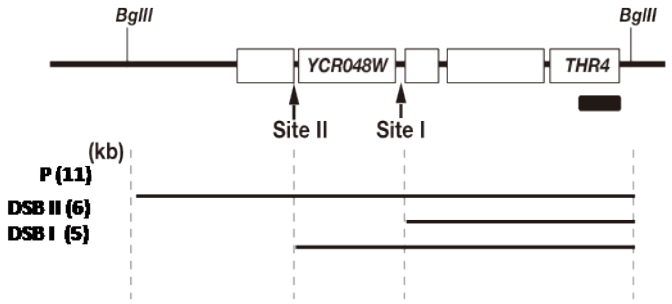
BglII
BglII
YCR048W
THR4
Site II
Site I
(kb)
P (11)
DSB II (6)
DSB I (5)

G

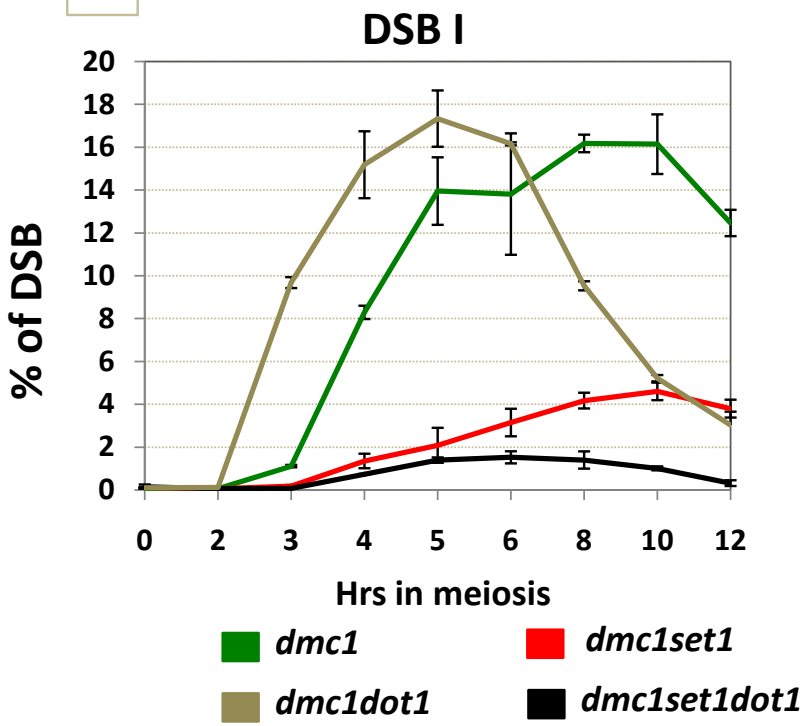
DSB I
% of DSB
20
18
16
14
12
10
8
6
4
2
0
0 2 3 4 5 6 8 10 12
Hrs in meiosis
dmc1
dmc1set1
dmc1dot1
dmc1set1dot1

Figure 6

A

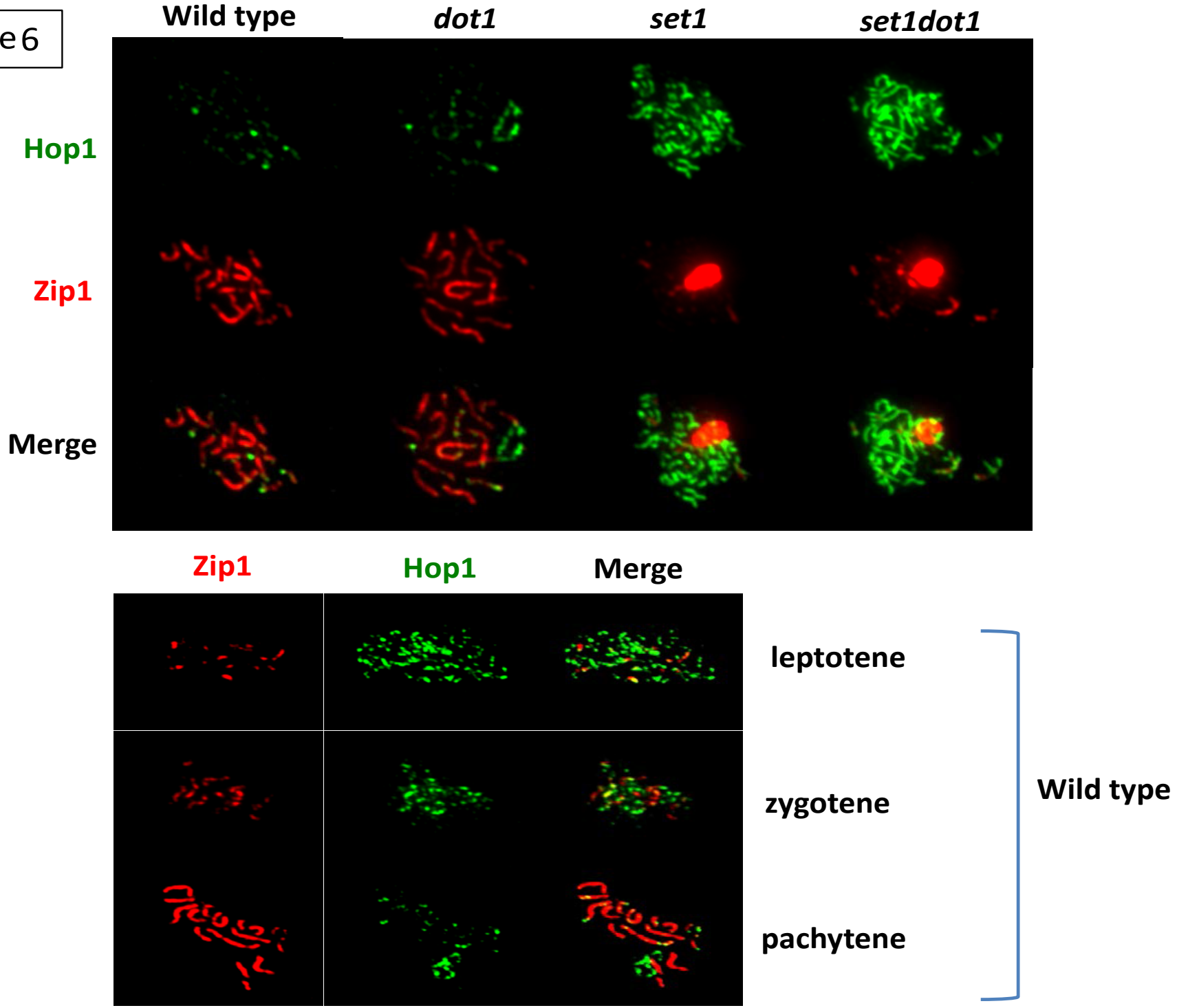
Wild type
dot1
set1
set1dot1
Hop1
Zip1
Merge
Zip1
Hop1
Merge
leptotene
zygotene
pachytene
Wild type

Figure 6

B

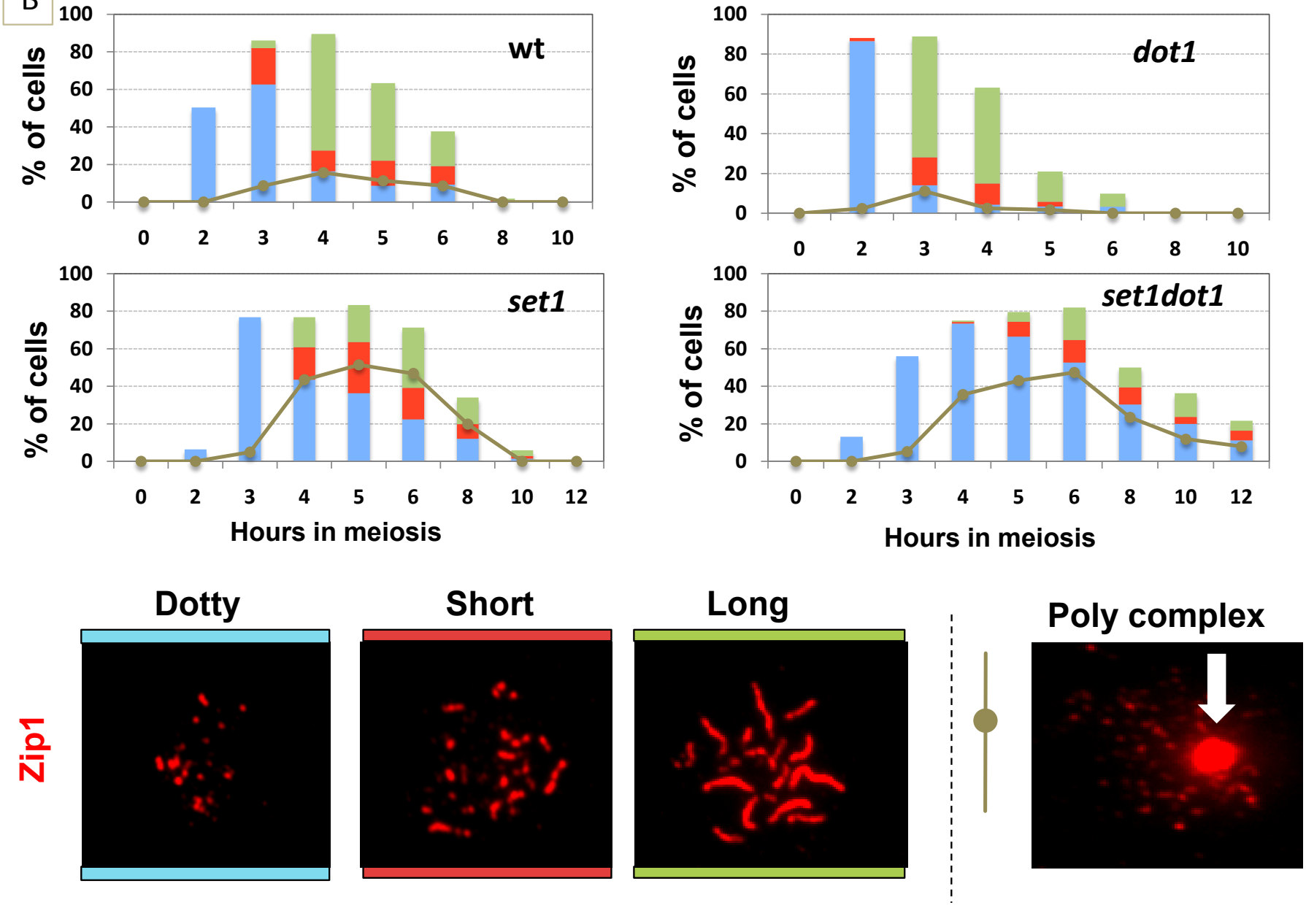
wt
dot1
set1
set1dot1
% of cells
100
80
60
40
20
0
0 2 3 4 5 6 8 10
0 2 3 4 5 6 8 10 12
Hours in meiosis
Dotty
Short
Long
Poly complex
Zip1

Figure 6

C

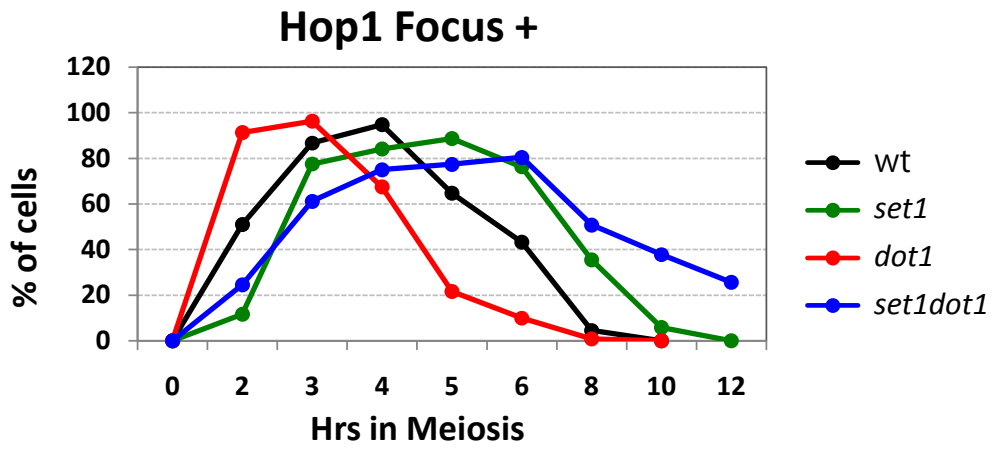
Hop1 Focus +
% of cells
120
100
80
60
40
20
0
0 2 3 4 5 6 8 10 12
Hrs in Meiosis
wt
set1
dot1
set1dot1

D

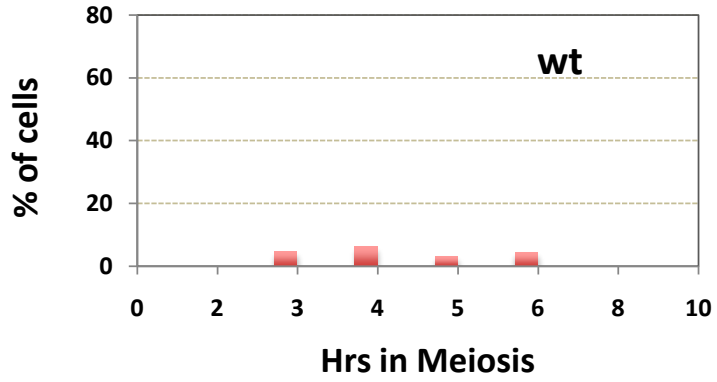
wt
% of cells
80
60
40
20
0
0 2 3 4 5 6 8 10
Hrs in Meiosis

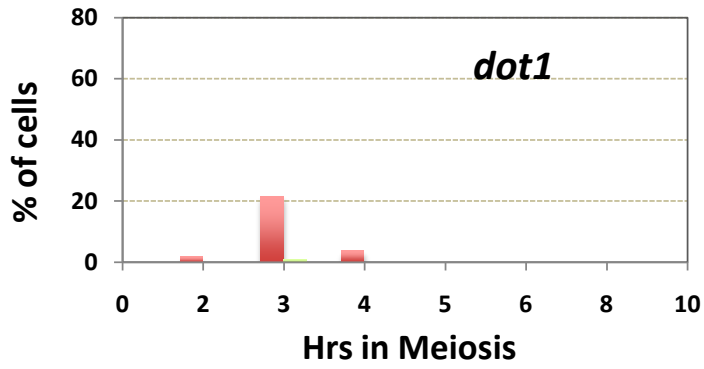
dot1
% of cells
80
60
40
20
0
0 2 3 4 5 6 8 10
Hrs in Meiosis

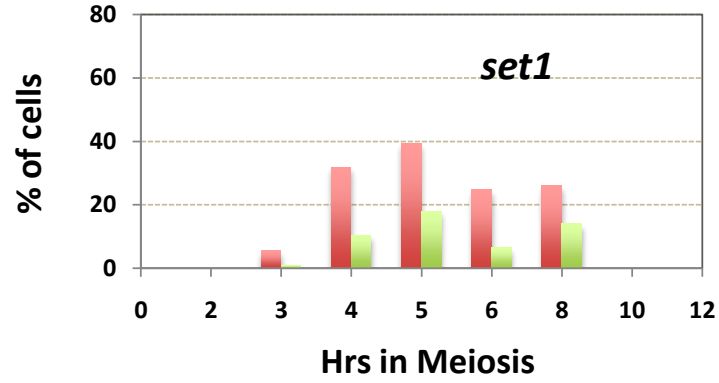
set1
% of cells
80
60
40
20
0
0 2 3 4 5 6 8 10 12
Hrs in Meiosis

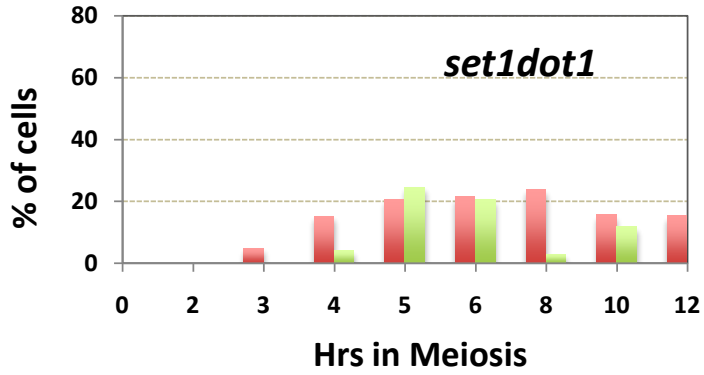
set1dot1
% of cells
80
60
40
20
0
0 2 3 4 5 6 8 10 12
Hrs in Meiosis

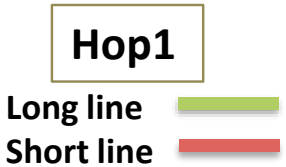
Hop1
Long line
Short line

Figure 7

A

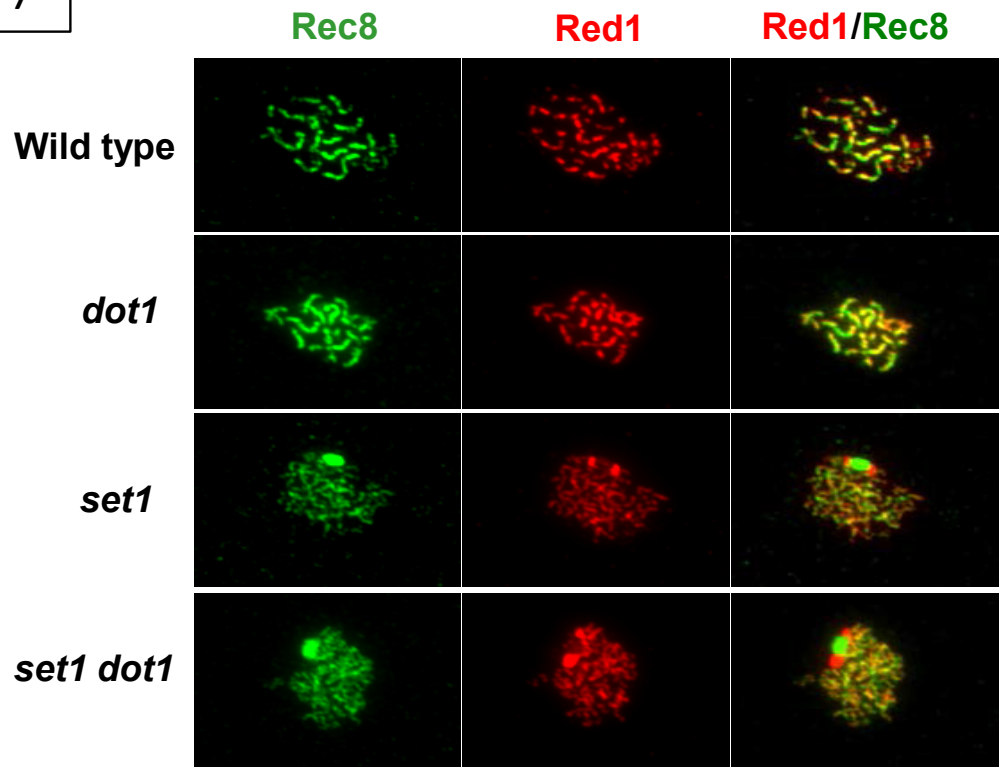

B

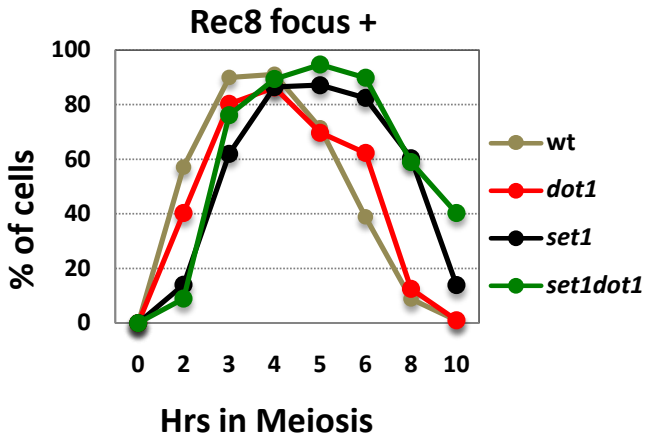

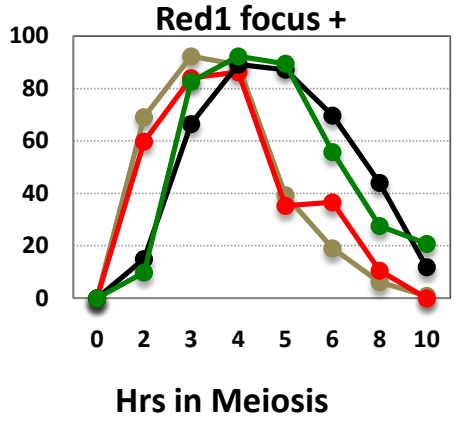

C

Poly complex

(Red1 /Rec8)

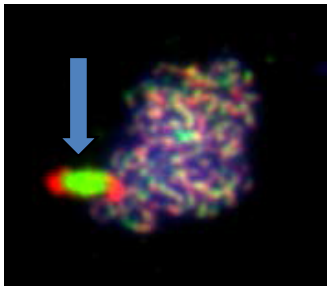

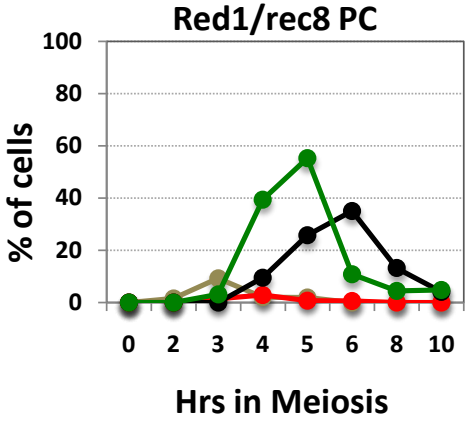

Figure 8

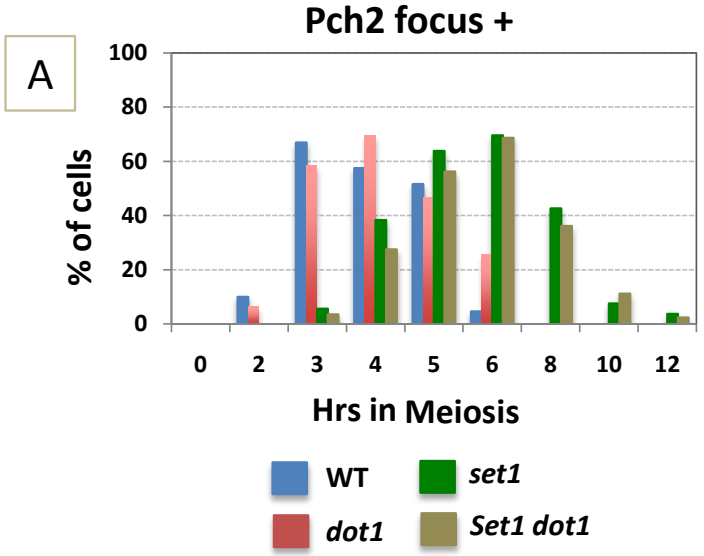
A
Pch2 focus +
% of cells
100
80
60
40
20
0
0 2 3 4 5 6 8 10 12
Hrs in Meiosis
WT
set1
dot1
Set1 dot1

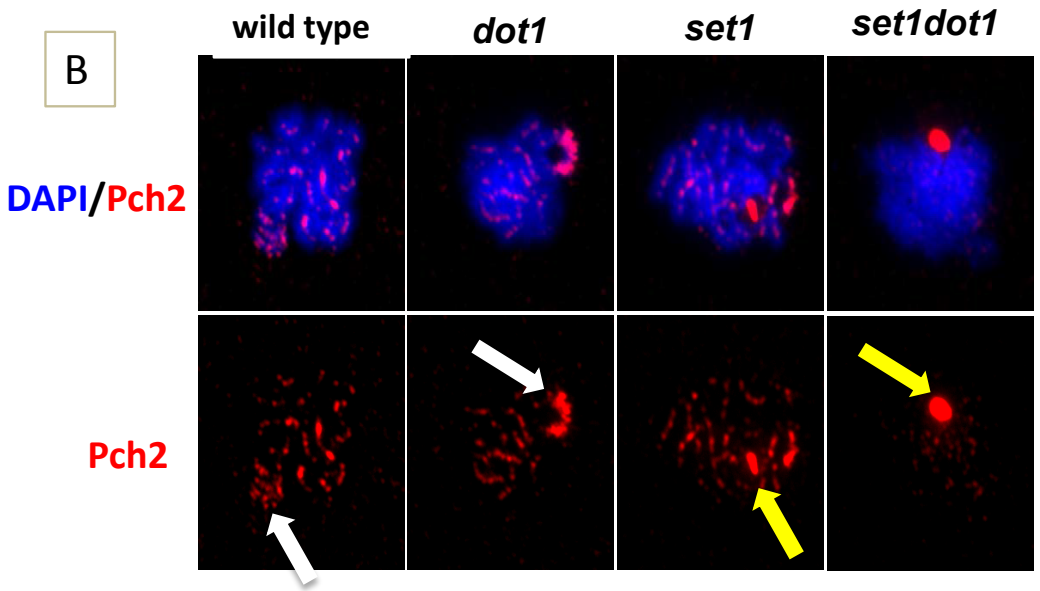
B
wild type
dot1
set1
set1dot1
DAPI/Pch2
Pch2

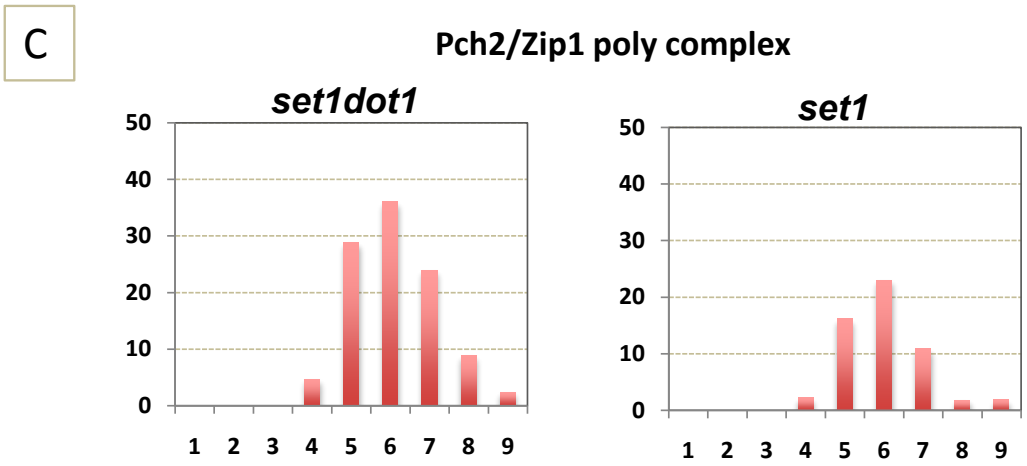
C
Pch2/Zip1 poly complex
set1dot1
set1
50
40
30
20
10
0
1 2 3 4 5 6 7 8 9

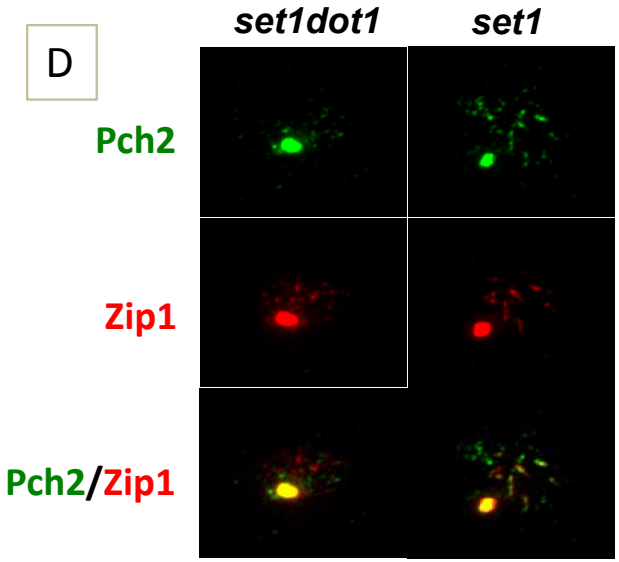
D
set1dot1
set1
Pch2
Zip1
Pch2/Zip1

Figure 9

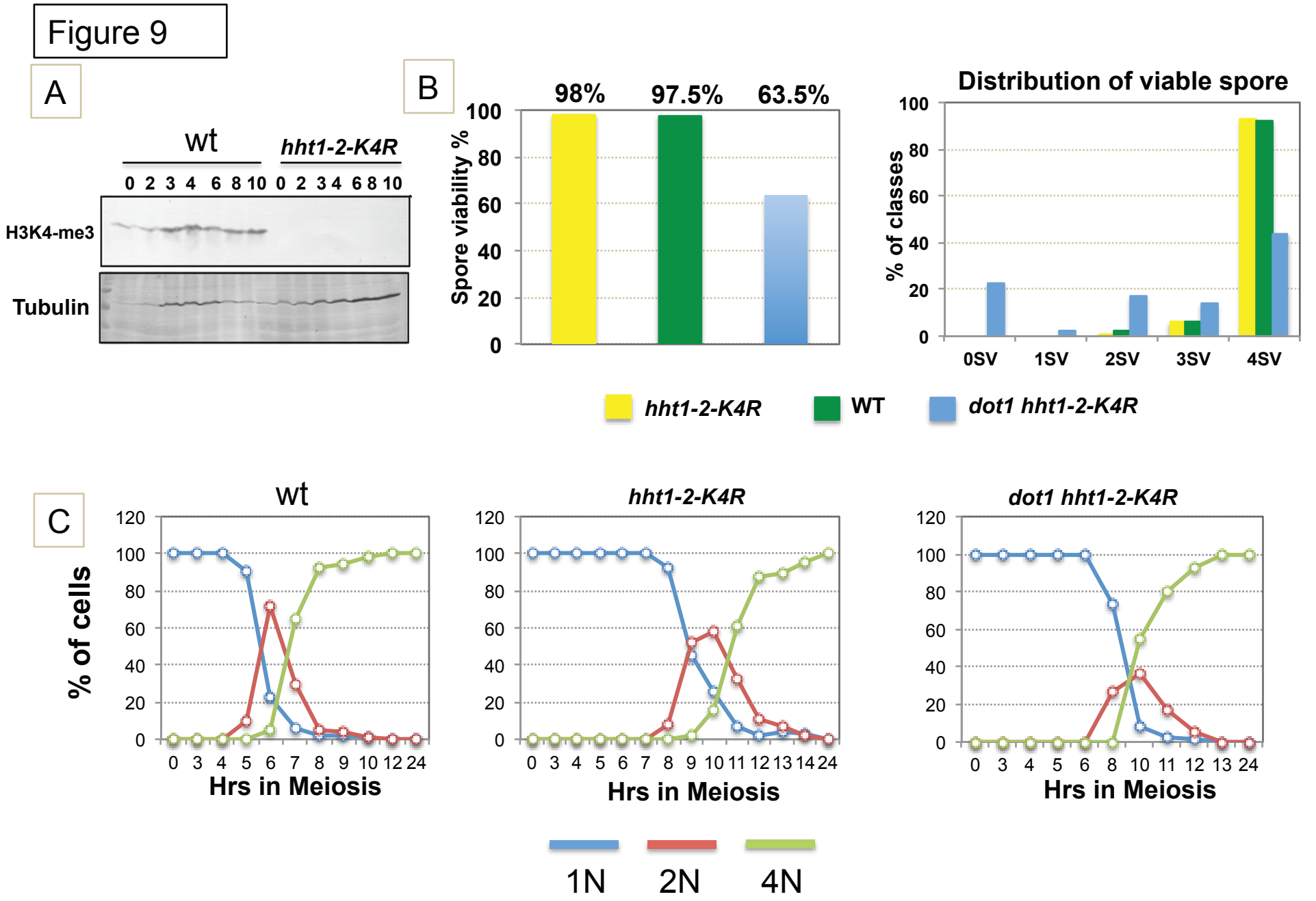
A
wt
hht1-2-K4R
0 2 3 4 6 8 10 0 2 3 4 6 8 10
H3K4-me3
Tubulin
B
98%
97.5%
63.5%
Spore viability %
100
80
60
40
20
0
Distribution of viable spore
% of classes
0SV
1SV
2SV
3SV
4SV
hht1-2-K4R
WT
dot1 hht1-2-K4R
C
wt
hht1-2-K4R
dot1 hht1-2-K4R
% of cells
120
100
80
60
40
20
0
0 3 4 5 6 7 8 9 10 12 24
0 3 4 5 6 7 8 9 10 11 12 13 14 24
0 3 4 5 6 8 10 11 12 13 24
Hrs in Meiosis
1N
2N
4N

Figure9

D

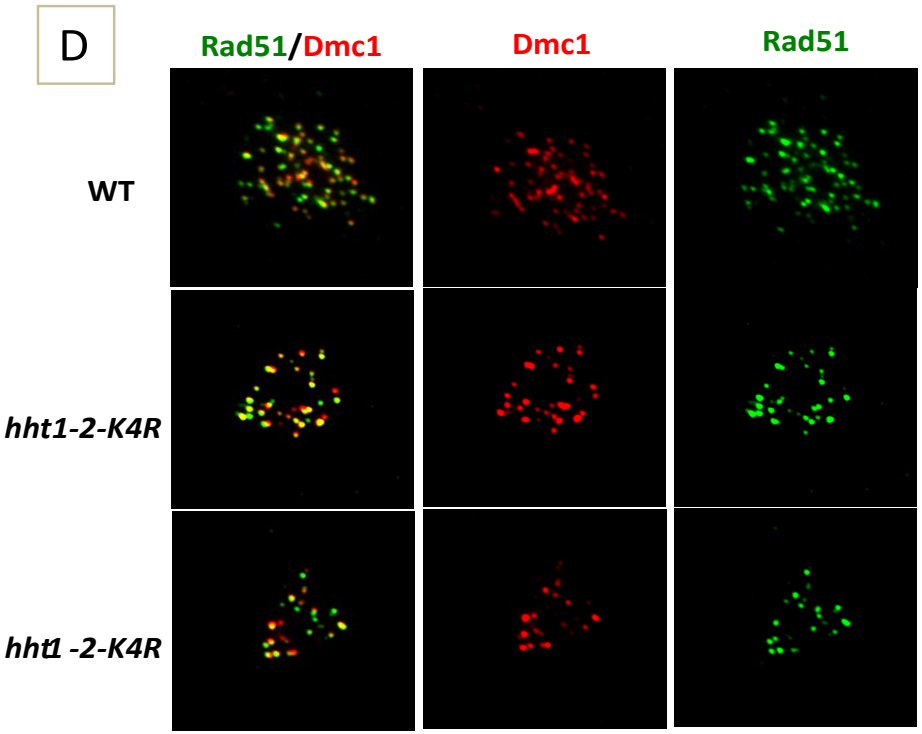
Rad51/Dmc1
Dmc1
Rad51
WT
hht1-2-K4R
hht1 -2-K4R

E

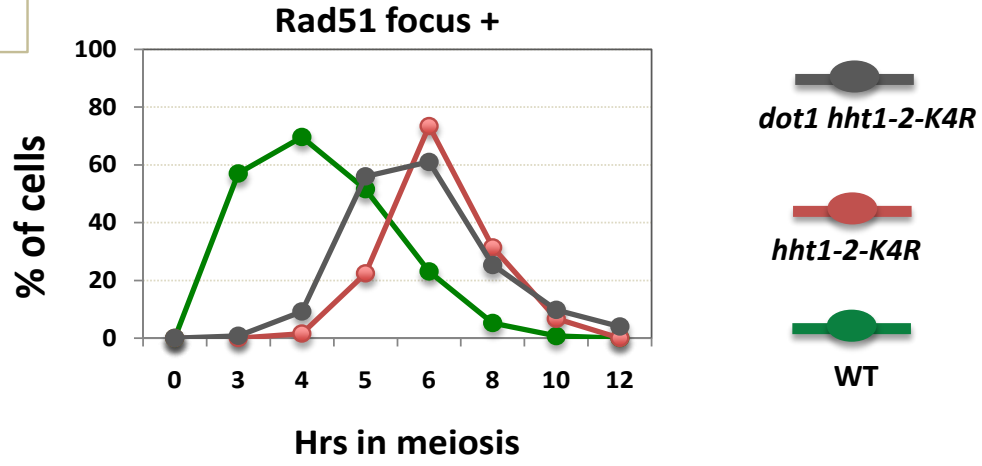
Rad51 focus +
% of cells
100
80
60
40
20
0
0 3 4 5 6 8 10 12
Hrs in meiosis
dot1 hht1-2-K4R
hht1-2-K4R
WT

F

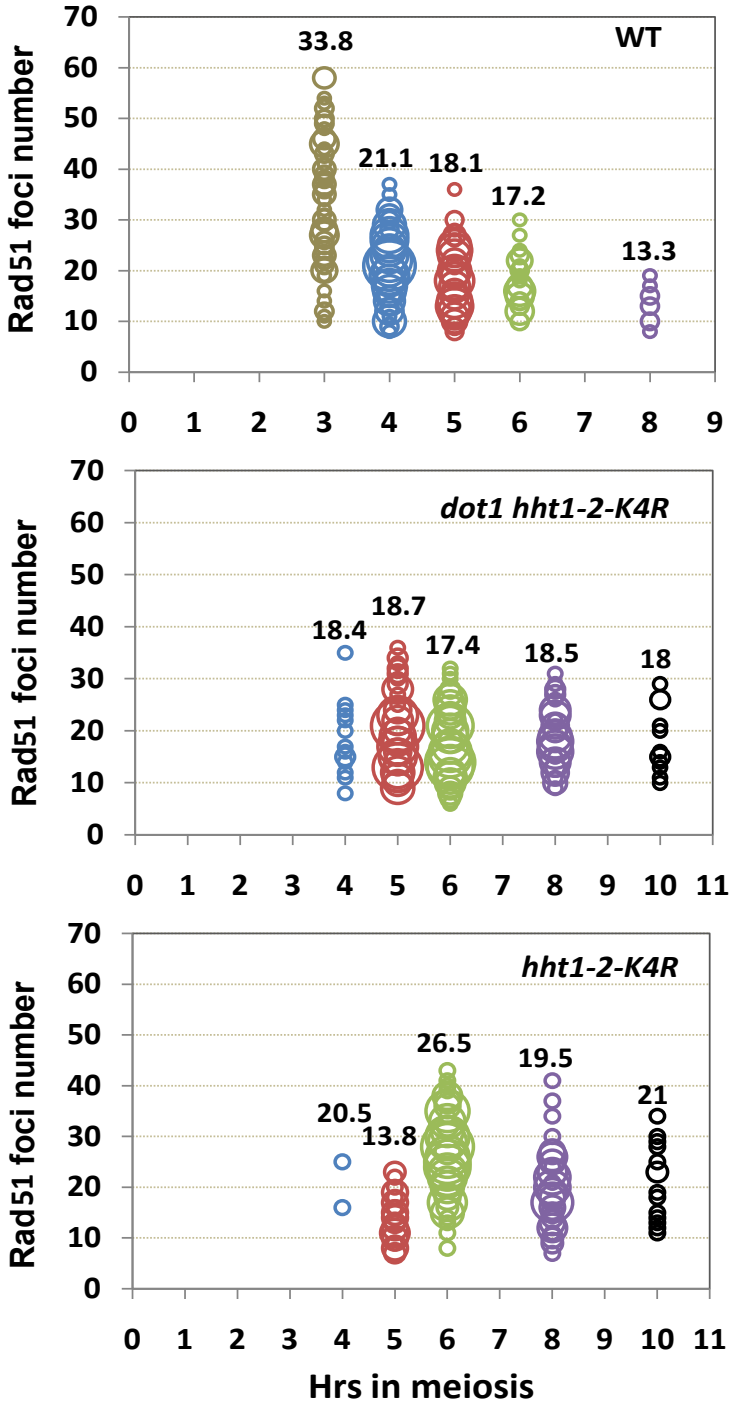
Rad51 foci number
WT
33.8
21.1
18.1
17.2
13.3
dot1 hht1-2-K4R
18.4
18.7
17.4
18.5
18
hht1-2-K4R
20.5
13.8
26.5
19.5
21
0 1 2 3 4 5 6 7 8 9 10 11
Hrs in meiosis

Figure 9

G

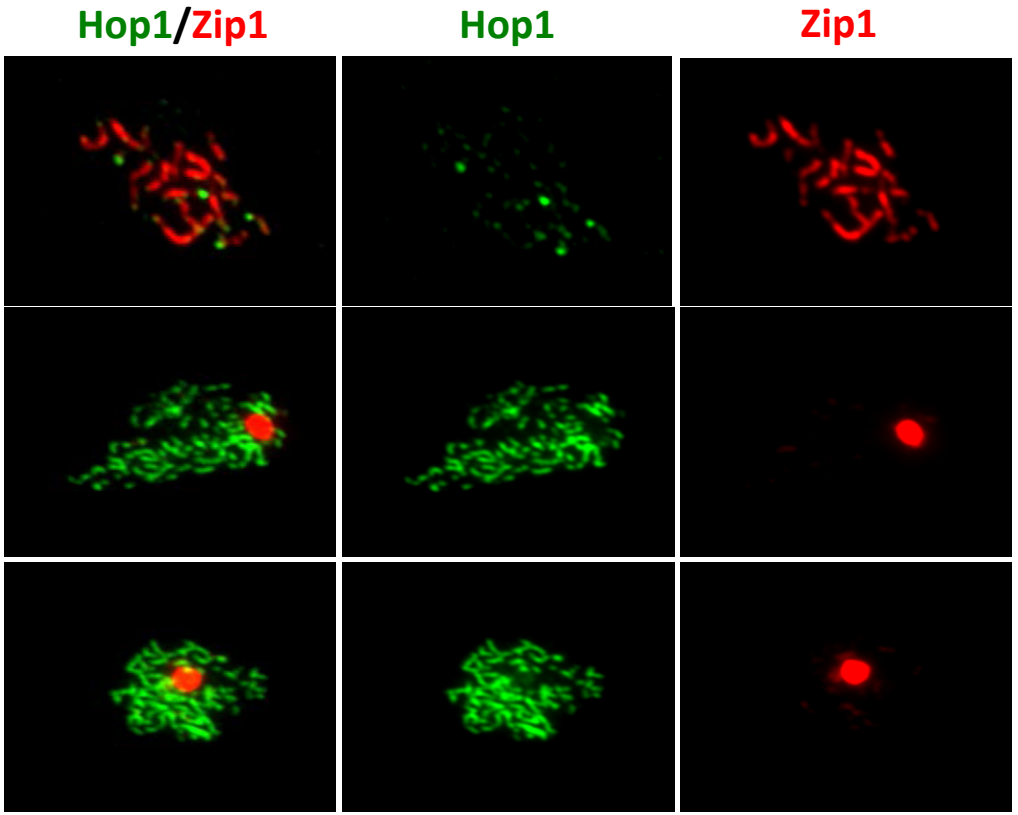
Hop1/Zip1
Hop1
Zip1
WT
hht1-2-K4R
dot1 hht1-2-K4R

H

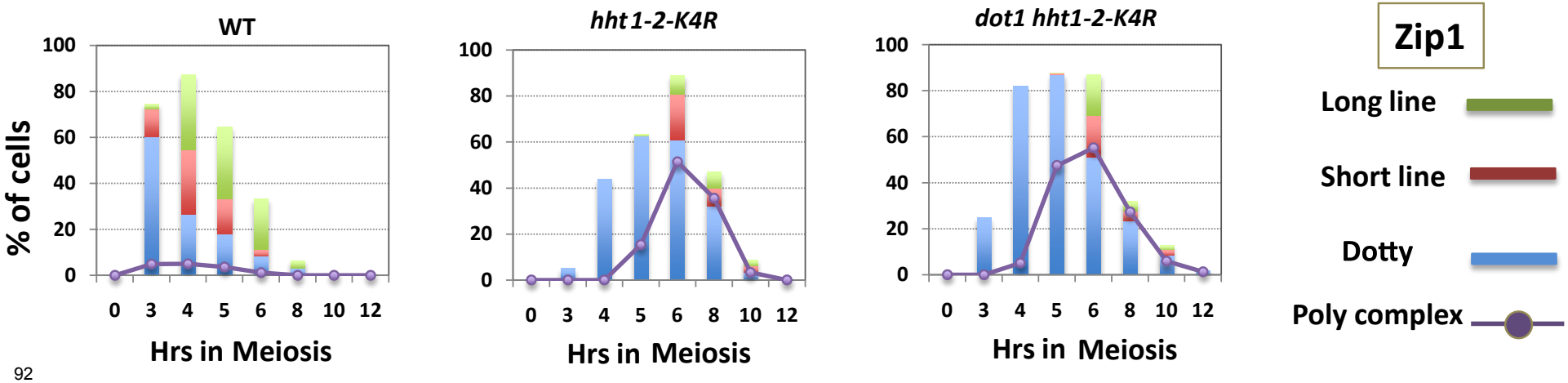
WT
hht1-2-K4R
dot1 hht1-2-K4R
% of cells
100
80
60
40
20
0
0 3 4 5 6 8 10 12
Hrs in Meiosis
Zip1
Long line
Short line
Dotty
Poly complex

Figure 10

A

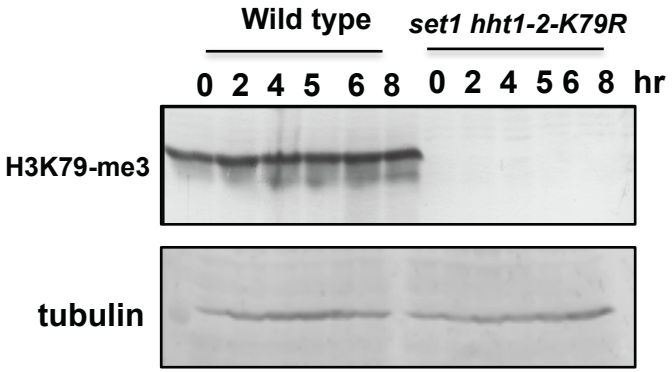

C

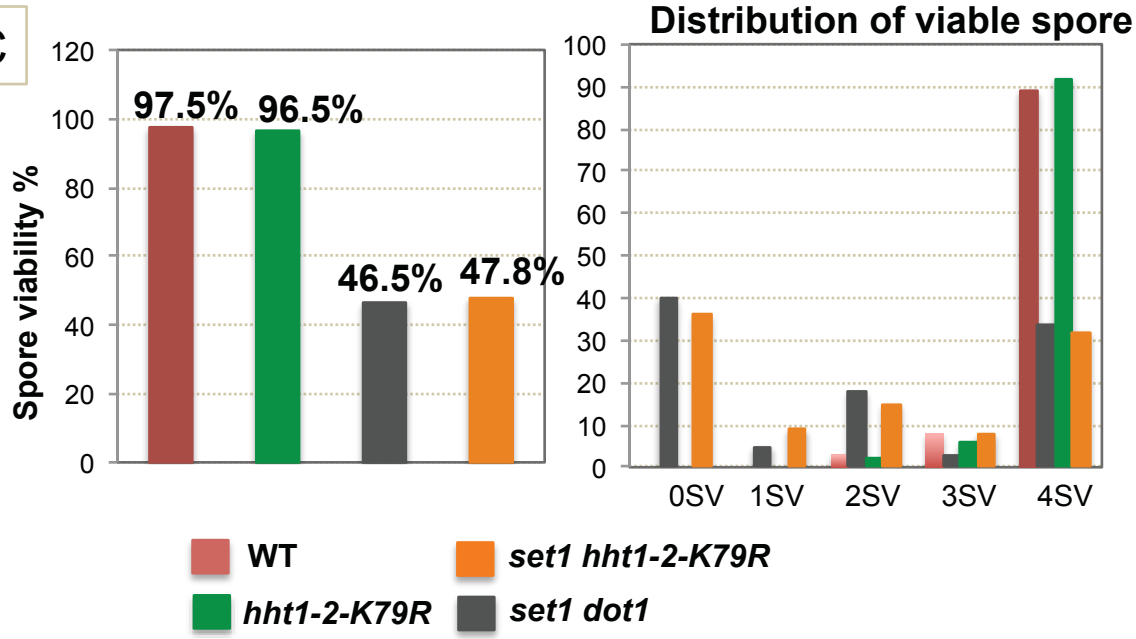

B

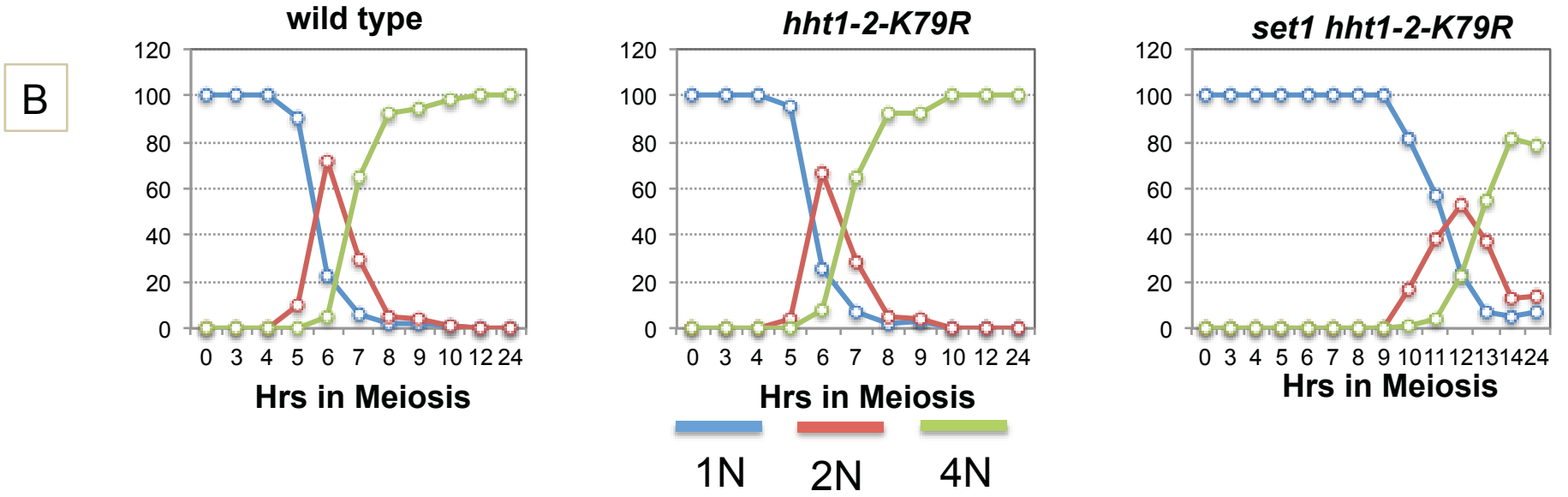

Figure 10

D

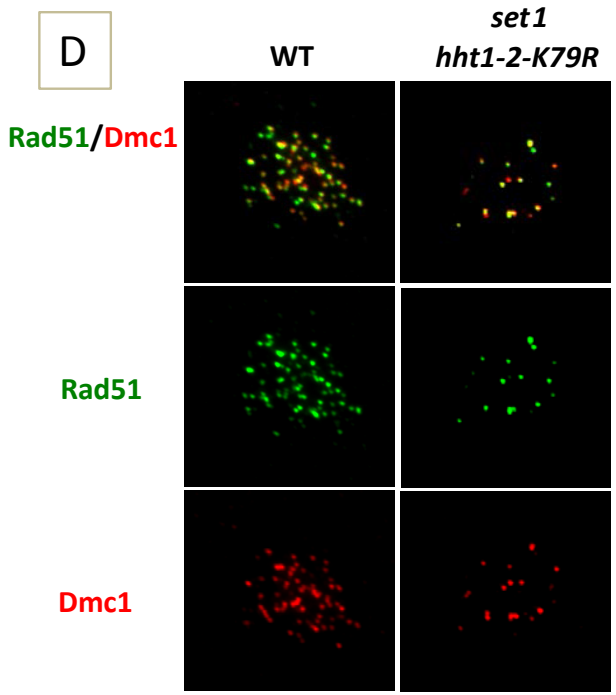
WT
set1
hht1-2-K79R
Rad51/Dmc1
Rad51
Dmc1

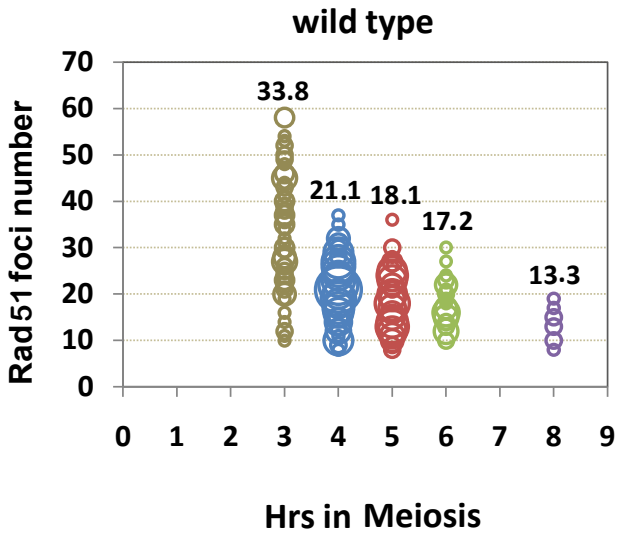
wild type
Rad51 foci number
33.8
21.1
18.1
17.2
13.3
Hrs in Meiosis

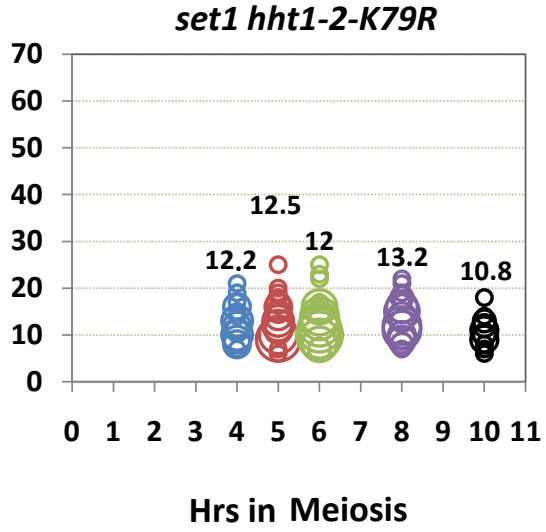
set1 hht1-2-K79R
12.2
12.5
12
13.2
10.8
Hrs in Meiosis

E

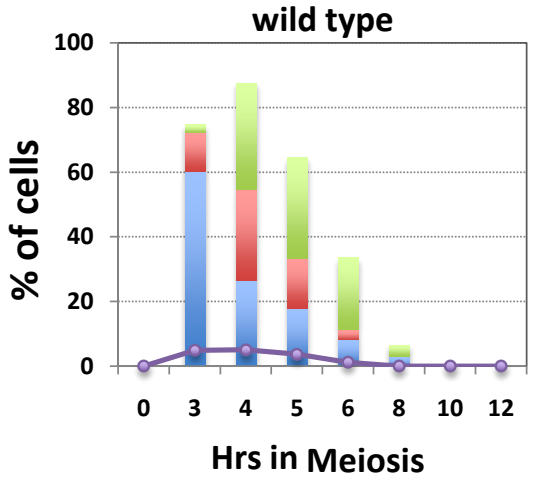
wild type
% of cells
Hrs in Meiosis

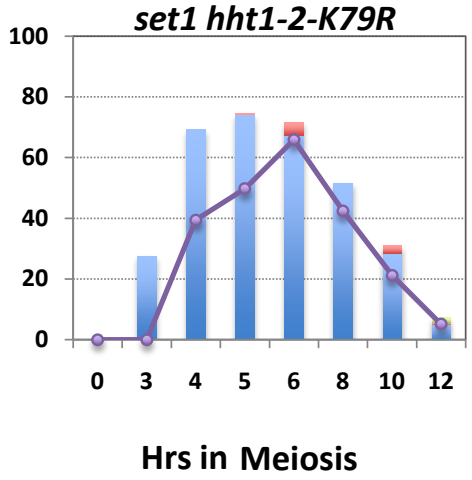
set1 hht1-2-K79R
Hrs in Meiosis

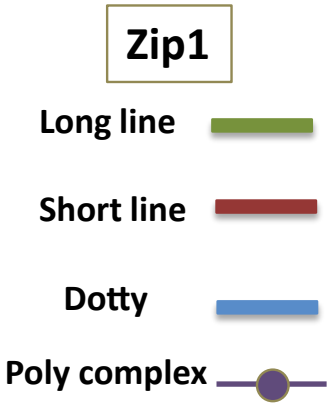
Zip1
Long line
Short line
Dotty
Poly complex

Figure 11

A

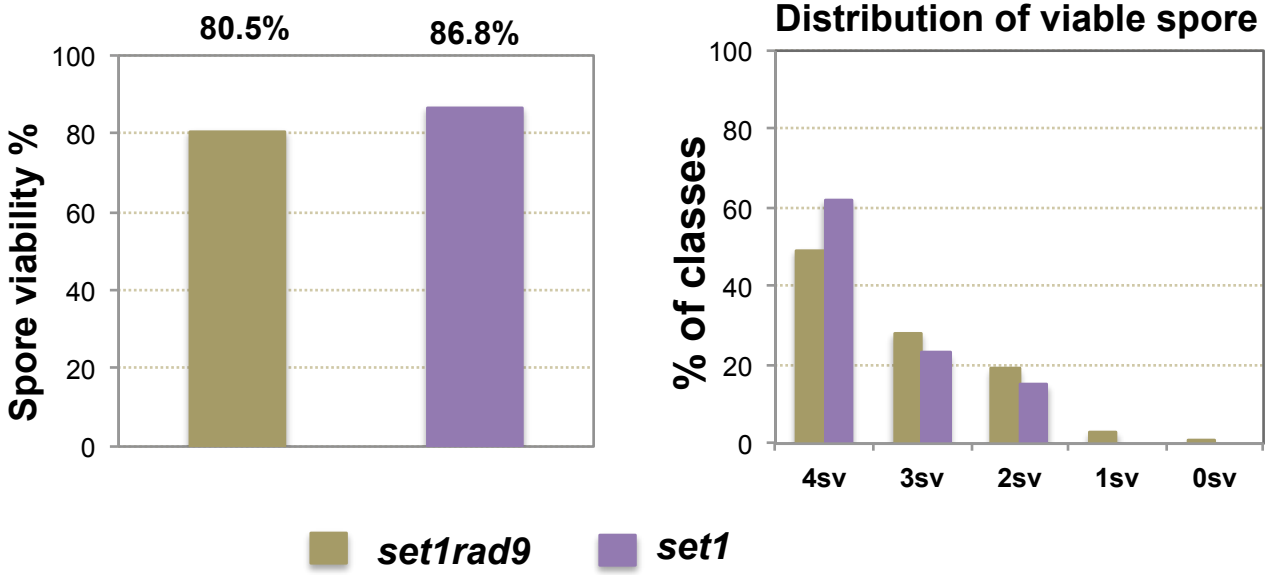
80.5%
86.8%
Spore viability %
100
80
60
40
20
0
Distribution of viable spore
% of classes
4sv
3sv
2sv
1sv
0sv
set1rad9
set1

B

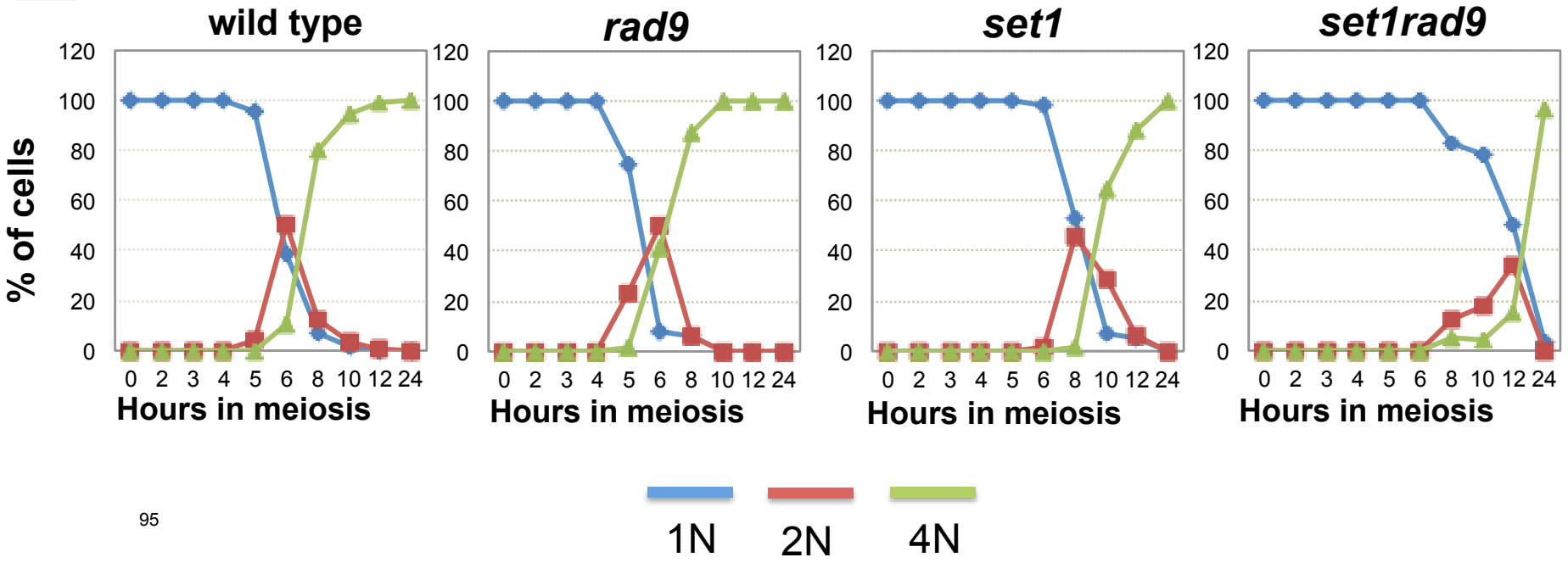
wild type
rad9
set1
set1rad9
% of cells
120
100
80
60
40
20
0
0 2 3 4 5 6 8 10 12 24
Hours in meiosis
1N
2N
4N

Figure 12

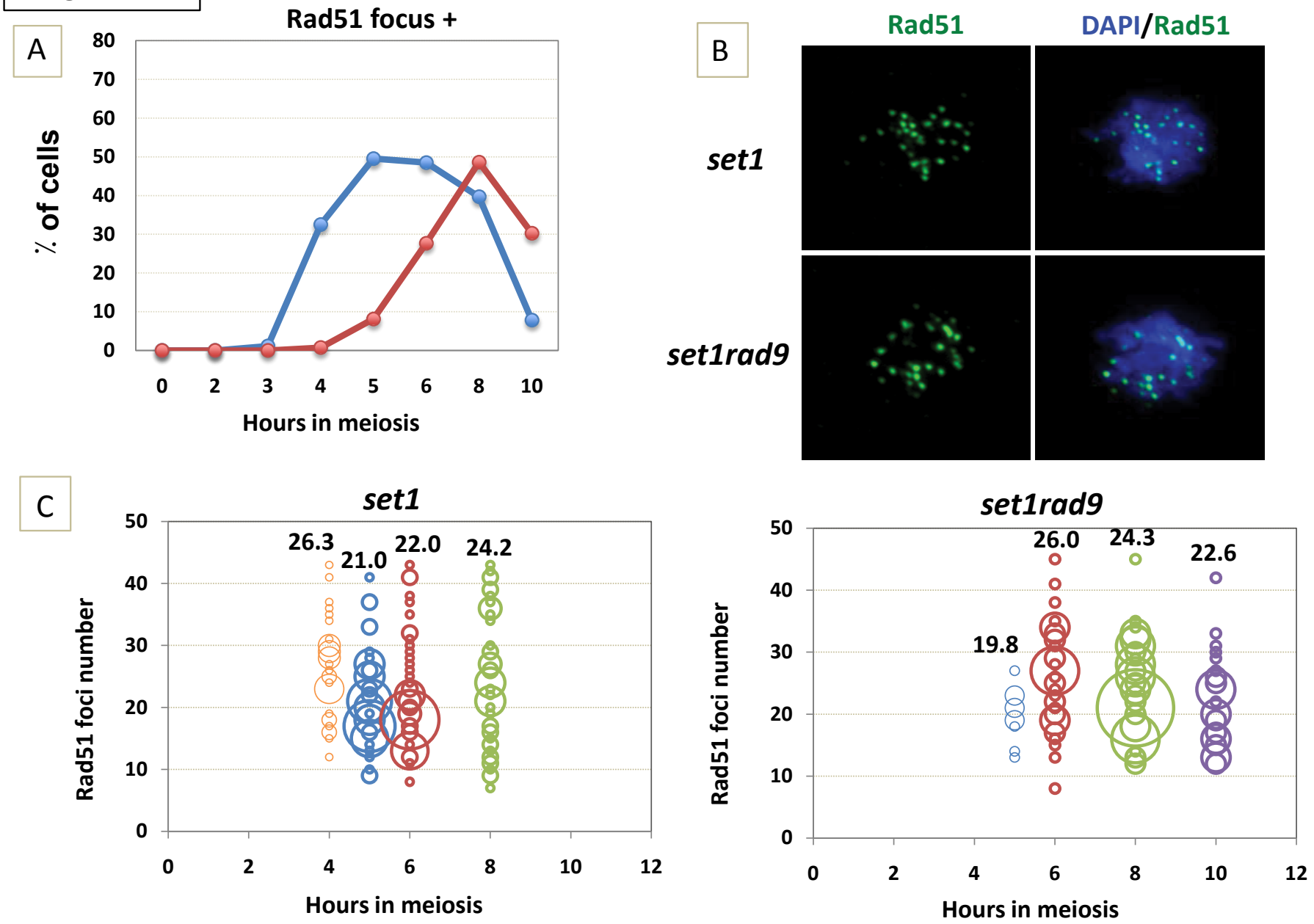
A
Rad51 focus +
% of cells
80
70
60
50
40
30
20
10
0
0 2 3 4 5 6 8 10
Hours in meiosis
B
Rad51
DAPI/Rad51
set1
set1rad9
C
set1
Rad51 foci number
50
40
30
20
10
0
26.3
21.0
22.0
24.2
0 2 4 6 8 10 12
Hours in meiosis
set1rad9
Rad51 foci number
50
40
30
20
10
0
19.8
26.0
24.3
22.6
0 2 4 6 8 10 12
Hours in meiosis

Figure 13

A

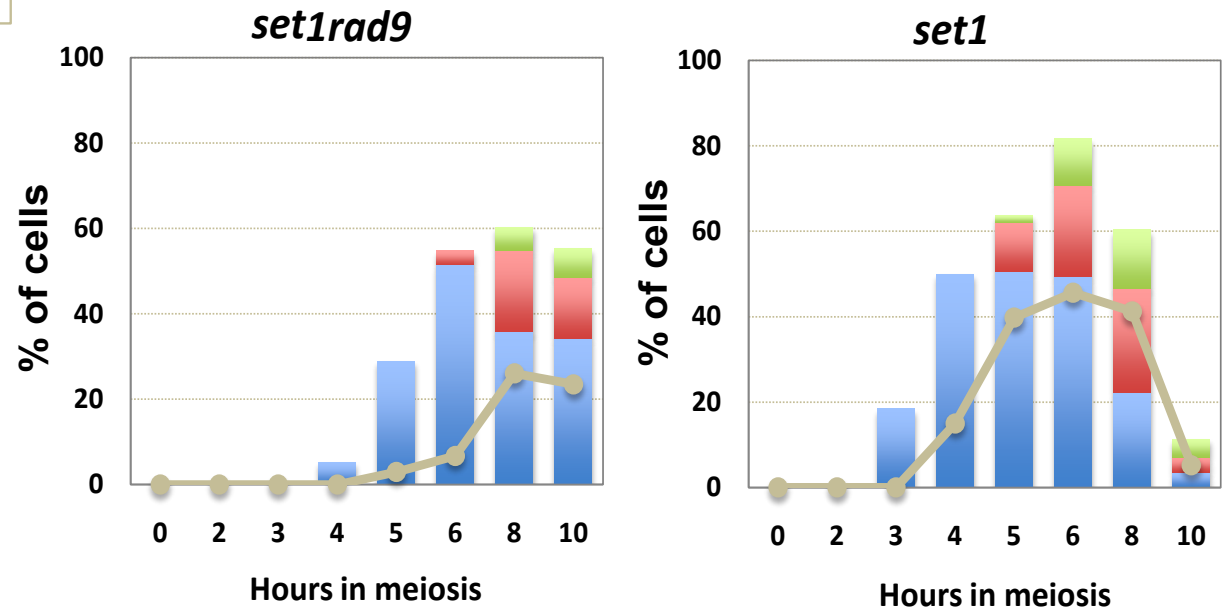
set1rad9
set1
100
80
60
40
20
0
% of cells
0 2 3 4 5 6 8 10
Hours in meiosis

B

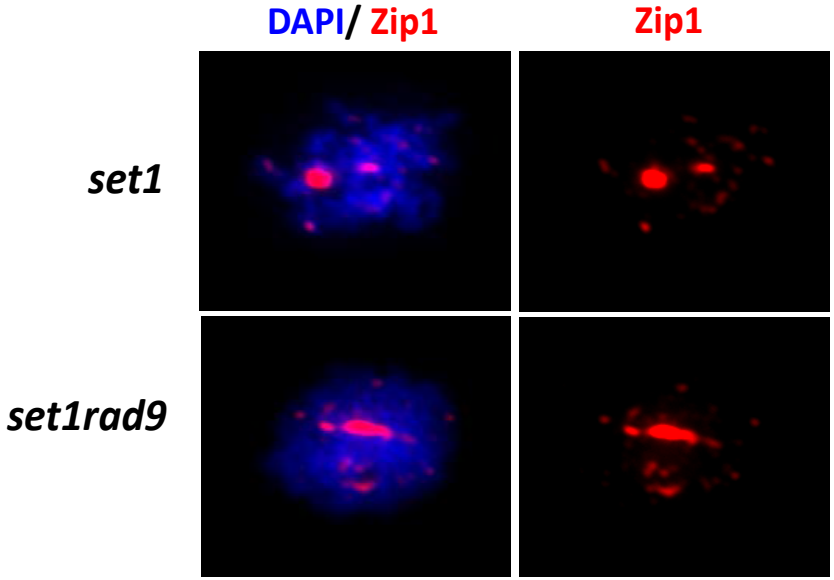
DAPI/ Zip1
Zip1
set1
set1rad9

Figures legend:

Figure 1:

Set1 and Dot1 play differential roles during meiosis.

(A) Meiotic divisions were analyzed by 4', 6'-diamidino-2-phenylindole (DAPI) staining. The percentage of cells entering MI, MII is plotted versus incubation time in SPM. (B) Percentage of spore viability in different strains, 100 tetrads were dissected. (C) Distribution of viable spores in tetrads. Vertical axis shows the percentage of each tetrad class and the horizontal axis represents the number of viable spores in a tetrad. (D) DNA contents in each cell were analyzed by using a fluorescence-activated cell sorter (FACS). (E) & (F) Meiotic lysates from different strains were analyzed by western blotting using anti- tubulin, Zip1, Hop1, Rec8, Red1, Cdc5 and Clb1 sera.

Figure 2:

The *set1* reduces amounts of meiotic DSBs.

(A) DSBs at the *HIS4-LEU2* locus in different strains were analyzed as described in Materials and Methods. (B) Quantification of DSB I fragment to a parental fragment is shown. (C) Schematic drawings of a meiotic recombination hotspot, *HIS4-LEU2* locus, on chromosome III. (D) Crossover (R2) and Non-crossover (R3) recombinants were analyzed by Southern blotting. Percentages of the recombinants are ratio of (R2) or (R3) recombinants to (P1) and (P2) parental fragments. (E) Quantification results are shown for different strains. (F) Schematic drawings of a meiotic recombination hotspot, *HIS4-LEU2* locus, on chromosome III.

Figure 3:

The *set1* and *set1 dot1* show reduction in Rad51-focus formation.

(A) Meiotic chromosome spreads isolated from cells after induction into meiosis were incubated with antibodies to Rad51 and Dmc1. Representative images are shown for each strain (B) Kinetics of Rad51- and Dmc1-focus positive cells. More than 100 nuclei were counted at each time point. A focus-positive cell was defined as a cell with more than five foci. (C) An average number of Rad51 foci in different strains.

All focus-positive cells were chosen and an average number of each focus is shown per a positive nucleus in blue color. The size of diameter of each circle corresponds with the number of a cell with defined numbers of foci.

Figure 4:

Dot1 plays a role in Rad51-focus formation in the absence of Set1.

(A) Meiotic divisions were analyzed by DAPI staining in different strains. The percentage of cells entering MI (2N) and MII (4N), as well as pre-meiotic cells (1N), are plotted versus incubation time in SPM. (B) Meiotic chromosome spreads isolated from different cells after induction into meiosis were incubated with antibodies against Rad51 (green). Representative images with or without DAPI staining (blue) are shown for each strain. (C) Kinetics of Rad51 focus-positive cells. More than 100 nuclei were counted at each time point. A focus-positive cell was defined as a cell with more than five foci. (D) An average number of Rad51 foci in different strains. All focus-positive cells were counted for focus numbers and an average number of each focus is shown per a positive nucleus in black color.

Figure 5:

Dot1 plays a role in DSB formation in the absence of Set1.

(A) DSBs along chromosome III were analyzed in different stains. Yeast chromosomes were separated by clamped homogeneous electric field and were detected by Southern blotting using a probe specific to the end of the left arm of the chromosome. (B) Quantification results. Values plotted with standard deviation bars are the mean of three independent experiments. (C) DSBs along chromosome IV were analyzed in different stains. Yeast chromosomes were separated by clamped homogeneous electric field gel electrophoresis and were detected by Southern blotting using a probe specific to the end of the left arm of this chromosome. (D) Quantification results of bands of specific regions shown (I-III). (E) DSBs at the *YCR048W* locus in different strains were analyzed as described in Materials and Methods. (F) Schematic drawings of a meiotic recombination hotspot; *YCR048W* locus on chromosome III. (G) Quantification of DSB I fragment to parental fragment is shown. Values are an average of two independent experiments with standard deviations.

Figure 6:

Set1 and Dot1 play a role in chromosome morphogenesis.

(A) Meiotic chromosome spreads for different mutants, isolated from cells after induction into meiosis were incubated with antibodies against Hop1 (green) and Zip1 (red). Representative images are shown for each strain. Lower panel shows staining of Hop1 and Zip1 for wild type cells at different stages in prophase-I. (B) Nuclear spreads from different strains were stained with anti-Zip1. Quantification of Zip1 staining was done for 3 different classes. Pictures show Zip1 staining, which was classified into three classes; dotty (blue), short (red) and long (green) and one more class (brown lines) show aggregates of Zip1 called poly complex as indicated by the white arrow. Representative staining images of Zip1 for each class are shown in bottom. (C) Kinetics of Hop1-positive cells. More than 100 nuclei were counted at each time point for different strains. (D) Hop1 accumulation was classified into short line (green) and long lines (red).

Figure 7:

Set1 and Dot1 play a role in chromosome morphogenesis.

(A) Nuclear spreads from different strains were stained with anti-Rec8 (green) and anti-Red1 (red). (B) Kinetics of Rec8- and Red1-positive cells. More than 100 nuclei were counted at each time point. (C) Quantification of Red1/Rec8 poly-complex in *set1* and *set1 dot1* (bottom). The Top picture shows the Red1/Rec8 poly-complex indicated by a blue arrow.

Figure 8:

Dot1 is required for proper Pch2 localization in the absence of Set1.

(A) Kinetics of Pch2-positive cells. Nuclear spreads from different strains were stained with anti-Pch2 (green) and anti-Zip1 (red). More than 100 nuclei were counted at each time point. (B) Representative images for Pch2 and Zip1 staining in different strains. White arrow shows the nucleolus and the yellow arrow shows the Pch2 polycomplex. (C) Quantification of Pch2/Zip1 polycomplex in *set1* and *set1dot1*. Cells positive for the polycomplex were counted and percentages were plotted. (D) Representative images for Pch2/Zip1 poly complex in *set1* and *set1dot1*.

Figure 9:

The histone H3K4 mutant is defective is SC formation.

(A) Meiotic lysates from wild type and *hht1-2-K4R* cells were analyzed by western blotting using anti-H3K4me3 and anti-tubulin. (B) Percentages of spore viability in different strains, 100 tetrads were dissected. Distribution of viable spores in tetrads, the vertical axis shows the percentage of each tetrad class and the horizontal axis represents a number of viable spores in a tetrad. (C) Meiotic divisions were analyzed by DAPI staining. The percentage of cells entering MI (2N), and MII (4N) as well as pre-meiotic cells (1N) are plotted over incubation time in SPM. (D) Meiotic chromosome spreads isolated from cells after induction into meiosis were incubated with antibodies against Rad51 (green) and Dmc1 (red). Representative images are shown for each strain. (E) Kinetics of Rad51-positive cells. More than 100 nuclei were counted at each time point. A focus-positive cell was defined as a cell with more than five foci. (F) Average numbers of Rad51 foci in different strains. All focus-positive cells were counted and an average number of each focus is shown per a positive nucleus in black color. (G) Meiotic chromosome spreads for different mutants isolated from cells after induction into meiosis were incubated with antibodies against Hop1 (green) and Zip1 (red). Representative images are shown for each strain. (H) Quantification of Zip1 staining classified into three classes; dotty (blue), short (red), and long (green), and also one more class showing aggregates of Zip1 called poly complex.

Figure 10:

Histone H3K79 methylation is critical for DSB formation as well as the synaptonemal complex assembly.

(A) Meiotic lysates from wild type and *set1 hht1-2-K79R* cells were analyzed by western blotting using anti-H3K79me3 and anti-tubulin. (B) Meiotic divisions were analyzed by DAPI staining. The percentage of cells entering MI (2N), and MII (4N) as well as pre-meiotic cells (1N) are plotted over incubation time in SPM. (C) Percentage of spore viability in different strains, 100 tetrads were dissected. Distribution of viable spores in tetrads, the vertical axis shows the percentage of each tetrad class and the horizontal axis represents the number of viable spores in a tetrad. (D) Meiotic chromosome spreads isolated from cells after induction into meiosis were

incubated with antibodies against Rad51 (green) and Dmc1 (red), an average number of Rad51 foci in different strains, all focus-positive cells were counted for focus and an average number of each focus is shown per a positive nucleus in black color. Representative images are shown for each strain. (E) Meiotic chromosome spreads for different mutants, isolated from cells after induction into meiosis were incubated with antibody against Zip1 (red), Quantification of Zip1 staining classified into three classes; dotty (blue), short (red) and long (green) and one more class show aggregates of Zip1 called poly complex.

Figure 11:

Rad9 might have a meiotic function in the absence of Set1.

(A) Percentage of spore viability in different strains (left). 100 tetrads were dissected. Distribution of viable spores in tetrads (right), the vertical axis shows the percentage of each tetrad class and the horizontal axis represents the number of viable spores in a tetrad. (B) Meiotic divisions for each strain were analyzed by DAPI staining. The percentage of cells entering MI (2N), and MII (4N) as well as pre-meiotic cells (1N) are plotted over incubation time in SPM.

Figure 12:

Rad9 does not contribute to the DSB formation in the absence of set1.

(A) Meiotic chromosome spreads isolated from cells after induction into meiosis were incubated with antibodies against Rad51 (green). Kinetics of Rad51 focus-positive cells is shown as a graph. More than 100 nuclei were counted at each time point. A focus-positive cell was defined as a cell with more than five foci. (B) Representative images with or without DAPI staining (blue) are shown for each strain. (C) An average number of Rad51 foci in different strains. All focus-positive cells were counted for focus and an average number of each focus is shown per a positive nucleus in black color.

Figure 13:

Rad9 does not contribute to the SC formation in the absence of set1.

(A) Meiotic chromosome spreads for different mutants, isolated from cells after induction into meiosis were incubated with antibody against Zip1 (red). The staining

patterns are classified into three classes and quantified in a graph; dotty (blue), short (red) and long (green) and one more class with aggregates of Zip1 called poly complex as described above. (B) Representative images are shown for each strain.

3-2. Discussion and models:

Previous reports on the roles of histone modification during meiosis have shown that two histone-modifications, H2BK123 ubiquitylation and H3K4 methylation play essential roles in the formation of meiotic DSBs (Sollier et al., 2004; Yamashita et al., 2004; Borde et al., 2009). So far, the role of histone H3K79 methylation in DSB formation has not yet been demonstrated. In this study, I showed a role of Dot1-dependent H3K79 methylation in DSB formation in the absence of Set1-dependent H3k4 methylation, which confirms the importance of this modification mark during meiotic recombination.

In this study, by using a cytological analysis of Rad51 foci, which marks a site of ongoing recombination (Bishop, 1994), I demonstrated that even in the absence of Set1-dependent H3K4 methylation, meiotic cells managed to form a relatively high amounts of DSBs around ¾ of levels detected in the wild type cells. In contrast to Borde et al. (2009) using genome wide mapping of the DSB sites detected as RPA-enriched sites by ChIP-chip, the absence of Set1 showed big reduction in DSBs levels. In this study, *set1* mutant showed a mild reduction of Rad51 focus number along the genome. Furthermore, DSB mapping on individual chromosomes in *set1* support the idea. Rad51 focus counting seems to be more reliable than ChIP to determine a steady number of DSBs in a nucleus. Although the previous studies

suggested an essential role of Set1 in DSB formation, my results suggest that the contribution of Set1-dependent H3K4 methylation in DSB formation is weaker than expected. This suggests the existence of other factors or determinants affecting DSB formation at least in the budding yeast.

Importantly, I found that the elimination of Dot1-dependent H3K79 methylation in the *set1* mutant background showed reduction of DSBs levels to about half to that detected in the *set1* single mutant. This indicates the involvement of this histone modification mark in DSB formation. Previous studies on other organisms confirm the involvement of multiple epigenetic marks in determining the site of initiation of meiotic recombination. For example, in fission yeast, Yamada and Ohta (2013) demonstrated that H3K9 acetylation is required to promote DSB formation, and also showed that meiotic DSBs levels in this yeast are not affected by the elimination of the H3K4 methylation. In my study, and even in the absence of both Set1 and Dot1, cells managed to form about 40-50% of the wild type levels of Rad51 foci, likely DSBs, suggesting the presence of other determinants for hotspot activity which might be another histone modification.

I also found a novel role for Set1-dependent H3K4 methylation in chromosome morphogenesis during meiosis, in particular, an essential role in the SC formation. Both the *set1* single and the *hht1-2-K4R* double mutants yield spores with high viability, indicating little defects during meiotic cell cycle. However, the cytological studies showed that both of the mutants showed a severe defect in the SC elongation. The SC elongation defect in these mutants is indicated by sustained loading of Hop1, which often forms linear lines unlike discontinues staining pattern seen in the wild type. This defect in SC elongation might be caused by abnormal assembly of chromosome axes proteins such as Rec8 and Red1, both of which

accumulate and form an aggregate-like structure, called polycomplex. This abnormal localization of the axes proteins has not been seen either in wild type or in other mutants defective in synapsis such as *zip1* or *dmc1* mutants (Smith and Roeder, 1997). This may suggest that the recombination defect seen in the absence of Set1 or H3K4 methylation; e.g reduction of DSBs, cannot account for the abnormal assembly of Hop1 and also the accumulation of Rec8-Red1 aggregates. This raises the possibility that Set1-dependent H3K4 methylation may actually play a direct role in the assembly of Red1 or Rec8 in the context of meiotic chromosomes. Other possibility might be that the reduction in DSBs level is directly connected to the defect in SC assembly. In this scenario, extra amounts of DSBs in wild type cells are required for normal chromosome synapsis rather than recombination. This idea is somehow consistent with a previous proposal of two types of DSBs; one for synapsis and the other for recombination (Zalevsky et al., 1999; Stahl et al., 2004).

The fact that *set1* single mutant shows reduced DSB formation compared to wild type with slight reduction in spore viability implies that the minimal amount of DSBs required for proper meiotic recombination is achieved in *set1* single mutant. As a result, the reduction in DSB formation has little impact on meiotic recombination products. In the case of the *set1 dot1* double mutant, more reduction in DSB formation is seen compared to *set1* single mutant. This suggests that an amount of DSB in the double mutant is not sufficient enough for proper meiotic recombination products, leading to big reduction in spore viability.

Results described here suggest that H3K79 methylation plays a role in DSB formation. Previous reports demonstrated that, histone H3K79 methylation is recognized by the Tudor domain of Rad9 in yeast (Grenon et al., 2007; Lydal et al., 1996). In this study I analyzed the *set1 rad9* double mutant for DSB formation. Using

the cytological analysis of Rad51 foci, I found that Rad9 does not contribute to DSB formation in the absence of Set1. At the moment, to confirm this, I am constructing the *set1 rad9 dmc1* triple mutant where DSBs are not repaired. This suggests that protein other than Rad9 reads this histone methyl mark. In future, I need to find the protein, which may recognize the H3K79 methylation mark and will study the role in DSB formation in the absence of Set1. Based on my results, I propose that meiotic chromosomes adapt different alternatives to create the recombination hotspot, possibly using different histone marks. This kind of multiple alternatives or flexibility for the determination of DSB sites may contribute to the rapid evolution of the recombination hotspots. In summary, I think that multiple histone modifications can affect a DSB hotspot activity. It has been reported that Spp1 protein can read the H3K4 methylation leading to the recruitment of Spo11 protein to the DSB site through the interaction of Spp1 with a Spo11 accessory protein Mer2 (Sommermeyer et al., 2013). In the absence of H3K4 methylation, the H3K79 methylation might work as a backup system to ensure the formation of a proper DSBs level, as a part of homeostatic control of DSBs. Indeed, in the absence of both Set1 and Dot1, cells can still manage to form a substantial level of DSBs, suggesting the presence of homeostatic control on DSB formation, which might be other histone modification, (Model I-I).

As mentioned above, I found the role of histone modification in SC elongation. I am now thinking two possibilities for the roles of histone methylation in the SC formation; first, the existence of a putative factor “X” which can read the methylation mark to promote a proper folding of axis structures by recruiting or stabilizing SC components. Other possibility, although not exclusive from the first possibility, histone methylation may induce specific chromosome structure; e.g.

proper folding of the chromosomes, which in turn modulates chromosome axis structures leading to the normal assembly of the SC components, (Model I-II).

Model I-I

Wild type
Normal DSB level

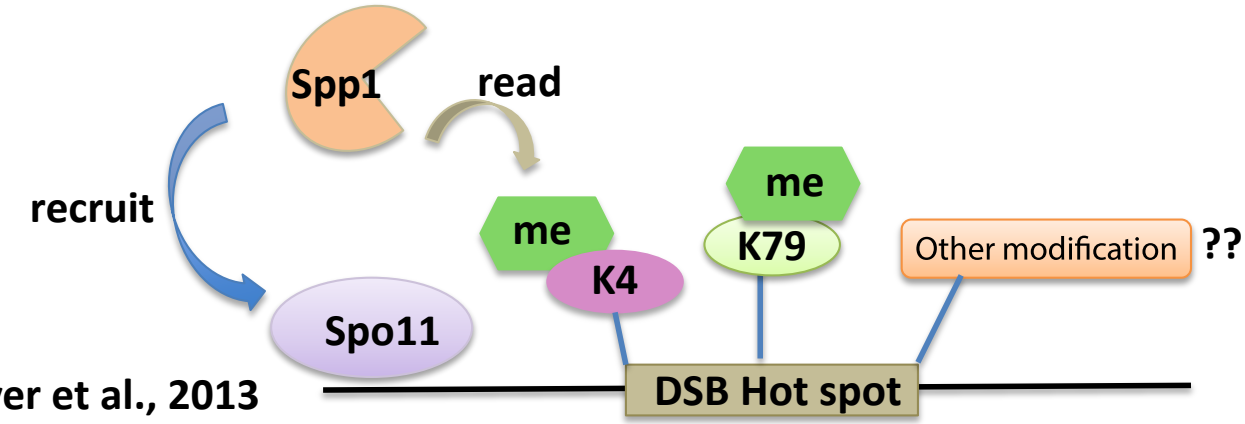

Sommermeyer et al., 2013

Absence of K4me (K4R) or *set1* mutants

Reduced DSB level

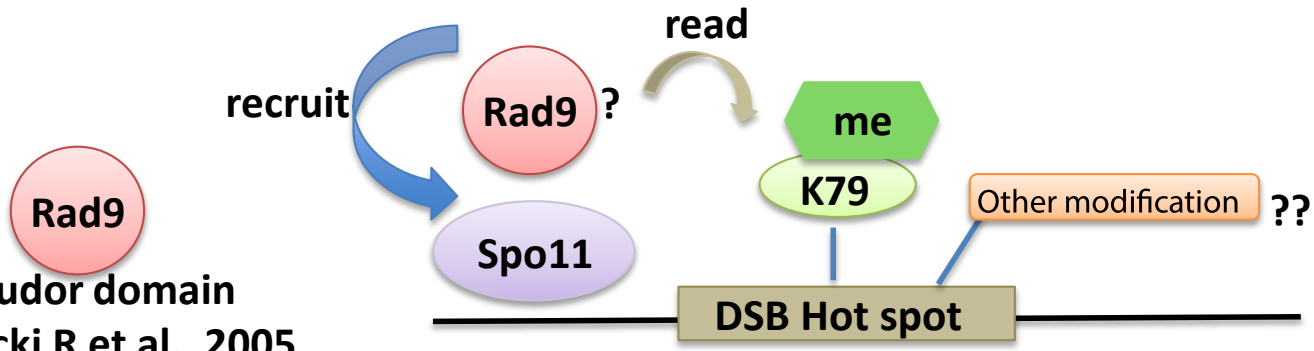

Wysocki R et al., 2005

Absence of K4me and K79me or *set1 dot1* mutant

More reduction in DSB level

Model I – II

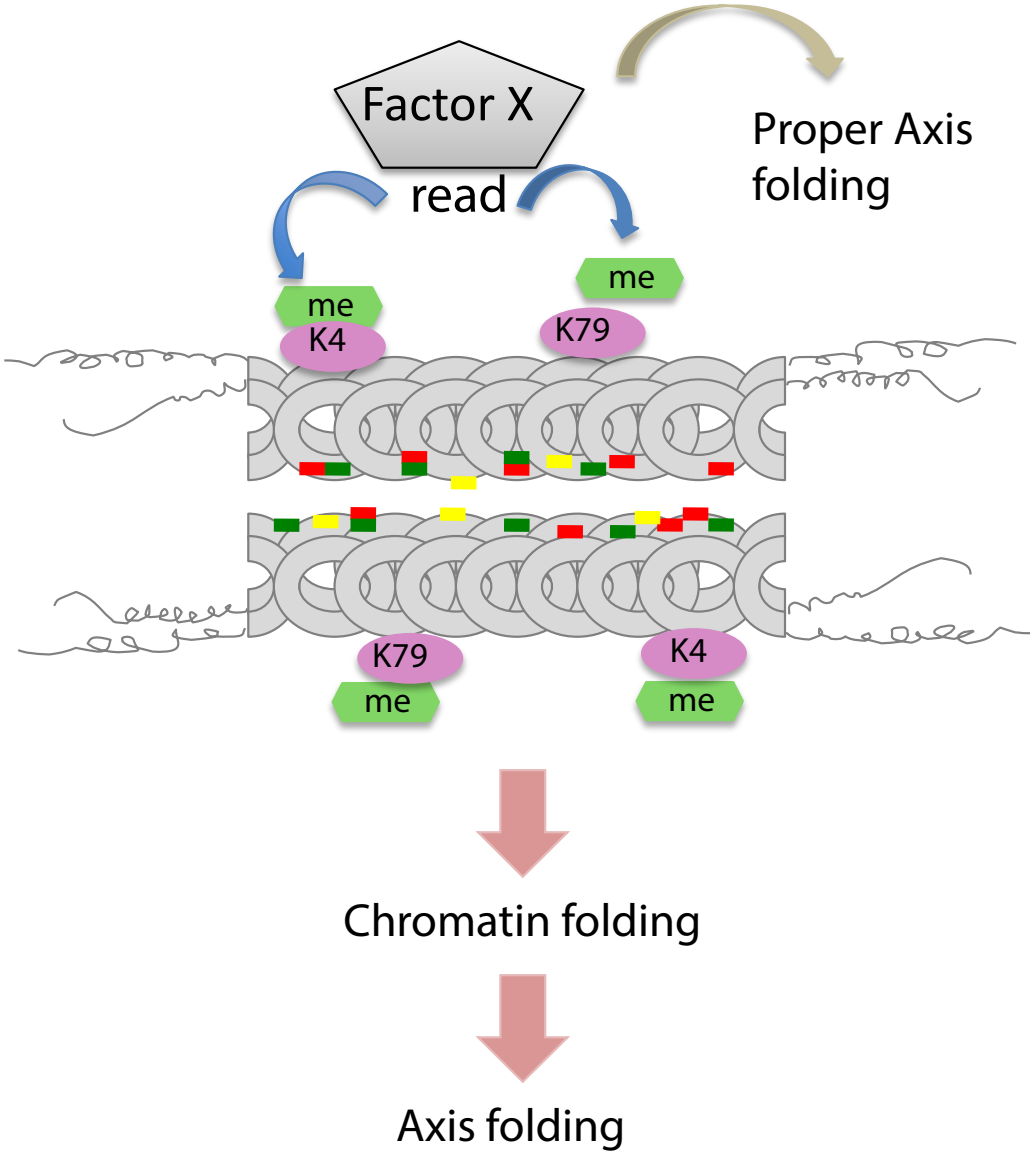
Factor X
read
Proper Axis
folding
me
K4
me
K79
K79
me
K4
me
Chromatin folding
Axis folding

References:

Agarwal, S., and G. S. Roeder, 2000 Zip3 provides a link between recombination enzymes and synaptonemal complex proteins. Cell 102**:** 245-255.

Aravind, L., D. R. Walker and E. V. Koonin, 1999 Conserved domains in DNA repair proteins and evolution of repair systems. Nucleic Acids Res 27**:** 1223-1242.

Bannister, A. J., and T. Kouzarides, 2011 Regulation of chromatin by histone modifications. Cell Res 21**:** 381-395.

Berger, S. L., 2002 Histone modifications in transcriptional regulation. Curr Opin Genet Dev 12**:** 142-148.

Bird, A. W., D. Y. Yu, M. G. Pray-Grant, Q. Qiu, K. E. Harmon *et al.*, 2002 Acetylation of histone H4 by Esa1 is required for DNA double-strand break repair. Nature 419**:** 411-415.

Bishop, D. K., 1994 RecA homologs Dmc1 and Rad51 interact to form multiple nuclear complexes prior to meiotic chromosome synapsis. Cell 79**:** 1081-1092.

Bishop, D. K., D. Park, L. Xu and N. Kleckner, 1992 DMC1: a meiosis-specific yeast homolog of E. coli recA required for recombination, synaptonemal complex formation, and cell cycle progression. Cell 69**:** 439-456.

Borde, V., N. Robine, W. Lin, S. Bonfils, V. Geli *et al.*, 2009 Histone H3 lysine 4 trimethylation marks meiotic recombination initiation sites. EMBO J 28**:** 99-111.

Borner, G. V., A. Barot and N. Kleckner, 2008 Yeast Pch2 promotes domainal axis organization, timely recombination progression, and arrest of defective recombinosomes during meiosis. Proc Natl Acad Sci U S A 105**:** 3327-3332.

Borner, G. V., N. Kleckner and N. Hunter, 2004 Crossover/noncrossover differentiation, synaptonemal complex formation, and regulatory surveillance at the leptotene/zygotene transition of meiosis. Cell 117**:** 29-45.

Brachet, E., V. Sommermeyer and V. Borde, 2012 Interplay between modifications of chromatin and meiotic recombination hotspots. Biol Cell 104**:** 51-69.

Brar, G. A., A. Hochwagen, L. S. Ee and A. Amon, 2009 The multiple roles of cohesin in meiotic chromosome morphogenesis and pairing. Mol Biol Cell 20**:** 1030-1047.

Cao, L., E. Alani and N. Kleckner, 1990 A pathway for generation and processing of double-strand breaks during meiotic recombination in S. cerevisiae. Cell 61**:** 1089-1101.

Carballo, J. A., A. L. Johnson, S. G. Sedgwick and R. S. Cha, 2008 Phosphorylation of the axial element protein Hop1 by Mec1/Tel1 ensures meiotic interhomolog recombination. Cell 132**:** 758-770.

Celeste, A., S. Petersen, P. J. Romanienko, O. Fernandez-Capetillo, H. T. Chen *et al.*, 2002 Genomic instability in mice lacking histone H2AX. Science 296**:** 922-927.

Cheng, C. H., Y. H. Lo, S. S. Liang, S. C. Ti, F. M. Lin *et al.*, 2006 SUMO modifications control assembly of synaptonemal complex and polycomplex in meiosis of Saccharomyces cerevisiae. Genes Dev 20**:** 2067-2081.

Chua, P. R., and G. S. Roeder, 1998 Zip2, a meiosis-specific protein required for the initiation of chromosome synapsis. Cell 93**:** 349-359.

Clerici, M., D. Mantiero, G. Lucchini and M. P. Longhese, 2006 The Saccharomyces cerevisiae Sae2 protein negatively regulates DNA damage checkpoint signalling. EMBO Rep 7**:** 212-218.

de los Santos, T., and N. M. Hollingsworth, 1999 Red1p, a MEK1-dependent phosphoprotein that physically interacts with Hop1p during meiosis in yeast. J Biol Chem 274**:** 1783-1790.

Dehe, P. M., and V. Geli, 2006 The multiple faces of Set1. Biochem Cell Biol 84**:** 536-548.

Dobson, M. J., R. E. Pearlman, A. Karaiskakis, B. Spyropoulos and P. B. Moens, 1994 Synaptonemal complex proteins: occurrence, epitope mapping and chromosome disjunction. J Cell Sci 107 (Pt 10)**:** 2749-2760.

Dong, H., and G. S. Roeder, 2000 Organization of the yeast Zip1 protein within the central region of the synaptonemal complex. J Cell Biol 148**:** 417-426.

Eijpe, M., H. Offenberg, R. Jessberger, E. Revenkova and C. Heyting, 2003 Meiotic cohesin REC8 marks the axial elements of rat synaptonemal complexes before cohesins SMC1beta and SMC3. J Cell Biol 160**:** 657-670.

Essers, J., A. B. Houtsmuller, L. van Veelen, C. Paulusma, A. L. Nigg *et al.*, 2002 Nuclear dynamics of RAD52 group homologous recombination proteins in response to DNA damage. EMBO J 21**:** 2030-2037.

Farmer, S., E. J. Hong, W. K. Leung, B. Argunhan, Y. Terentyev *et al.*, 2012 Budding yeast Pch2, a widely conserved meiotic protein, is involved in the initiation of meiotic recombination. PLoS One 7**:** e39724.

Fischle, W., B. S. Tseng, H. L. Dormann, B. M. Ueberheide, B. A. Garcia *et al.*, 2005 Regulation of HP1-chromatin binding by histone H3 methylation and phosphorylation. Nature 438**:** 1116-1122.

Fukuda, T., K. Kugou, H. Sasanuma, T. Shibata and K. Ohta, 2008 Targeted induction of meiotic double-strand breaks reveals chromosomal domain-

dependent regulation of Spo11 and interactions among potential sites of meiotic recombination. Nucleic Acids Res 36**:** 984-997.

Govin, J., J. Dorsey, J. Gaucher, S. Rousseaux, S. Khochbin *et al.*, 2010 Systematic screen reveals new functional dynamics of histones H3 and H4 during gametogenesis. Genes Dev 24**:** 1772-1786.

Greon, M., T. Costelloe, S.Jimeno, A. O'Shaughnessy, J. Fitzgerald *et al*.,2007 Docking onto chromatin via the *Sacharomyces cerevisiae* Rad9 Tudor domain. Yeast 24: 105-119.

Handel, M. A., and J. C. Schimenti, 2010 Genetics of mammalian meiosis: regulation, dynamics and impact on fertility. Nat Rev Genet 11**:** 124-136.

Harrington, L. A., and B. J. Andrews, 1996 Binding to the yeast SwI4,6-dependent cell cycle box, CACGAAA, is cell cycle regulated in vivo. Nucleic Acids Res 24**:** 558-565.

Hawley, R. S., 2011 Solving a meiotic LEGO puzzle: transverse filaments and the assembly of the synaptonemal complex in Caenorhabditis elegans. Genetics 189**:** 405-409.

Hernandez-Hernandez, A., G. H. Vazquez-Nin, O. M. Echeverria and F. Recillas-Targa, 2009 Chromatin structure contribution to the synaptonemal complex formation. Cell Mol Life Sci 66**:** 1198-1208.

Herskowitz, I., 1988 Life cycle of the budding yeast Saccharomyces cerevisiae. Microbiol Rev 52**:** 536-553.

Hirano, T., 2002 The ABCs of SMC proteins: two-armed ATPases for chromosome condensation, cohesion, and repair. Genes Dev 16**:** 399-414.

Ho, H. C., and S. M. Burgess, 2011 Pch2 acts through Xrs2 and Tel1/ATM to modulate interhomolog bias and checkpoint function during meiosis. PLoS Genet 7**:** e1002351.

Hochwagen, A., and A. Amon, 2006 Checking your breaks: surveillance mechanisms of meiotic recombination. Curr Biol 16**:** R217-228.

Hollingsworth, N. M., L. Goetsch and B. Byers, 1990 The HOP1 gene encodes a meiosis-specific component of yeast chromosomes. Cell 61**:** 73-84.

Hollingsworth, N. M., and L. Ponte, 1997 Genetic interactions between HOP1, RED1 and MEK1 suggest that MEK1 regulates assembly of axial element components during meiosis in the yeast Saccharomyces cerevisiae. Genetics 147**:** 33-42.

Hollingsworth, N. M., L. Ponte and C. Halsey, 1995 MSH5, a novel MutS homolog, facilitates meiotic reciprocal recombination between homologs in Saccharomyces cerevisiae but not mismatch repair. Genes Dev 9**:** 1728-1739.

Hong, E. J., and G. S. Roeder, 2002 A role for Ddc1 in signaling meiotic double-strand breaks at the pachytene checkpoint. Genes Dev 16**:** 363-376.

Hunter, N., 2003 Synaptonemal complexities and commonalities. Mol Cell 12**:** 533-535.

Hunter, N., 2008 Hop1 and the meiotic DNA-damage response. Cell 132**:** 731-732.

Hunter, N., and N. Kleckner, 2001 The single-end invasion: an asymmetric intermediate at the double-strand break to double-holliday junction transition of meiotic recombination. Cell 106**:** 59-70.

Huyen, Y., O. Zgheib, R. A. Ditullio, Jr., V. G. Gorgoulis, P. Zacharatos *et al.*, 2004 Methylated lysine 79 of histone H3 targets 53BP1 to DNA double-strand breaks. Nature 432**:** 406-411.

Joshi, N., A. Barot, C. Jamison and G. V. Borner, 2009 Pch2 links chromosome axis remodeling at future crossover sites and crossover distribution during yeast meiosis. PLoS Genet 5**:** e1000557.

Keeney, S., C. N. Giroux and N. Kleckner, 1997 Meiosis-specific DNA double-strand breaks are catalyzed by Spo11, a member of a widely conserved protein family. Cell 88**:** 375-384.

Kerr, G. W., S. Sarkar and P. Arumugam, 2012 How to halve ploidy: lessons from budding yeast meiosis. Cell Mol Life Sci 69**:** 3037-3051.

Klein, F., P. Mahr, M. Galova, S. B. Buonomo, C. Michaelis *et al.*, 1999 A central role for cohesins in sister chromatid cohesion, formation of axial elements, and recombination during yeast meiosis. Cell 98**:** 91-103.

Kniewel, R., and S. Keeney, 2009 Histone methylation sets the stage for meiotic DNA breaks. EMBO J 28**:** 81-83.

Kouzarides, T., 2007 Chromatin modifications and their function. Cell 128**:** 693-705.

Krogan, N. J., J. Dover, A. Wood, J. Schneider, J. Heidt *et al.*, 2003 The Paf1 complex is required for histone H3 methylation by COMPASS and Dot1p: linking transcriptional elongation to histone methylation. Mol Cell 11**:** 721-729.

Krogh, B. O., and L. S. Symington, 2004 Recombination proteins in yeast. Annu Rev Genet 38**:** 233-271.

Lao, J. P., and N. Hunter, 2010 Trying to avoid your sister. PLoS Biol 8**:** e1000519.

Lazzaro, F., V. Sapountzi, M. Granata, A. Pellicioli, M. Vaze *et al.*, 2008 Histone methyltransferase Dot1 and Rad9 inhibit single-stranded DNA accumulation at DSBs and uncapped telomeres. EMBO J 27**:** 1502-1512.

Leu, J. Y., and G. S. Roeder, 1999 The pachytene checkpoint in S. cerevisiae depends on Swe1-mediated phosphorylation of the cyclin-dependent kinase Cdc28. Mol Cell 4**:** 805-814.

Li, B., M. Carey and J. L. Workman, 2007 The role of chromatin during transcription. Cell 128**:** 707-719.

Loidl, J., H. Scherthan and D. B. Kaback, 1994 Physical association between nonhomologous chromosomes precedes distributive disjunction in yeast. Proc Natl Acad Sci U S A 91**:** 331-334.

Longhese, M. P., D. Bonetti, I. Guerini, N. Manfrini and M. Clerici, 2009 DNA double-strand breaks in meiosis: checking their formation, processing and repair. DNA Repair (Amst) 8**:** 1127-1138.

Lui, D. Y., C. K. Cahoon and S. M. Burgess, 2013 Multiple opposing constraints govern chromosome interactions during meiosis. PLoS Genet 9**:** e1003197.

Lydall, D., Y. Nikolsky, D. K. Bishop and T. Weinert, 1996 A meiotic recombination checkpoint controlled by mitotic checkpoint genes. Nature 383**:** 840-843.

Lynn, A., R. Soucek and G. V. Borner, 2007 ZMM proteins during meiosis: crossover artists at work. Chromosome Res 15**:** 591-605.

Mahadevaiah, S. K., J. M. Turner, F. Baudat, E. P. Rogakou, P. de Boer *et al.*, 2001 Recombinational DNA double-strand breaks in mice precede synapsis. Nat Genet 27**:** 271-276.

Marston, A. L., and A. Amon, 2004 Meiosis: cell-cycle controls shuffle and deal. Nat Rev Mol Cell Biol 5**:** 983-997.

Matos, J., M. G. Blanco, S. Maslen, J. M. Skehel and S. C. West, 2011 Regulatory control of the resolution of DNA recombination intermediates during meiosis and mitosis. Cell 147**:** 158-172.

Mets, D. G., and B. J. Meyer, 2009 Condensins regulate meiotic DNA break distribution, thus crossover frequency, by controlling chromosome structure. Cell 139**:** 73-86.

Min, J., Q. Feng, Z. Li, Y. Zhang and R. M. Xu, 2003 Structure of the catalytic domain of human DOT1L, a non-SET domain nucleosomal histone methyltransferase. Cell 112**:** 711-723.

Miyazaki, T., D. A. Bressan, M. Shinohara, J. E. Haber and A. Shinohara, 2004 In vivo assembly and disassembly of Rad51 and Rad52 complexes during double-strand break repair. EMBO J 23**:** 939-949.

Miyazaki, W. Y., and T. L. Orr-Weaver, 1994 Sister-chromatid cohesion in mitosis and meiosis. Annu Rev Genet 28**:** 167-187.

Mosammaparast, N., and Y. Shi, 2010 Reversal of histone methylation: biochemical and molecular mechanisms of histone demethylases. Annu Rev Biochem 79**:** 155-179.

Nakagawa, T., and R. D. Kolodner, 2002 Saccharomyces cerevisiae Mer3 is a DNA helicase involved in meiotic crossing over. Mol Cell Biol 22**:** 3281-3291.

Nakagawa, T., and H. Ogawa, 1999 The Saccharomyces cerevisiae MER3 gene, encoding a novel helicase-like protein, is required for crossover control in meiosis. EMBO J 18**:** 5714-5723.

Nicolette, M. L., K. Lee, Z. Guo, M. Rani, J. M. Chow *et al.*, 2010 Mre11-Rad50-Xrs2 and Sae2 promote 5' strand resection of DNA double-strand breaks. Nat Struct Mol Biol 17**:** 1478-1485.

Nislow, C., E. Ray and L. Pillus, 1997 SET1, a yeast member of the trithorax family, functions in transcriptional silencing and diverse cellular processes. Mol Biol Cell 8**:** 2421-2436.

Novak, J. E., P. B. Ross-Macdonald and G. S. Roeder, 2001 The budding yeast Msh4 protein functions in chromosome synapsis and the regulation of crossover distribution. Genetics 158**:** 1013-1025.

Ontoso, D., I. Acosta, F. van Leeuwen, R. Freire and P. A. San-Segundo, 2013 Dot1-dependent histone H3K79 methylation promotes activation of the Mek1 meiotic checkpoint effector kinase by regulating the Hop1 adaptor. PLoS Genet 9**:** e1003262.

Page, S. L., and R. S. Hawley, 2004 The genetics and molecular biology of the synaptonemal complex. Annu Rev Cell Dev Biol 20**:** 525-558.

Perez-Hidalgo, L., S. Moreno and P. A. San-Segundo, 2003 Regulation of meiotic progression by the meiosis-specific checkpoint kinase Mek1 in fission yeast. J Cell Sci 116**:** 259-271.

Peterson, C. L., and M. A. Laniel, 2004 Histones and histone modifications. Curr Biol 14**:** R546-551.

Recht, J., T. Tsubota, J. C. Tanny, R. L. Diaz, J. M. Berger *et al.*, 2006 Histone chaperone Asf1 is required for histone H3 lysine 56 acetylation, a modification associated with S phase in mitosis and meiosis. Proc Natl Acad Sci U S A 103**:** 6988-6993.

Rockmill, B., and G. S. Roeder, 1988 RED1: a yeast gene required for the segregation of chromosomes during the reductional division of meiosis. Proc Natl Acad Sci U S A 85**:** 6057-6061.

Roeder, G. S., and J. M. Bailis, 2000 The pachytene checkpoint. Trends Genet 16**:** 395-403.

San-Segundo, P. A., and G. S. Roeder, 1999 Pch2 links chromatin silencing to meiotic checkpoint control. Cell 97**:** 313-324.

San-Segundo, P. A., and G. S. Roeder, 2000 Role for the silencing protein Dot1 in meiotic checkpoint control. Mol Biol Cell 11**:** 3601-3615.

Sawada, K., Z. Yang, J. R. Horton, R. E. Collins, X. Zhang *et al.*, 2004 Structure of the conserved core of the yeast Dot1p, a nucleosomal histone H3 lysine 79 methyltransferase. J Biol Chem 279**:** 43296-43306.

Schulze, J. M., J. Jackson, S. Nakanishi, J. M. Gardner, T. Hentrich *et al.*, 2009 Linking cell cycle to histone modifications: SBF and H2B monoubiquitination machinery and cell-cycle regulation of H3K79 dimethylation. Mol Cell 35**:** 626-641.

Schwacha, A., and N. Kleckner, 1997 Interhomolog bias during meiotic recombination: meiotic functions promote a highly differentiated interhomolog-only pathway. Cell 90**:** 1123-1135.

Serrentino, M. E., E. Chaplais, V. Sommermeyer and V. Borde, 2013 Differential association of the conserved SUMO ligase Zip3 with meiotic double-strand break sites reveals regional variations in the outcome of meiotic recombination. PLoS Genet 9**:** e1003416.

Shilatifard, A., 2006 Chromatin modifications by methylation and ubiquitination: implications in the regulation of gene expression. Annu Rev Biochem 75**:** 243-269.

Shilatifard, A., 2008 Molecular implementation and physiological roles for histone H3 lysine 4 (H3K4) methylation. Curr Opin Cell Biol 20**:** 341-348.

Shinohara, A., S. Gasior, T. Ogawa, N. Kleckner and D. K. Bishop, 1997 Saccharomyces cerevisiae recA homologues RAD51 and DMC1 have both distinct and overlapping roles in meiotic recombination. Genes Cells 2**:** 615-629.

Shinohara, A., H. Ogawa and T. Ogawa, 1992 Rad51 protein involved in repair and recombination in S. cerevisiae is a RecA-like protein. Cell 69**:** 457-470.

Shinohara, A., and T. Ogawa, 1998 Stimulation by Rad52 of yeast Rad51-mediated recombination. Nature 391**:** 404-407.

Shinohara, A., and M. Shinohara, 2004 Roles of RecA homologues Rad51 and Dmc1 during meiotic recombination. Cytogenet Genome Res 107**:** 201-207.

Shinohara, M., S. L. Gasior, D. K. Bishop and A. Shinohara, 2000 Tid1/Rdh54 promotes colocalization of rad51 and dmc1 during meiotic recombination. Proc Natl Acad Sci U S A 97**:** 10814-10819.

Shinohara, M., S. D. Oh, N. Hunter and A. Shinohara, 2008 Crossover assurance and crossover interference are distinctly regulated by the ZMM proteins during yeast meiosis. Nat Genet 40**:** 299-309.

Shinohara, M., K. Sakai, T. Ogawa and A. Shinohara, 2003 The mitotic DNA damage checkpoint proteins Rad17 and Rad24 are required for repair of double-strand breaks during meiosis in yeast. Genetics 164**:** 855-865.

Singer, M. S., A. Kahana, A. J. Wolf, L. L. Meisinger, S. E. Peterson *et al.*, 1998 Identification of high-copy disruptors of telomeric silencing in Saccharomyces cerevisiae. Genetics 150**:** 613-632.

Smith, A. V., and G. S. Roeder, 1997 The yeast Red1 protein localizes to the cores of meiotic chromosomes. J Cell Biol 136**:** 957-967.

Sollier, J., W. Lin, C. Soustelle, K. Suhre, A. Nicolas *et al.*, 2004 Set1 is required for meiotic S-phase onset, double-strand break formation and middle gene expression. EMBO J 23**:** 1957-1967.

Sommermeyer,V., C. Béneut, E. Chaplais, M.E. Serrentino and V. Borde, 2013 Spp1, a member of the Set1 Complex, promotes meiotic DSB formation in promoters by tethering histone H3K4 methylation sites to chromosome axes. Mol Cell 49: 43-54.

Sourirajan, A., and M. Lichten, 2008 Polo-like kinase Cdc5 drives exit from pachytene during budding yeast meiosis. Genes Dev 22**:** 2627-2632.

Stahl, F. W., H. M. Foss, L. S. Young, R. H. Borts, M. F. Abdullah *et al.*, 2004 Does crossover interference count in Saccharomyces cerevisiae? Genetics 168**:** 35-48.

Storlazzi, A., L. Xu, L. Cao and N. Kleckner, 1995 Crossover and noncrossover recombination during meiosis: timing and pathway relationships. Proc Natl Acad Sci U S A 92**:** 8512-8516.

Storlazzi, A., L. Xu, A. Schwacha and N. Kleckner, 1996 Synaptonemal complex (SC) component Zip1 plays a role in meiotic recombination independent of SC polymerization along the chromosomes. Proc Natl Acad Sci U S A 93**:** 9043-9048.

Sym, M., J. A. Engebrecht and G. S. Roeder, 1993 ZIP1 is a synaptonemal complex protein required for meiotic chromosome synapsis. Cell 72**:** 365-378.

Symington, L. S., 2002 Role of RAD52 epistasis group genes in homologous recombination and double-strand break repair. Microbiol Mol Biol Rev 66**:** 630-670, table of contents.

Takahashi, Y. H., and A. Shilatifard, 2010 Structural basis for H3K4 trimethylation by yeast Set1/COMPASS. Adv Enzyme Regul 50**:** 104-110.

Thompson, E. A., and G. S. Roeder, 1989 Expression and DNA sequence of RED1, a gene required for meiosis I chromosome segregation in yeast. Mol Gen Genet 218**:** 293-301.

Tsubouchi, H., and H. Ogawa, 1998 A novel mre11 mutation impairs processing of double-strand breaks of DNA during both mitosis and meiosis. Mol Cell Biol 18**:** 260-268.

Tsubouchi, T., H. Zhao and G. S. Roeder, 2006 The meiosis-specific zip4 protein regulates crossover distribution by promoting synaptonemal complex formation together with zip2. Dev Cell 10**:** 809-819.

Tung, K. S., and G. S. Roeder, 1998 Meiotic chromosome morphology and behavior in zip1 mutants of Saccharomyces cerevisiae. Genetics 149**:** 817-832.

Usui, T., S. S. Foster and J. H. Petrini, 2009 Maintenance of the DNA-damage checkpoint requires DNA-damage-induced mediator protein oligomerization. Mol Cell 33**:** 147-159.

Usui, T., H. Ogawa and J. H. Petrini, 2001 A DNA damage response pathway controlled by Tel1 and the Mre11 complex. Mol Cell 7**:** 1255-1266.

van Leeuwen, F., P. R. Gafken and D. E. Gottschling, 2002 Dot1p modulates silencing in yeast by methylation of the nucleosome core. Cell 109**:** 745-756.

Vermeulen, M., H. C. Eberl, F. Matarese, H. Marks, S. Denissov *et al.*, 2010 Quantitative interaction proteomics and genome-wide profiling of epigenetic histone marks and their readers. Cell 142**:** 967-980.

Wan, L., T. de los Santos, C. Zhang, K. Shokat and N. M. Hollingsworth, 2004 Mek1 kinase activity functions downstream of RED1 in the regulation of meiotic double strand break repair in budding yeast. Mol Biol Cell 15**:** 11-23.

Wysocki, R., A. Javaheri, S. Allard, F. Sha, J. Cote *et al.*, 2005 Role of Dot1-dependent histone H3 methylation in G1 and S phase DNA damage checkpoint functions of Rad9. Mol Cell Biol 25**:** 8430-8443.

Yamada, T., and K. Ohta, 2013 Initiation of meiotic recombination in chromatin structure. J Biochem 154**:** 107-114.

Yamashita, K., M. Shinohara and A. Shinohara, 2004 Rad6-Bre1-mediated histone H2B ubiquitylation modulates the formation of double-strand breaks during meiosis. Proc Natl Acad Sci U S A 101**:** 11380-11385.

Zalevsky, J., A. J. MacQueen, J. B. Duffy, K. J. Kemphues and A. M. Villeneuve, 1999 Crossing over during Caenorhabditis elegans meiosis requires a conserved MutS-based pathway that is partially dispensable in budding yeast. Genetics 153**:** 1271-1283.

Zhu, Z. H., S. Mori, H. Oshiumi, K. Matsuzaki, M. Shinohara *et al.*, 2010 Cyclin-dependent kinase promotes formation of the synaptonemal complex in yeast meiosis. Genes to Cells 15**:** 1036-1050.

Zickler, D., and N. Kleckner, 1998 The leptotene-zygotene transition of meiosis. Annu Rev Genet 32**:** 619-697.

Table one:
Strain list

Strain No.	Genotypes
NKY1543	*MAT α, ho::LYS2, lys2, ura3, leu2::hisG, his4X-LEU2(BamHI)-URA3, arg4-nsp*
NKY1303	*MAT **a**, ho::LYS2, lys2, ura3, leu2::hisG, his4B-LEU2(MluI), arg4-bgl*
MBY005	NKY1303 with *dot1::KanMX6*
MBY006	NKY1543 with *dot1::KanMX6*
MBY015	NKY1303 with *set1:: KlURA3*
MBY016	NKY1543 with *set1::KlURA3*
MBY037	NKY1303 with *dot1::KanMX6, set1:: KlURA3*
MBY039	NKY1543 with *dot1::KanMX6, set1::KlURA3*
MBY211	NKY1303 with *hht1-K4R, hht2-K4R*
MBY218	NKY1543 with *hht1-K4R, hht2-K4R*
MBY152	NKY1303 with *hht1-K79R, hht2-K79R*
MBY151	NKY1543 with *hht1-K79R, hht2-K79R*
MBY219	NKY1303 with *hht1-K79R, hht2-K79R, set1:: KlURA3*
MBY221	NKY1543 with *hht1-K79R, hht2-K79R, set1:: KlURA3*
MBY233	NKY1303 with *hht1-K4R, hht2-K4R, dot1::KanMX6*
MBY237	NKY1543 with *hht1-K4R, hht2-K4R, dot1::KanMX6*
MBY009	NKY1303 with *dmc1::URA3*
MBY010	NKY1543 with *dmc1::URA3*
MBY003	NKY1303 with *dmc1::URA3, dot1::KanMX6*
MBY004	NKY1543 with *dmc1::URA3, dot1::KanMX6*
MBY021	NKY1303 with *dmc1::URA3, set1::KlURA3*
MBY022	NKY1543 with *dmc1::URA3, set1::KlURA3*
MBY282	NKY1303 with *dmc1::URA3, set1::KlURA3, dot1::KanMX6*
MBY285	NKY1543 with *dmc1::URA3, set1::KlURA3, dot1::KanMX6*
MBY133	NKY1303 with *50S::URA3*
MBY132	NKY1543 with *50S::URA3*
MBY175	NKY1303 with *dot1::KanMX6*, *50S::URA3*
MBY163	NKY1543 with *dot1::KanMX6*, *50S::URA3*
MBY171	NKY1303 with *pch2::TRIP1*, *50S::URA3*
MBY159	NKY1543 with *pch2::TRIP1*, *50S::URA3*
MBY245	NKY1303 with *pch2::TRIP1*, *50S::URA3, dot1::KanMX6*
MBY243	NKY1543 with *pch2::TRIP1*, *50S::URA3, dot1::KanMX6*
MBY258	NKY1303 with *tel1::TRIP1*, *50S::URA3*
MBY259	NKY1543 with *tel1::TRIP1*, *50S::URA3*
MBY251	NKY1303 with *hht1-K79R, hht2-K79R, 50S::URA3*
MBY252	NKY1543 with *hht1-K79R, hht2-K79R, 50S::URA3*

Table two:
Primer list

Cloning for HTT1
5’ AGCTATCCGGAATTCGGGGGAGAAGCGCTCGGAACA 3’
5’ TCGACTCCCAAGCTTGACACCTACCACGTATGCGG 3’
K4R mutagenesis for HHT1
5’ ATGGCCAGAACGCGTCAAACAGCAAGA 3’
5’ TCTTGCTGTTTGACGCGTTCTCGGCAT 3’
Cloning for HTT2
5’ CCGAATTCCAAACACGTATGTATCTAGCCG 3’
5’ CCCGCGGCCGCGTGTTGAATCCTGCGAATC 3
K4R mutagenesis for HHT2
5’ ATGGCCAGAACGCGTCAAACAGCAAGA 3’
5’ ATGGCCAGAACGCGTCAAACAGCAAGA 3’

Acknowledgment

Thanks God for your mercy and grace upon me for finishing my PhD. Completing a PhD is truly an exhausting, emotional struggle. You are forced to confront all of your fears, insecurities and doubts you have about yourself and somehow overcome them, and I would not have been able to complete this journey without the aid and support of countless people over the past five years.

I must first express my sincere gratitude towards my supervisors, Professor Akira Shinohara and Dr. Miki Shinohara, your patient guidance, kindness, encouragement as well as the advice you have provided have been invaluable to me, I have been extremely lucky to have a supervisor who cared so much about my work. Your leadership, support, attention to detail, hard work, and scholarship have set an example I hope to match some day.

I would like to thank Dr. Saori Mori for her guidance and teaching during my first year. I am extremely grateful to Dr. Hiroyuki Sasanuma, for his great efforts to explain things clearly and simply, he responded to my questions and queries so promptly, he helped me a lot throughout my PhD course; he provided good teaching, good company, and lots of good ideas. I would like to thank Dr. Takehiko Usui for the *hht1,2 k79R* strain. I would like to thank Dr. Terasawa for valuable discussions and support. My special thanks to Dr. Prasada Rao who as a good friend was always willing to help and give his best suggestions, I really enjoyed the time we spent here, and It would have been a lonely lab without him.

I owe my deepest gratitude and appreciation to our lab technicians and managers for their kind support, my research would not have been possible without their generous help. Many thanks to all current and past members of our laboratory, they each helped make my time in the PhD course more fun and interesting, I have been enjoying doing research with all of you.

I would like to acknowledge the support from the administration office in the Institute for protein research. Over these five years, I have enjoyed the aid of several fellowships and scholarships, I would like to thank Graduate school of science, JASSO, JGC-S (Nikki Saneyoshi) and institute for protein research for the generous financial aid.

I would like to thank my thesis committee members, Profs. Tajima, Takisawa and Dr. Miki Shinohara for your scientific input towards my research, and for your wonderful advice and feedback. I would like to thank my friends Nouri, Haneih, Abdol, Haredy, yousef, Elyas and Ghalawingi, for cheering me up, for helping me get through the difficult times, and for all the emotional support, entertainment, and caring they provided.

Most importantly, none of this would have been possible without the love and patience of my parents, sisters and brother. My parents to whom this thesis is dedicated to, you raised me, supported me, taught me and loved me, thank you for instilling in me confidence and a drive for pursuing my PhD, thank you for all the scarifies you have made for me, words can not express how grateful I am for all that you are doing in order to build a brighter tomorrow for me.